JOSÉ ALEXANDER RODRÍGUEZ

PIRÓLISE DE RESÍDUOS AGRÍCOLAS E INDUSTRIAIS E USO POTENCIAL DO BIOCARVÃO COMO CONDICIONADOR DE REJEITOS DE MINERAÇÃO

Tese apresentada à Universidade Federal de Viçosa, como parte das exigências do Programa de Pós-Graduação em Solos e Nutrição de Plantas, para obtenção do título de *Doctor Scientiae.*

VIÇOSA
MINAS GERAIS - BRASIL
2017

Ficha catalográfica elaborada pela Biblioteca Central da Universidade Federal de Viçosa - Campus Viçosa

T
R696p
2017

Rodríguez, José Alexander, 1979-
Pirólise de resíduos agrícolas e industriais e uso potencial do biocarvão como condicionador de rejeitos de mineração / José Alexander Rodríguez. – Viçosa, MG, 2017.
1 tese eletrônica (xi, 96 f.): il. (algumas color.).

Inclui anexos.
Orientador: Teógenes Senna de Oliveira.
Tese (doutorado) - Universidade Federal de Viçosa.
Inclui bibliografia.
Disponível em: https://www.locus.ufv.br/

1. Biocombustíveis. 2. Pirólise. 3. Carvão. 4. Resíduos agrícolas. 5. Resíduos de animais. I. Universidade Federal de Viçosa. Departamento de Solos. Programa de Pós-Graduação em Solos e Nutrição de Plantas. II. Título.

CDD 22. ed. 662.88

Bibliotecário(a) responsável: Alice Regina Pinto CRB6 2523

JOSÉ ALEXANDER RODRÍGUEZ

Pirólise de resíduos agrícolas e industriais e uso potencial do biocarvão como condicionador de rejeitos de mineração

Tese apresentada à Universidade Federal de Viçosa, como parte das exigências do Programa de Pós-Graduação em Solos e Nutrição de Plantas, para obtenção do título de *Doctor Scientiae*.

APROVADA: 24 de março de 2017

Maria Eugenia Ortiz Escobar

Etelvino Henrique Novotny

Raphael Bragança Alves Fernandes

Igor Rodrigues de Assis
(Coorientador)

Teogenes Senna de Oliveira
(Orientador)

Ao meu amor e família, por não fazerem fácil meu caminho;
porque me fez mais forte e dedicado!

Aos amigos que fiz no Brasil e na UFV, sempre os levarei
no meu coração, amigos para sempre!

Ao professor Teógenes pela paciência, apoio e confiança
de conseguir o objetivo

Dedico.

AGRADECIMENTOS

A Deus pela presença em todos os momentos da minha vida.

À Universidade Federal de Viçosa e ao Programa de Pós-Graduação em Solos e Nutrição de Plantas, pela oportunidade de realização do curso.

À Comissão de Aperfeiçoamento de Pessoal do Nível Superior (CAPES), pela concessão da bolsa de estudos.

Ao Programa de Alianças pela Educação e Capacitação (PAEC) entre a Organização dos Estados Americanos (OEA) e o grupo Coimbra de Universidades Brasileiras (GCUB), pela intermediação.

Ao Professor Teógenes Senna de Oliveira e Leônidas Melo, pela orientação e apoio essencial para realização de mais este projeto de vida.

Aos Professores Igor Rodrigues e Maria Catarina Megumi Kasuya pelo apoio e ensinamentos.

Ao professor Jairo Tronto do Campus da UFV em Rio Paranaíba pelo apoio com as análises de FTIR.

Aos professores Julio Neves e Raphael Fernandes e funcionários do Departamento de Solos, em especial Luciana, Cláudio, Carlos Fonseca, Janílson, José Francisco (Chico) e Adriana pelas ajudas inestimáveis, exemplos de profissionais!

Aos estagiários Márcio Maitano, Emerson Fialho e Joésio Souza pelas colaborações nas atividades de laboratório.

A todas as pessoas que participaram da minha formação e do meu convívio diário, muito obrigado!

SUMÁRIO

LISTA DE ABREVIAÇÕES

Å	Angstrom 1 Å= 10^{-10} m
ABRELPE	Associação Brasileira de Empresas de Limpeza Pública e Resíduos Especiais
ACP	Análise de componentes principais
ANOVA	Análise de variância
ASE	Área superficial específica
ASTM	American Society for Testing and Materials
C	Carbono
Ca	Cálcio
CE	Condutividade elétrica
Cfx	Carbono fixo
CO	Carbono orgânico
CRA	Capacidade retenção de água
CTC	Capacidade de troca catiônica
CW	Resíduos de madeira da construção
CW+PVC	Resíduos de madeira da construção e PVC
CW+TR	Resíduos de madeira da construção e pneu
Disp	Elementos disponíveis
DMP	Diâmetro médio ponderado
DRX	Difratometria de raios X
Fe	Ferro
FTIR	Espectroscopia no infravermelho com transformada de Fourier
H	Hidrogênio
H+Al	Acidez potencial
IBI	International Biochar Initiative
ICP-OES	Espectroscopia absorção atômica com plasma indutivamente acoplado
IPEA	Instituto de Pesquisa Econômica Aplicada
IVB	Índice de viabilidade do biocarvão
K	Potássio
m	Saturação de alumínio
Mg	Magnésio
Mn	Manganês
Na	Sódio
O	Oxigênio
P	Fósforo
pH_{KCl}	pH em KCl
PL	Resíduos de cama de frango
PL+CW	Resíduos de cama de frango e madeira da construção
PL+PVC	Resíduos de cama de frango e PVC
PL+SM	Resíduos de cama de frango e dejetos de suíno
PL+TR	Resíduos de cama de frango e pneu
PN	Poder de neutralização
PVC	Policloruro de vinilo
PVC	Resíduos de PVC
R^2	Coeficiente de determinação
Rej	Rejeito
RS	Porcentagem de resíduos de biocarvão
S	Enxofre

SB	Soma de bases
SM	Resíduos de dejeto de Suíno
SM+CW	Resíduos de dejeto de suíno e madeira da construção
SM+PVC	Resíduos de dejeto de suíno e PVC
SM+TR	Resíduos de dejeto de suíno e pneu
Sol	Solução do solo\substrato
T	Capacidade de troca catiônica a pH 7,0
t	Capacidade de troca catiônica efetiva
Tc	Teores de cinzas
TR	Resíduos de pneu
Tr	Teores de elementos trocáveis
TR+PVC	Resíduos de pneu e PVC
Tv	Teores de compostos voláteis
V	Saturação de bases

RESUMO

RODRIGUEZ, Jose Alexander, D.Sc., Universidade Federal de Viçosa, março de 2017. **Pirólise de resíduos agrícolas e industriais e uso potencial do biocarvão como condicionador de rejeitos de mineração.** Orientador: Teógenes Senna de Oliveira. Coorientadores: Igor Rodrigues de Assis e Leônidas Carrijo Azevedo Melo.

A degradação ambiental pela inadequada utilização das terras e disposição dos resíduos agrícolas, industriais e urbanos está aumentando no mundo, o que exige novas e rápidas alternativas ambientalmente sustentáveis. A pirólise é um processo que tem se apresentado como uma opção limpa de gestão de resíduos pela sua decomposição térmica em altas temperaturas na ausência do oxigênio produzindo carvão, gases e óleo, produtos que podem ser aproveitados sem geração de resíduos. Neste trabalho, objetivou-se identificar as características e potencialidades agronômicas e ambientais dos biocarvões produzidos por pirólise e co-pirólise (mistura dos resíduos em proporções de 1:1, w:w) lentas em diferentes temperaturas, utilizando dois resíduos sólidos agrícolas (dejetos de suíno - SM e de cama de frango - PL) e três industriais (madeira da construção - CW, pneu - TR e plástico PVC - PVC), levando-os a uma utilização mais aproveitável. Os resíduos foram selecionados considerando critérios de quantidade gerada e disposição final. Os materiais foram submetidos a cinco temperaturas: 300, 400, 500, 600 e 700 ºC, em ambiente com restrição de oxigênio, com taxa de aquecimento de 10 ºC min^{-1}, mantidos durante uma hora na temperatura desejada. Antes e após a transformação térmica, avaliaram-se as seguintes propriedades físico-químicas: rendimento (RS), teor de cinzas (Tc), compostos voláteis (Tv), C fixo (Cfx) e orgânico (CO), composição elementar, grupos funcionais, mineralogia, macro e micronutrientes, pH, condutividade elétrica (CE), poder neutralizante (PN), capacidade de retenção de água (CRA), capacidade de troca catiônica (CTC) e diâmetro médio ponderado das partículas (DPM). Os biocarvões foram estratificados pelas características intrínsecas dos biocarvões e as propriedades restritivas de uso em solo/substrato, utilizando análise de componentes principais (ACP) e índice de viabilidade do biocarvão (IVB), além de critérios delimitados pelos teores de C fixo (Cfx), cinzas (Tc) e materiais voláteis (Tv). Utilizou-se também estratificações já estabelecidas na literatura e aplicadas por organismos institucionais. O biocarvão classificado como o mais viável segundo as propriedades restritivas de uso em solo/substrato, PL600, foi utilizado num experimento de casa de vegetação em pirólise e co-pirólise com resíduos industriais (TR, CW e PVC). Rejeitos de mineração de Fe e Mn foram tratados com biocarvões na dose de 5% (m/m) e após incubação

cultivado com crotalaria (*Crotalaria juncea*) em vasos. Avaliaram-se o crescimento e as alterações na solução do solo e nas propriedades químicas dos rejeitos. Os biocarvões PL e TR, seguidos de SM e CW foram os que apresentaram maiores potencialidades para uso na produção de biocarvões considerando os resultados de pH, CRA, CTC, H:C, O:C, Cfx, elementos disponíveis e ausência de contaminantes inorgânicos. O R_{PVC} apresentou potencialidades como disponibilidade de P e Ca, além de alta CRA, porém, a elevada CE e o teor total de Pb pode restringir seu uso como condicionador de solo. Por outro lado, biocarvões produzidos em co-pirólise com os resíduos industriais (principalmente TR e CW) podem ter suas características melhoradas (ex. CE e pH) para uso como condicionador de solo. A estratificação segundo as propriedades restritivas de uso em solo/substrato é uma ferramenta útil para estratificar os melhores biocarvões para determinado uso. A combinação dos parâmetros teores de Cfx, Tc e Tve mostrou-se adequada para a identificação das potencialidades agronômicas e ambientais dos biocarvões, pois é rápida e de baixo custo. No experimento de casa de vegetação, os efeitos dos biocarvões dependeram muito mais das interações com o tipo de substrato do que das características do biocarvão, pois observaram-se os maiores valores de CE e pH nos tratamentos com rejeitos de Fe do que Mn, assim como menores disponibilidades de macro e micronutrientes no rejeito de Fe. Os tratamentos que apresentaram melhor desenvolvimento de plantas foram aqueles com CW nos dois rejeitos, PL+TR e PL+CW no rejeito de Mn e TR no rejeito de Fe, o que confirma as diferenças no sinergismo entre os biocarvões e o substrato. Os fatores mais limitantes em ambos rejeitos foram o pH e CE.

ABSTRACT

RODRIGUEZ, Jose Alexander, D.Sc., Universidade Federal de Viçosa, March, 2017. **Pyrolysis of agricultural and industrial residues and the potential use of biochar as a conditioner for mining tailings.** Adviser: Teógenes Senna de Oliveira. Co-advisers: Igor Rodrigues de Assis and Leônidas Carrijo Azevedo Melo.

Environmental degradation due to inadequate land use and disposal of agricultural, industrial and urban wastes is increasing worldwide, requiring new and fast environmentally sustainable alternatives. Pyrolysis is a process that has been presented as a clean alternative of waste management by its thermal decomposition at high temperatures in the absence of oxygen producing coal, gases and oil, products that can be used without generation of waste. The objective of this work was to identify the agronomic and environmental characteristics and potentials of the biochar produced by pyrolysis and co-pyrolysis (mixing of residues in 1: 1, w / w ratios) at different temperatures using two solid agricultural residues (swine manure - SM and poultry litter- PL) and three industrial ones (construction wood - CW, Tire - TR and PVC plastic - PVC). The residues were selected because they present high potential of generating negative impacts to the environment, considering quantity generated criteria and final disposal. The materials were subjected to five temperatures (300, 400, 500, 600 and 700 ºC) in an oxygen-restricted environment, with a heating rate of 10 ºC min-1, and kept for one hour at the desired temperature. The following physicochemical properties were evaluated: yield, ash, volatile compounds, fixed and organic C, elemental composition, functional groups, mineralogy, macro and micro nutrients, pH, electrical conductivity, Neutralizing power (PN), water retention capacity (CRA), cation exchange capacity (CTC) and particle size distribution (DPM). The biochar were classified by their intrinsic characteristics and the restrictive properties of soil / substrate use, using principal component analysis (PCA) and the formulation of biobial viability index (IVB). In addition, biofuel quality criteria delimited by fixed C (Cfx), ashes (Tc) and volatile materials (Tv) were established. Stratifications already established in the literature and applied by institutional bodies were also used. Biochar classified as the most viable according to the restrictive properties of use in soil/substrate, PL600, was used in a greenhouse experiment in pyrolysis and co-pyrolysis with industrial waste (TR, CW and PVC). Fe and Mn mining were treated with 5% (w / w) biochar and after incubation Crotalaria (Crotalaria juncea) was grown in pots. It was evaluated the development of the plants, besides the changes in soil solution and the chemical properties of the tailings. The biofuels PL and TR, followed by SM and CW were

the ones with the highest potential for use in the production of biochar considering the results of pH, CRA, CTC, H: C, O: C and C Fx and available elements and absence of contaminants Inorganic acids. The RPVC presented potentials such as availability of phosphorus and calcium, in addition to high CRA, but the high EC and total Pb content may restrict its use as soil conditioner. On the other hand, biofuels produced in co-pyrolysis with industrial waste (mainly Tire and Wood from the construction) can have their improved characteristics (eg EC and pH) for use as a soil conditioner. Due to the high variability in the properties of the biochar, it was not possible to establish the best pyrolysis temperature for each raw material, aiming to produce biochar with desirable characteristics. In this sense, the classification proposed in this work is a useful tool to select the best biochar for a particular use. The combination of the parameters of fixed C, ash and volatile compounds were adequate for the identification of the agronomic and environmental potential of biofuels, which is a relevant result, since the immediate analysis is a quick and low cost evaluation, leading to Conclusions similar to those obtained by methods that use up to 20 or more variables. In the greenhouse experiment, it was observed that the effect of the biochar depended more on the synergism with the type of substrate, than on the characteristics of the bio-carbon, as it was observed higher values of EC and pH in the treatments with Fe Mn, as well as lower availability of macro and micronutrients in the Fe residue. The treatments that showed the best development of plants were those with CW in both residues, PL+TR and PL+CW in the Mn and TR residue in the Fe residue, confirming the differences in the synergism between the biofuels and the substrate. The limiting factors in both wastes were pH and EC.

INTRODUÇÃO GERAL

O mundo vive hoje dois grandes problemas que têm provocado cada vez mais interesse e preocupação a todos pelo impacto ambiental, econômico e à saúde humana. O primeiro é o aumento da utilização da terra de forma inadequada degradando áreas produtivas e, o segundo, é a geração de resíduos com potenciais danos ambientais se não forem devidamente tratados. Esses dois problemas agravam-se com o crescimento da população, pois ocasiona o aumento do consumo e a utilização dos recursos do planeta, o que leva ao desequilíbrio do ambiente, gerando áreas degradadas e a insustentabilidade ambiental.

Essas alterações no ambiente ganharam grande impulso com o advento da Revolução Industrial. A produção em massa de bens de consumo, a necessidade de recursos ou matérias primas e a geração de resíduos tomou dimensões sem precedentes na história da humanidade. No início da civilização, os resíduos gerados eram basicamente constituídos de restos vegetais e excrementos humanos e animais, materiais de fácil degradação. Porém, com o aumento da industrialização, os resíduos também se tornaram mais industrializados e de difícil destinação, não sendo mais possível a simples disposição direta em cursos d'água, solo ou atmosfera.

A disposição inadequada de resíduos apresenta-se como um dos problemas ambientais mais críticos da atualidade. O passivo ambiental oriundo da contaminação pela disposição final incorreta é ainda corrente em muitas instalações rurais, industriais e urbanas. A taxa de geração de resíduos é muito maior, aumentando a utilização de lixões e/ou aterros sanitários.

Os resíduos sólidos comuns e perigosos estão causando problemas ambientais em áreas urbanas, rurais e industriais, uma vez que geram impacto ambiental negativo ameaçando a sustentabilidade ambiental. Dada a necessidade de reduzir o passivo ambiental, representado pelos estoques de resíduos e de áreas degradadas, faz-se necessária a criação de soluções sustentáveis, o que pode ser conseguido mediante processos intrínsecos de eliminação de resíduos e recuperação de áreas degradadas, alternativas que têm se tornado mais comuns (MENCH et al., 2010). Alternativas de correção têm que ser rentáveis, possíveis de aplicação in situ; gerando interações com os componentes do sistema tratado, assegurando simultaneamente condições que promovam e estimulem a restauração ecológica (BEESLEY et al., 2011).

A utilização dos resíduos como matéria-prima em novos processos agrícolas ou industriais é uma alternativa sustentável na gestão de resíduos sólidos, sendo de grande

importância socioambiental e econômica. Os resíduos podem ser classificados em dois grandes grupos: agrícolas e industriais, sendo que os agrícolas são oriundos da fase agrícola do cultivo/criação de determinada espécie vegetal ou animal no campo ou os produzidos no processamento de produtos agrícolas. Os resíduos industriais são resultantes dos processos produtivos em instalações industriais (Artigo 13 da Política Nacional de Resíduos Sólidos; PNRS, 2010).

O uso dos resíduos sólidos como matéria-prima para novos processos agrícolas e/ou industriais apresenta algumas vantagens: valor energético na geração de energia e/ou biocombustíveis; o aproveitamento para a produção agrícola como fertilizante; a redução da exigência por lixões ou de aterros sanitários e, consequentemente, com eliminação de pragas, entre outros problemas sanitários; a melhoria da paisagem; e a redução da contaminação do ar, água e solo (MARTÍNEZ-LOZANO, 2009). A grande desvantagem, seja como fonte de energia, fertilizantes para culturas ou de alimentos para animais é o custo do transporte do local de coleta até a unidade de processamento central. Nesse sentido, o aproveitamento e gestão vai depender dos benefícios das tecnologias aplicadas para sua utilização (SPOKAS, 2010), especialmente porque os benefícios ambientais, sociais e econômicos superam os custos da obtenção dos resíduos (GALINATO; YODER; GRANATSTEIN, 2011).

A conversão de resíduos para a produção de carvão pelo processo de pirólise tem se apresentado como uma das opções de aproveitamento de resíduos agrícolas ou industriais não contaminados (TSAI et al., 2012). A pirólise constitui-se como um processo de decomposição térmica, entre 300 e 800 ºC, na ausência total ou parcial de oxigênio, convertendo a matéria-prima dos resíduos agrícolas ou industriais em três produtos: carvão (sólido), óleo (combustível líquido) e gás combustível, contendo CO, CO2, H2, CH4 e outros hidrocarbonetos (LEHMANN; JOSEPH, 2015). O uso do produto da pirólise no solo incorpora o prefixo “bio” pelo fato de intervir nos processos naturais, tanto físicos como químicos do solo (LEHMANN; JOSEPH, 2015), o que leva ao uso do termo biocarvão para se referir ao produto sólido da pirólise.

As propriedades físicas e químicas de biocarvões são influenciadas pela natureza e estado físico do material utilizado, pela temperatura de pirólise, conteúdo de oxigênio e tempo de residência (SPOKAS, 2010). As condições de pirólise influenciam principalmente a recalcitrância química dos compostos aromáticos, tornando-os mais estáveis quanto maior for

a temperatura (WU et al., 2011), o tempo de retenção e menor presença de ar (BRUUN et al., 2012).

Os biocarvões podem ser utilizados na recuperação de áreas degradadas como corretivo do solo na melhoria das propriedades e funções físicas, químicas e biológicas para o desempenho ambiental (WOOLF et al., 2010). Entre as funções potenciais dos biocarvões destacam-se a resistência ou estabilidade à degradação (de centenas a vários milhares de anos) (LEHMANN; JOSEPH, 2015), com consequente sequestro e redução das emissões de carbono para a atmosfera (MIMMO et al., 2014); a adsorção de contaminantes orgânicos e inorgânicos (KASOZI; NKEDI-KIZZA; GAO, 2010); a melhoria da retenção de água, capacidade de troca catiônica e interações com a ciclagem de nutrientes por meio de aumento no pH do solo (MUKHERJEE; ZIMMERMAN; HARRIS, 2011); a redução na lixiviação de nutrientes (SCHULZ; DUNST; GLASER, 2013); e a melhoria da estrutura do solo, promovendo o aumento da drenagem e das interações com as comunidades microbianas (JEFFERY et al., 2011).

As características e a otimização dos efeitos do biocarvão são reguladas pela seleção da matéria prima e pela técnica de produção, o que define sua aplicação ambiental ou agronômica especifica. Dessa condição emergem diferentes tipos de carvão e em várias escalas, necessitando de sistemas de produção específicos (IPPOLITO; LAIRD; BUSSCHER, 2012). A escolha da matéria-prima é um dos fatores mais importantes para produção de biocarvão, pois devem ser considerados os custos ambientais, sociais e financeiros (BEESLEY et al., 2013). Nesse sentido, a produção e utilização de biocarvão necessita de um desenho especifico, uma vez que a seleção da matéria-prima deve ser direcionada pela disponibilidade e finalidade do biocarvão.

Diante do exposto, é clara a necessidade de aprofundar nos conhecimentos acerca da conversão dos resíduos agrícolas e industriais pelo processo de pirólise. Nesse contexto, o presente trabalho tem como objetivo geral aprofundar nos conhecimentos acerca da conversão dos resíduos agrícolas e industriais pelo processo de pirólise e co-pirólise, a fim de conhecer as características físico-químicas do biocarvão produzido, o que leva ao direcionamento da sua utilização de uma forma, mas aproveitável, como por exemplo na revegetação das áreas degradadas pela mineração de ferro e manganês.

Para alcançar o objetivo do presente trabalho o primeiro capítulo intitulado “Influência da temperatura de pirólise e matéria-prima nas propriedades dos biochars produzidos a partir

de resíduos agrícolas e industriais" teve como objetivo avaliar o efeito da temperatura de pirólise nas características físico-químicas de biocarvões produzidos a partir de resíduos industriais e agrícolas por pirólise lenta e suas comparações. O capítulo 2, intitulado "A copirólise de resíduos agrícolas e industriais altera a composição e estabilidade dos biochars e pode melhorar seus benefícios agrícolas e ambientais" objetivou utilizar o processo de co-pirólise lenta como ferramenta para melhorar as características e potencialidades agronômicas e ambientais dos biocarvões produzidos em diferentes temperaturas, utilizando dois resíduos sólidos agrícolas e três industriais. O capítulo 3, intitulado "classificando do potencial de biochars de resíduos agrícolas e industriais para a recuperação de rejeitos de mineração de Fe e Mg" teve como objetivo propor formas de estratificação de biocarvões produzidos de resíduos agrícolas e industriais utilizando suas propriedades físicas e químicas tornando as escolhas e, ou, interpretações da sua qualidade e usos, mais eficientes. O capítulo 4, intitulado "crescimento da crotalaria em rejeitos da mineração de Fe e Mn condicionados com fertilizantes e biocarvões" o objetivo foi avaliar o crescimento da crotalaria (Crotalaria juncea) em rejeitos de mineração de Fe e Mn, condicionados com biocarvões derivados de resíduo agrícola (cama de frango: PL) e industriais (pneu: TR, plástico PVC: PVC e madeira da construção: CW) produzidos por pirólise e co-pirólise lenta a 600 ºC (PL+CW; PL+TR e PL+PVC).

Referências

BEESLEY, L. et al. A review of biochars' potential role in the remediation, revegetation and restoration of contaminated soils. **Environmental Pollution**, v. 159, n. 12, p. 3269–3282, 2011.

BEESLEY, L. et al. Biochar addition to an arsenic contaminated soil increases arsenic concentrations in the pore water but reduces uptake to tomato plants (Solanum lycopersicum L.). **Science of the Total Environment**, v. 454–455, p. 598–603, 2013.

BRUUN, E. W. et al. Effects of slow and fast pyrolysis biochar on soil C and N turnover dynamics. **Soil Biology and Biochemistry**, v. 46, p. 73–79, 2012.

GALINATO, S. P.; YODER, J. K.; GRANATSTEIN, D. The economic value of biochar in crop production and carbon sequestration. **Energy Policy**, v. 39, n. 10, p. 6344–6350, 2011.

IPPOLITO, J. A.; LAIRD, D. A.; BUSSCHER, W. J. Environmental Benefits of Biochar. **Journal of Environment Quality**, v. 41, n. 4, p. 967, 2012.

JEFFERY, S. et al. A quantitative review of the effects of biochar application to soils on crop productivity using meta-analysis. **Agriculture, Ecosystems and Environment**, v. 144, n. 1, p. 175–187, 2011.

KASOZI, G. N.; NKEDI-KIZZA, P.; GAO, B. I. N. Catechol and Humic Acid Sorption onto a Range of Laboratory Produced Black Carbons (Biochars).pdf. v. 44, n. 16, p. 6189–6195, 2010.

LEHMANN, J.; JOSEPH, S. **Biochar for environmental management: Science, technolgy and implementation**. New York: Earthscan, 2015.

MARTÍNEZ-LOZANO, S. **Evaluación de la biomasa como recurso energético renovable en Cataluña**. [s.l: s.n.].

MENCH, M. et al. Successes and limitations of phytotechnologies at field scale: Outcomes, assessment and outlook from COST Action 859. **Journal of Soils and Sediments**, v. 10, n. 6, p. 1039–1070, 2010.

MIMMO, T. et al. Effect of pyrolysis temperature on miscanthus (Miscanthus × giganteus) biochar physical, chemical and functional properties. **Biomass and Bioenergy**, v. 62, n. 0, p. 149–157, 2014.

MUKHERJEE, A.; ZIMMERMAN, A. R.; HARRIS, W. Surface chemistry variations among a series of laboratory-produced biochars. **Geoderma**, v. 163, n. 3–4, p. 247–255, 2011.

SCHULZ, H.; DUNST, G.; GLASER, B. Positive effects of composted biochar on plant growth and soil fertility. **Agronomy for Sustainable Development**, v. 33, n. 4, p. 817–827, 2013.

SPOKAS, K. A. Review of the stability of biochar in soils: predictability of O:C molar ratios. **Carbon Management**, v. 1, n. 2, p. 289–303, 2010.

TSAI, W. T. et al. Textural and chemical properties of swine-manure-derived biochar pertinent to its potential use as a soil amendment. **Chemosphere**, v. 89, n. 2, p. 198–203, 2012.

WOOLF, D. et al. **Sustainable biochar to mitigate global climate change.Nature communications**Nature Publishing Group, , 2010. Disponível em: <http://dx.doi.org/10.1038/ncomms1053>

WU, H. et al. Removal and Recycling of Inherent Inorganic Nutrient Species in Mallee Biomass and Derived Biochars by Water Leaching. p. 12143–12151, 2011.

CAPÍTULO 1

INFLUENCE OF PYROLYSIS TEMPERATURE AND FEEDSTOCK ON THE PROPERTIES OF BIOCHARS PRODUCED FROM AGRICULTURAL AND INDUSTRIAL WASTES

Journal of Analytical and Applied Pyrolysis 149 (2020) 104839

Contents lists available at ScienceDirect

Journal of Analytical and Applied Pyrolysis

journal homepage: www.elsevier.com/locate/jaap

Influence of pyrolysis temperature and feedstock on the properties of biochars produced from agricultural and industrial wastes

José Alexander Rodriguez[a,c], José Ferreira Lustosa Filho[a,*], Leônidas Carrijo Azevedo Melo[b], Igor Rodrigues de Assis[a], Teógenes Senna de Oliveira[a]

[a] Department of Soils, Federal University of Viçosa, 36570-900, Viçosa, MG, Brazil
[b] Department of Soil Science, Federal University of Lavras, 37200-000, Lavras, MG, Brazil
[c] Faculty of Veterinary Medicine and Zootechnics, Autonomous University Foundation of the Americas, South Avenue 98-56, Pereira, R/da, Colombia

ARTICLE INFO

Keywords:
Biochar stability
Biochar potentiality
Tire
PVC
Construction wood
Swine manure
Poultry litter

ABSTRACT

Pyrolysis of waste materials aiming to produce biochar has been considered as an effective strategy to add value and to recycle such materials. The properties of the produced biochars depends on pyrolysis temperature and feedstock type, for example. Some waste materials have been still poorly studied. The objective of this study was to evaluate the changes in physicochemical characteristics, mineral composition, X-ray diffraction (XRD), Fourier transform infrared spectroscopy (FTIR) of biochars derived from agricultural and industrial wastes produced by different pyrolysis temperatures and feedstocks. Two agricultural solid wastes (poultry litter - PL and swine manure - SM) and three industrial wastes (construction wood - CW, tire - TR and PVC plastic - PVC) were pyrolyzed at five temperatures (300, 400, 500, 600 and 700 °C) in an oxygen-limited environment at a heating rate of 10 °C min^{-1} for one hour. Increased pyrolysis temperature reduced the yield of solids and volatile compounds and increased pH in water and $K_{soluble}$ in all studied biochars. Nevertheless, the temperature caused no significant changes in electrical conductivity, water-soluble nutrients and total elements, and CEC, in the industrial wastes (CW, TR and PVC). The XRD patterns revealed similarities in mineral formation among the studied biochars, including quartz, sylvite, calcite and dolomite. Data of FTIR spectra evidenced the presence of aromatic and aliphatic functional groups. The results obtained enable the design of biochars for a desired purpose, which might be solutions for agronomic and environmental issues, taking into account the effects of pyrolysis temperature and the type of waste to be processed.

1. Introduction

In Brazil, agricultural and industrial activities produce large amounts of wastes. The reuse and correct disposal of these wastes can represent serious environmental concerns. Thus, their efficient recovery is extremely important for global sustainability, higher profitability of the agricultural and industrial sector and promotion of the concept of circular economy. For example, Brazil is the second largest producer of poultry meat in the world, and the amount of poultry litter generated annually is estimated to be 8–10 million tons [1]. In 2016, the number of tires discarded in Brazil was close to 500,000 tons [2]. This fact is worrisome, because this number tends to increase exponentially [3]. Globally, the market of polyvinyl chloride (PVC) is expected to reach an installed capacity of about 60 million tons by 2020, with almost 75 % of its production intended for applications in construction products such as plastic pipes and electrical and hydraulic accessories [4]. According to these authors, PVC wastes are 100 % recyclable; however, in the case of waste generated in urban areas, recycling represents only 15–20%, and the largest volume is discarded in public landfills or disposed of directly into the environment.

Pyrolysis is a thermal decomposition process often performed at temperatures between 300 and 800 °C in either total or partial absence of oxygen. It is a process that is now considered one of the alternatives in the use of agricultural or industrial waste due to the thermal conversion into biochar (solid), bio-oil (liquid fuel) and fuel gas (CO, CO_2, H_2, CH_4 and other hydrocarbons) [5]. Biochar can be used in power generation, as soil conditioner and in the decontamination of environments [6].

The agronomic and environmental potential of biochar application in the soil is broad, including the improvement of physical, chemical and biological characteristics [7]. Its resistance or stability to degradation for hundreds to thousands of years [5] favors C sequestration

* Corresponding author.
E-mail addresses: filhoze04@hotmail.com, jose.lustosa@ufv.br (J.F. Lustosa Filho).

https://doi.org/10.1016/j.jaap.2020.104839
Received 3 March 2020; Received in revised form 21 April 2020; Accepted 1 May 2020
Available online 06 May 2020

and reduces its emissions to the atmosphere [8]. These potentialities are influenced by the nature and physical state of the material, pyrolysis temperature, oxygen content and residence time [9], conditioning the physical and chemical characteristics of biochar from different feedstocks [10].

Biochar properties can be significantly influenced when different types of feedstock and/or pyrolysis conditions, especially temperature, are used for the production [8,11–14]. The biochar derived from relatively high pyrolysis temperature is more depleted of H and O but possesses a larger proportion of aromatic C [15]. Consequently, it presents greater chemical recalcitrance and resistance to microbial and chemical decomposition in the soil [16]. In addition, increasing pyrolysis temperature generally increases the biochar pH, by producing more alkaline components, the electrical conductivity, the ash contents, the exchangeable and soluble cations [17,18]. Biochars are characterized by porous structures with a high surface area, which increase the adsorption capacity for the retention of moisture and nutrients in the soil [16,19]. On the other hand, the biochar yields, acidic functional groups concentration, volatile matter content and cation exchange capacity decrease with the increase of the temperature [20,21]. The biochar feedstock type, or the original material that the biochar is derived from is known also to affect the total organic carbon, fixed carbon and mineral elements of the biochar [22]. Although there are many recent studies with biochar from different sources, origins and purposes of use [5], very little has been studied about the pyrolytic conversion of industrial wastes compared to animal wastes aiming to evaluate its potential for agronomic and environmental use. Therefore, a detailed characterization study of these materials aiming to evaluate their potential or limitation is needed. This study aimed to evaluate the effects of pyrolysis temperature on the physical and chemical characteristics of biochars produced from animal and industrial wastes by slow pyrolysis. Moreover, we aimed to compare the industrial wastes derived biochars with animal wastes derived biochars in order to evaluate their potential applications.

2. Material and methods

2.1. Selection of wastes

The materials used for biochar production were selected by consulting state inventories of agricultural and industrial solid wastes, recompiled in the 2012 National Solid Waste Plan and in the 2015 Solid Waste Panorama Report [23,24]. Two agricultural wastes (poultry litter and swine manure) and three industrial solid wastes (wood generated in the construction sector, tire and PVC plastic) were selected considering the greatest potential for causing negative impacts on the environment, according to the criteria of generated quantity and final disposal. Besides that, our aim was to select feedstocks with contrasting physical and chemical attributes. In addition, these feedstocks were chosen because of the great availability of these materials in many regions of Brazil and worldwide. Agricultural residues are rich in nutrients and can be used as organic fertilizers. However, if applied *in natura*, they can act as vectors of animal diseases and might become a source of pollution. Therefore, they must first go through a composting process or some other process capable of eliminating undesirable effects. Industrial wastes are generated in large quantities and most of it are discarded in public land fills or disposed directly into the environment, which might lead to water and soil contamination due to the presence of toxic elements and pathogens [25].

The civil construction wood wastes were collected from a field located in the Federal University of Viçosa (UFV), whereas the PVC and tire residues wastes were acquired from recycling companies. The poultry litter and swine manure were collected in animal rearing facilities on the Campus of the Federal University of Viçosa. The poultry litter samples were composed of wood shavings and had been kept on a poultry production farm for 18 months, while swine manure was collected in the animal gestation sector and air-dried. The physicochemical properties of the feedstocks are presented in Table S1.

2.2. Production and characterization of biochars

The wastes, thereafter named feedstocks, were ground for separation on a 4-mm-mesh sieve and dried at 65 °C for 48 h. The mixtures were placed in hermetically sealed stainless steel cylinders (10.6 cm in diameter and 42 cm in height) and placed in an electric muffle furnace with technical specifications of 10 °C min^{-1} heating rate, which was adapted with a condenser through an iron tube to allow the release of gases during pyrolysis and bio-oil collection. An air-free environment was achieved inside the cylinders during pyrolysis, as their lid and the furnace door were airtight, and the continuous emission of pyrolysis volatiles prevented air from diffusing in through the hole in the lid. A schematic figure of the pyrolysis system can be found in Lustosa Filho et al. [26]. Pyrolysis was carried out at temperatures of 300, 400, 500, 600 and 700 °C, at heating rate of 10 °C min^{-1}, until reaching the final pre-defined temperature with one hour of holding time, after which the muffle was switched off and allowed to slowly cool down to room temperature [27]. The heating rate of 10 °C min^{-1} was chosen because it is the most common one used in slow pyrolysis in biochar studies [12–14,28].

The produced biochars were termed as PL (biochar from poultry litter), SM (biochar from swine manure), CW (biochar from construction wood), TR (biochar from tire) and PVC (biochar from PVC), followed by the corresponding pyrolysis temperature (e.g. PL300, abbreviation for biochar produced from poultry litter pyrolyzed at 300 °C).

The physical analyses of the biochars were performed using 100 g of each biochar in triplicates to determine (i) the percentage of biochar residues (YS) by difference between weights, according to ASTM Standard D3172 -13 [29]; (ii) mean weight diameter of particles (MWD) determined from the distribution of particles according to the International Biochar Initiative [30]; and (iii) water holding capacity (WHC) for substrates determined in a pressure chamber at 33 kPa for 72 h [31].

For chemical analyses, biochar samples were ground and passed through a 60-mesh sieve (0.25 mm), dried in an oven at 65 ± 2 °C for 48 h to remove moisture and standardize its content to < 10 % [32], determining the following attributes: (i) proportions of volatile compounds (Vol) [33], modified by Enders et al. [34]; (ii) proportions of ash (Ash) [33]; (iii) content of fixed C (Cfx) and yield of fixed C (Y_{Cfx}) [29]; (iv) elemental composition in elemental analyzer, determining C, H, N and O [35]; (v) electrical conductivity (EC) and pH in water by potentiometry in 1:20 solution, after rest of 12 h and stirring of suspension [36]; (vi) neutralizing power (NP) determined by the acid/base titrimetric method [37]; (vii) cation exchange capacity (CEC) determined by the method of saturation with NH_4OAC (1.0 mol L^{-1}) and Phenate method using colorimetry [38]; (viii) contents of elements dissolved in water (Ca, K, P, Mg, S, Na, Fe, Mn and Zn) [39] and total (Ca, K, P, Mg, S, Na, Fe, Mn, Zn, Mo, B, Ba, Al, Cu, As, Pb, Se, Cd, Co, Cr) [40], with K determined by flame photometry, Ca by atomic absorption spectroscopy and the other elements by inductively coupled plasma atomic emission spectroscopy (ICP-AES); (ix) identification of minerals of the crystalline phases by X-ray powder diffractometry (XRD), using a PAN analytical device, X` Pert Powder model, with cobalt tube, nickel filter in the range from 4 to 50°2θ, scanning speed of 10°2θ and interpretation according to Chen [41]. and (x) identification of functional groups by molecular absorption spectrophotometry in the infrared region with Fourier transform (FTIR) (Jasco FTIR 4100), using spectra obtained with 60 scans, with wavenumber from 4000 to 400 cm^{-1} and resolution of 4 cm^{-1}, in KBr tablets and interpretation according to Barbosa [42].

The results of the analyses of the physical and chemical characteristics of the produced biochars were evaluated according to a

completely randomized design with split plots, adopting three replicates. The temperatures were considered the main plot and the different biochars were evaluated in the subplots. Analysis of variance (ANOVA) was performed using linear regression to evaluate the effects of pyrolysis temperature on the different attributes of the biochars, choosing the best models based on the best fit and significance ($p < 0.05$) of R^2 and coefficients. The means of the biochars produced from the various wastes were compared by the Tukey test ($p < 0.05$). All analyses were performed using the software package SPSS 22 [43].

3. Results and discussion

3.1. Temperature and composition of biochars

In general, the values and behaviors found for the studied biochars can be considered comparable to those observed by other authors, despite the methodological differences in biochar production and evaluation [8,14,22,28,34,38,44–51]. The analysis of variance of the results identified that the main effects and the interaction between biochars and temperature were significant ($P < 0.01$ or $P < 0.05$) for the vast majority of the analyzed variables (Table S1). There were exceptions, and significance of the main effects was found for $K_{soluble}$, Mg_{Total}, P_{Total}, Mo_{Total}, Zn_{Total}, Mn_{Total}, Al_{Total}, Cu_{Total}, As_{Total}, Pb_{Total} and Cd_{Total} (biochars), $Mn_{soluble}$ (temperature), and S_{total} and Fe_{total} (biochars and temperature). Absence of significance ($P > 0.05$ or $P > 0.01$, F test) was only observed for Se_{Total} (Table S6). Nevertheless, the interaction was decomposed to identify possible differences (Table S5 and S6).

The results show that the increase in pyrolysis temperature caused several effects on the attributes of the produced biochars. Reductions of yield of solids, proportions of volatile compounds and increases in pH in water and $K_{soluble}$ were observed. The other attributes (mean weight diameter of particles, water holding capacity, proportions of ash, content of fixed C, yield of fixed C, neutralizing power, soluble and total elements) were dependent on the type of raw material, with predominance of quadratic models in their responses (Table S2 and S3). There were also cases, such as for the attributes electrical conductivity, cation exchange capacity and water-soluble nutrients (P, Mg, S, Na, Fe, Mn and Zn) and total elements (Ca, P, Mg, Fe, Mn, Zn, Mo, Ba, Al, Cu, Pb and Cr), in which the temperature did not alter their behavior, especially industrial wastes (construction wood, tire and PVC plastic) (Table S2 and S3). Increments followed by reduction and vice versa, such as in the neutralizing power, cation exchange capacity and $Ca_{soluble}$, for instance, reduction ($P_{soluble}$) or increase (e.g. water holding capacity) in the attributes with temperature were also observed (Table S2 and S3).

In the comparisons among biochars at each studied temperature, there was also no behavior common to all conditions, such as higher values of attributes in biochars from agricultural or even industrial wastes, or higher values at lower temperatures and lower values at higher temperatures or vice versa (Table 1 and 2). Overall, the absolute values of some attributes were similar, although there were significant differences ($P < 0.05$). Some attributes stood out due to their values and the large differences among biochars; for example, the electrical conductivity was much higher in biochars from PVC residues ($P < 0.05$) (Table 1).

However, it is evident that the biochars reflect the composition of the used wastes, since positive and high correlation coefficients ($P < 0.01$ or $P < 0.05$) were identified for the vast majority of the evaluated attributes in the wastes and the same ones measured in the biochars for each studied temperature (Table S7).

Although positive, some attributes presented low and non-significant coefficients ($P > 0.05$). Contents of water-soluble elements (Ca, Zn, Fe and Mn), electrical conductivity and cation exchange capacity are examples of negative coefficients common to all studied temperatures, in which some is significant, such as the water holding capacity (600 °C) (Table S7).

The results are consequences of physical and chemical processes inherent to the experimental conditions: reduction of mass and its volatilization by the action of temperature [14,52], expressed by the increase in proportions of ash, content of fixed C and the reduction of proportions of volatile compounds and yield of solids, which is highly associated with the oxidation of organic compounds, predominantly formed by primary macro-elements (C, H, N and O). The behavior of the chemical elements, whether evaluated individually in soluble form or based on attributes that express their set as a whole (pH in water, neutralizing power or electrical conductivity) are altered with the increase in temperature. The studied pyrolysis temperatures are higher than the boiling points of phosphorus and sulfur, for example, which are 280.5 °C and 444.6 °C, respectively [53]. In some cases, there were increases and reductions in their contents, which depend on the type of waste (Table 2).

In this context, the attributes cation exchange capacity and water holding capacity, together with the mean weight diameter of particles and particle distribution deserve to be highlighted among the obtained results because the incorporation of biochars might have repercussions on various ecological-environmental processes [34,38]. It was found that the cation exchange capacity was not affected by temperature for almost all types of biochars ($\hat{Y} = \overline{Y}$), but with differences between the averages of each of them when compared at each temperature, reflecting differences between wastes of agricultural origin (poultry litter and swine manure) and industrial origin (construction wood, tire and PVC plastic) or even between those of natural origin (poultry litter, swine manure and construction wood) or synthetic origin (tire and PVC plastic). The cation exchange capacity is associated with functional groups that compose the portion of carbonaceous materials transformed after pyrolysis [54]. The increase in pyrolysis temperature is responsible for removing volatile materials that compose the acid functional groups that are present in the structure of the materials [55]. The cation exchange capacity might change with the oxidation of biochars when exposed to the environment, increasing its value as the functional groups increase [56], which was not observed in the present study.

As for the water holding capacity, which is highly dependent on cation exchange capacity [38], there was an increase in some biochars, precisely in those of industrial/synthetic origin (PVC plastic and tire) with great polluting potential. These same biochars also showed the highest values of water holding capacity for temperatures higher than 500 °C. The values are considered high, which are typical of clay loam, loamy and clayey soils and correspond to 21, 30 and 38 %, respectively [38]. The incorporation of these biochars into the soil could increase its water holding capacity, which can be quite interesting depending on the condition of use and provided that they have no other negative characteristics.

Changes in biochar particle size are not always associated with thermal transformations of the wastes used for their production. It was observed that biochars produced from construction wood and PVC plastic had the highest values of mean weight diameter of particles at all pyrolysis temperatures, while the lowest values occurred for the biochars produced from poultry litter (300 and 700 °C), swine manure (400 and 500 °C) and tire (600 °C) (Table 1). These results are confirmed by the particle-size distribution data, and those biochars produced from construction wood and PVC plastic also showed the highest proportions of particles (> 4.00 mm). These biochars have low vulnerability to breakage, whereas biochars produced from poultry litter, swine manure and tire were characterized by moderate stability to breakage. These results are evident according to the mean weight diameter of particles data and the distribution of particles between 2.12 and 4.99 mm, which is a range that represents moderate to high stability (Fig. 1).

The observed differences might be associated with the contraction and expansion promoted by temperature variations, which weaken the

Table 1
Means of physical and chemical attributes of biochars produced from the agricultural wastes poultry litter (PL) and swine manure (SM) and from the industrial wastes construction wood (CW), tire (TR) and PVC plastic (PVC), subjected to pyrolysis temperatures of 300, 400, 500, 600 and 700 °C.

Temperature °C	Biochar	YS %	MWD mm	WHC kg kg^{-1}	Vol %	Ash %	Cfx %	Y_{Cfx} %	EC dSm^{-1}	pH in water	NP %
	PL	69.1e	2.58d	0.52ab	50.7b	19.0c	27.5c	19.0c	2.60b	8.13a	11.6b
	SM	76.8d	3.36c	0.61a	39.8c	36.8a	19.3d	14.8d	1.41c	7.17c	54.6a
300	CW	80.0c	4.81a	0.35bc	44.3c	2.57e	50.9a	40.6a	0.08d	7.54b	6.93b
	TR	95.6a	4.14b	0.05 d	57.2a	13.1d	28.3c	27.1b	0.08d	6.95d	59.5a
	PVC	83.5b	4.65a	0.24cd	27.9d	32.5b	33.5b	24.6b	13.0a	6.31e	41.9a
	PL	52.2c	2.83c	0.51ab	44.1a	26.5c	25.4c	13.3d	0.76b	9.99a	25.4c
	SM	51.3c	2.12e	0.66a	27.9c	45.5a	21.2c	10.9e	0.46b	8.95b	69.8a
400	CW	42.3d	4.91a	0.36bc	42.5a	3.71e	49.2b	20.8b	0.07b	9.63a	10.9d
	TR	83.3a	2.61d	0.19c	31.3c	6.99d	59.9a	49.8a	0.06b	7.89c	43.7b
	PVC	79.4b	4.71b	0.29bc	35.9b	38.0b	23.1c	18.3c	16.4a	7.36d	32.7bc
	PL	47.1b	3.33c	0.48c	19.0b	26.9c	49.4c	23.3b	2.21b	10.7a	23.8d
	SM	40.9c	2.16d	0.61b	17.2c	57.8a	22.1e	9.02c	0.83b	10.6a	68.6a
500	CW	30.9d	5.92a	0.39d	22.2a	3.69e	70.1b	21.7b	0.07b	8.75c	12.0e
	TR	46.9b	2.29d	0.81a	3.96d	10.3d	84.0a	39.4a	0.25b	8.94c	48.2b
	PVC	65.4a	4.55b	0.84a	18.6b	42.3b	34.5d	22.5b	97.0a	9.60b	41.2c
	PL	45.2b	2.91c	0.45c	9.82bc	27.8c	57.5b	26.0b	10.9b	10.6ab	24.8d
	SM	38.9c	2.86c	0.60b	11.2ab	42.8b	43.0c	16.7d	0.84b	9.59ab	71.7a
600	CW	24.0d	5.56a	0.47c	11.8ab	4.22e	78.2a	18.7cd	0.09b	9.51ab	5.98e
	TR	37.6c	2.74d	0.84a	7.93c	12.0d	77.6a	29.1a	0.44b	8.55b	49.7b
	PVC	56.6a	4.65b	0.80a	12.6a	49.5a	37.5d	21.2c	146a	11.8a	38.6c
	PL	44.1b	1.63d	0.44c	8.78bc	30.9c	54.1c	23.8b	2.63b	10.5c	21.7c
	SM	39.7c	3.22c	0.57bc	8.71bc	63.9a	23.5e	9.40d	0.96b	11.3b	77.0a
700	CW	21.3d	6.48a	0.54bc	10.7ab	3.80e	77.2b	16.4c	0.10b	10.3d	21.4c
	TR	35.9c	3.06c	0.79ab	3.45c	10.9d	83.5a	29.9a	0.25b	10.2d	56.9b
	PVC	49.1a	4.99b	0.99a	14.3a	51.2b	34.0d	16.7c	165a	11.5a	30.3c

Temperature °C	CEC	Water-soluble elements								
		Ca	K	P	Mg	S	Na	Fe	Mn	Zn
	cmol$_c$ kg^{-1}	g kg^{-1}								
	38.5a	1.64ab	33.4a	5.15a	1.88a	2.42a	5.05a	0.21a	6E-3a	1.5E-3b
	32.2a	0.50b	15.3ab	3.98b	1.94a	1.21b	3.14b	0.03ab	5E-3a	0.03b
300	19.0b	2.23a	0.48b	0.22c	0.09b	0.26bc	0.21c	3E-3b	4E-3a	5E-4b
	5.53c	0.63b	0.13b	8.5E-3c	0.04b	0.26bc	0.05c	2E-2b	5E-3a	0.37a
	8.18c	0.67b	0.08b	4.5E-3c	0.62b	0.09c	0.08c	5E-4b	3E-3a	0.31a
	22.9a	1.01a	36.2a	2.88a	1.11ab	2.03a	4.57a	0.01a	1.5E-3ab	5E-4a
	20.8a	2.37a	7.10a	1.08b	0.62ab	0.31b	1.49ab	7.5E-3ab	1E-3ab	3E-3a
400	9.81a	2.02a	0.53a	0.41b	0.19b	0.88ab	1.31ab	2.5E-3ab	2E-3ab	5E-4a
	9.69a	2.29a	0.10a	0.04b	0.04b	0.42b	0.26b	1.5E-3ab	0.00b	1E-3a
	13.5a	3.25a	0.09a	0.01b	1.77a	0.12b	0.07b	5E-4b	3.5E-3a	1.4E-2a
	14.6b	1.44b	39.2a	1.17a	0.25b	2.04a	2.90a	3E-3a	0.00a	0.00a
	67.2a	2.54a	17.7a	1.97a	0.51b	0.57b	1.29b	1.7E-2a	4E-3a	1E-3a
500	61.5a	2.64a	0.69a	0.22 b	0.01b	0.34ab	0.22b	1.5E-3a	0.00a	0.00a
	51.9ab	2.72a	0.49a	0.03b	0.10b	0.86b	0.61b	0.00a	0.00a	1E-3a
	50.8ab	3.61a	0.05a	0.01b	1.41a	0.10b	0.04b	0.00a	0.00a	0.00a
	15.5a	1.55b	47.2a	0.73b	0.33b	1.95a	3.54a	5E-4a	0.00a	0.00a
	47.8a	0.83b	9.60a	1.63a	0.50a	0.97ab	0.73b	4E-3a	0.00a	5E-4a
600	30.0a	2.55b	1.47b	0.01c	0.02c	0.55b	0.39b	1E-3a	0.00a	0.00a
	21.0a	3.96a	0.81b	0.01c	0.32b	1.85a	0.75b	0.00a	1.5E-3a	0.29a
	31.9a	4.09a	0.09b	0.01c	0.01c	0.06b	0.10b	0.00a	0.00a	5E-4a

(*continued on next page*)

Table 1 (*continued*)

Temperature °C	CEC	Water-soluble elements								
		Ca	K	P	Mg	S	Na	Fe	Mn	Zn
	$cmol_c\ kg^{-1}$	$g\ kg^{-1}$								
	13.2ab	2.26a	50.6a	0.36b	0.22b	1.93ab	2.98a	1E-3a	0.00a	0.00a
	20.6ab	1.06a	16.8b	0.86a	0.67a	2.60a	0.77b	1.5E-3a	0.00a	0.00a
700	39.5a	2.48a	1.79c	0.01b	0.01b	0.43c	0.38b	2E-3a	0.00a	0.00a
	10.9b	3.15a	0.58c	0.01b	0.17b	0.94bc	0.57b	0.00a	0.00a	0.00a
	25.1ab	2.37a	0.29c	0.01b	0.01b	0.07c	0.18b	0.00a	0.00a	0.00a

YS: yield of solids; MWD: mean weight diameter; WHC: water holding capacity; Vol: proportions of volatile compounds; Ash: proportion of ashes; Cfx: content of fixed carbon; Y_{Cfx}: yield of fixed carbon; EC: electrical conductivity; NP: neutralizing power; CEC: cation exchange capacity. Different letters indicate significant differences between wastes at the same temperature ($p < 0.05$) by Tukey test.

structure of the material [57], producing biochars more vulnerable to breakage, increasing the proportion of smaller particles. In addition, the friction between particles also contributes to changes in particle-size distribution, which varies with the raw material [5]. Biochars produced from poultry litter, swine manure and tire, which had the highest proportions of smaller particles (Fig. 1), might have greater potential for use in soil as conditioner, since they facilitate reactions or interactions with the medium [55,58].

The thermal transformations of the materials begin in temperature ranges between 120 and 300 °C, characterized by dehydration and beginning of degradation and formation of free radicals originated from the thermal action on the air oxygen and molecules [5,59]. Less reactive volatile compounds or tar are released within the range from 300 to 600 °C and, in the last range, above 600 °C, the production of gases is higher because the rates of mass and heat transfer are higher, which are the most representative kinetic ranges of the pyrolysis process. It is in this last temperature range that several elements are lost, such as N, H and O, but with the concentration of C, making the produced biochar to be more stable or recalcitrant [22].

3.2. Thermal transformations of biochars

Elemental composition (Table 3) enables identifying thermal transformations through the elemental ratios H:C and O:C, using the Van Krevelen diagram (Fig. 2) developed to represent the degree of carbonization of the pyrolyzed material. Oxigen:Carbon ratios have been used to measure the degree of aging of biochars, while H:C ratios are used to measure their aromaticity [5]. When the H:C ratio is low, the presence of compounds with aromatic structure is greater and, therefore, there is higher stability [13,47].

The H:C and O:C molecular ratios of the biochars indicate that the thermal transformation of the materials make them more carbonaceous as pyrolysis temperature increases (Fig. 2). Carbon contents increase and there is loss of part of some elements, such as H and O, especially at temperatures from 600 and 700 °C (Table 3), which clearly demonstrates the appearance of more resistant structures [34], except for biochars made from PVC. As for PVC, at temperatures below 450 °C, the majority of weight loss is due to the dehydrochlorination, while at higher temperatures (> 500 °C) the hydrocarbon release plays an important role causing a significant decrease in the C content [60]

The molecular ratio of H:C decreased faster than that of O:C with increasing temperatures, indicating that H is more easily lost at lower pyrolysis temperatures than O. The H:C ratios of all biochars produced (over 300 °C) were lower than 0.15, which can be considered low, except for biochars made from PVC (ranged from 0.15 − 0.28), indicating high stability or recalcitrance. Specifically because of the aromatic characteristics of their composition, these biochars present potential use for C sequestration in soil [61].

The dotted line (Fig. 2) indicates that the increase in pyrolysis temperature causes the molecular ratios to decrease and the degree of aromaticity to increase [62]. This behavior might be associated with a positive relationship between the molecular ratios H:C and O:C ($R^2 = 0.54$). The line parallel to the O:C axis indicates that H:C ratio values ≤ 0.10 belong to biochars with graphite structures [5,62], which ensures greater stability (Fig. 2).

3.3. Structural transformations

The thermal transformations of the wastes can also be characterized by XRD, enabling the detection of crystalline mineral phases in the different biochars [5] (Fig. 3). The diffractograms revealed peaks of crystallinity at different positions, highlighting the mineralogical similarities between biochars. Quartz, sylvite, calcite and dolomite were detected, as also observed by Gai et al. [45], Lustosa Filho et al. [26], Gupta et al. [63] and Pariyar et al. [13]. However, differences were observed between the evaluated pyrolysis temperatures.

Table 2
Means of total contents of elements in biochars produced from the agricultural wastes poultry litter (PL) and swine manure (SM) and from the industrial wastes construction wood (CW), tire (TR) and PVC plastic (PVC), subjected to pyrolysis temperatures of 300, 400, 500, 600 and 700 °C.

Temperature °C	Waste	Ca	K	P	Mg	S	Na	Fe	Mn	Zn
		g kg^{-1}						mg kg^{-1}		
300	PL	42.4a	21.2a	28.5b	4.83b	2.29a	3.35a	970bc	90.0a	110b
	SM	11.6c	9.77b	83.0a	7.24a	2.00a	1.85a	1310b	40.0ab	840b
	CW	39.9a	0.73c	1.43b	0.10c	0.48c	0.42a	260c	80.0a	10.0b
	TR	13.7c	0.20c	1.50b	1.31c	0.97bc	0.07a	4720a	90.0a	4140a
	PVC	29.6b	0.04c	0.12b	6.07ab	1.09b	0.04a	180c	10.0b	1960ab
400	PL	30.9c	30.1a	37.0b	5.50a	3.01a	4.36a	1420ab	120a	200b
	SM	13.1d	12.8b	95.3a	7.85a	2.51ab	2.25a	1840a	150a	1060ab
	CW	79.1a	0.82c	1.04b	0.12b	0.51c	0.39a	380b	110a	20.0b
	TR	14.9d	0.28c	1.62b	0.09b	1.73abc	0.06a	260b	6.30a	5130a
	PVC	53.6b	0.03c	0.11b	6.51a	1.30bc	0.03a	410b	13.0a	2010ab
500	PL	82.3b	34.2a	38.2b	6.03a	3.04a	4.77a	1390ab	160a	220b
	SM	9.20e	14.9b	109a	7.95a	2.85a	2.28a	1740a	150a	1210b
	CW	89.1a	1.00c	1.13b	0.10b	0.89a	0.49a	590ab	110a	50.0b
	TR	23.3d	0.41c	1.91b	0.13b	2.74a	0.07a	500ab	10.0a	6020a
	PVC	34.3c	0.05c	0.00b	7.21a	1.70a	0.03a	220b	10.0a	2300ab
600	PL	79.4b	36.9a	44.9a	6.56a	3.90a	7.12a	1350a	130a	260b
	SM	15.1c	17.3b	121b	9.24a	3.83a	3.73a	1760a	50.0a	1230ab
	CW	134a	1.14c	1.25b	0.23b	1.09a	0.58a	490b	120a	20.0b
	TR	29.4c	0.44c	2.27b	0.16b	3.70a	0.09a	400b	10.0a	6310a
	PVC	74.5b	0.05c	0.00b	8.62a	2.15a	0.06a	340b	10.0a	2540ab
700	PL	19.8bc	35.6a	37.5b	5.78a	4.08ab	5.26a	1180b	100a	130b
	SM	28.1ab	17.6b	127a	9.81a	5.27a	3.52a	1720a	40.0b	1180b
	CW	31.4a	1.05c	1.14b	0.10b	1.28b	0.45a	430c	120a	20.0ab
	TR	16.8c	0.75c	2.15b	0.23b	6.41ab	0.09a	550c	10.0b	6170a
	PVC	5.49d	0.05c	0.00b	7.37a	1.98ab	0.03a	340c	10.0b	2130ab

Temperature °C	Mo	B	Ba	Al	Cu	As	Pb	Se	Cd	Co	Cr
	mg kg^{-1}										
300	2.50a	25.0a	30.0ab	480c	50.0b	0.68ab	0.00b	1.80a	0.49a	1.60bc	22.0b
	0.47a	5.90b	70.0a	530c	100b	0.38ab	0.00b	1.60a	0.57a	5.90ab	16.0b
	0.30a	5.20b	40.0ab	270c	30.0b	1.70a	0.00b	2.70a	0.41a	6.30c	9.80b
	6.10a	3.50b	30.0b	2210b	40.0b	0.11b	3.40b	1.20a	1.60a	9.30a	270a
	3.30a	4.80b	60.0ab	4050a	1360a	0.00b	930a	1.90a	2.10a	0.85c	12.0b
400	3.40a	34.0a	42.0ab	590b	90.0b	0.55ab	0.00b	1.50a	0.54b	1.90bc	21.0ab
	0.72a	9.80b	88.0a	640b	120b	0.01ab	0.00b	1.70a	0.74ab	6.90a	13.0b
	0.37a	3.60b	43.0ab	350b	20.0b	1.10a	0.00b	2.10a	0.36b	0.76c	39.0a
	0.52a	3.50b	5.00b	270b	50.0b	0.95ab	5.20b	2.40a	0.54b	5.50ab	7.80b
	0.35a	6.40b	69.0a	4280b	1360a	0.00b	960a	2.30a	0.27b	1.20c	36.0a
500	3.90a	39.0b	48.0ab	740b	97.0b	0.21a	0.00b	2.20a	0.63b	2.10b	28.0a
	0.58a	7.60b	99.0a	740b	140b	0.55a	0.00b	1.70a	0.69b	7.80a	9.30ab
	0.41a	6.00b	600ab	400b	36.0b	1.50a	0.00b	2.40a	0.40b	0.68b	9.80ab
	0.43a	4.00b	7.70b	370b	130b	0.53a	5.70b	2.30a	0.74ab	6.90a	3.80b
	0.32a	10.0a	79.0a	5100a	1500a	0.00a	1100a	2.00a	2.90a	0.94b	16.0ab

(*continued on next page*)

Table 2 (*continued*)

Temperature °C	Mo	B	Ba	Al	Cu	As	Pb	Se	Cd	Co	Cr
	mg kg^{-1}							mg			
	4.10a	44.0a	42.0bc	870b	100b	0.31a	0.00b	2.70a	0.58a	2.30b	25.0b
	0.60a	9.80bc	120a	840b	130b	0.26a	0.00b	2.20a	0.71a	8.80a	12.0bc
600	0.42a	6.40bc	69.0abc	390b	41.0b	0.60a	0.00b	2.80a	0.39a	6.60b	13.0bc
	0.45a	5.30c	9.60c	480b	18.0b	0.90a	1.10b	3.10a	0.79a	7.20a	5.90c
	0.27a	23.0b	100ab	6900a	1900a	0.00a	1400a	2.70a	0.59a	1.30b	44.0a
	3.90a	30.0a	41.0ab	710b	70.0b	0.21a	0.00b	1.90a	0.47a	2.10b	16.0ab
	0.59b	12.0ab	120a	910b	160b	0.20a	0.00b	1.50a	0.71a	9.10a	5.40b
700	0.47b	4.10b	67.0ab	380b	36.0b	1.00a	0.00b	2.40a	0.40a	7.70b	28.0ab
	0.28b	3.40b	12.0b	520b	36.0b	0.56a	12.0b	1.80a	0.75a	7.60a	3.00b
	0.25b	12.0ab	80.0ab	5300a	1700a	0.00a	1100a	3.20a	0.37a	1.10b	41.0a

Different letters indicate significant differences between wastes at the same temperature ($p < 0.05$) by Tukey test.

For poultry litter, it was possible to identify the presence of quartz (SiO2) (4.26 and 2.01 Å), sylvite (KCl) (3.15 and 2.22 Å) and K-feldspar ($KAlSi_3O_8$) (4.17; 3.74 and 3.34 Å) (Fig. 3a). As the pyrolysis temperature increased, there were increases or decreases in some peaks, indicating thermal transformation in the pyrolysis process [45]. In poultry litter biochars produced between 300 and 700 °C, the peak at 4.26 Å, present in non-pyrolyzed wastes, was not observed, which suggests the formation of graphite, confirmed by the peak 1.80 Å. On the other hand, the content of sylvite (3.15 Å) increases in the biochars from 300 up to 700 °C, also confirmed by the peak at 2.22 Å [64]. The increase in the size of the peaks at 3.15 and 2.22 Å with the increase in pyrolysis temperature also suggests that sylvite contents increased with the increase in pyrolysis temperature, which is consistent with the high contents of K_{total} (Table 2), besides the appearance of confirmatory peaks (2.88 and 2.57 Å) of nephelite ((Na, K)$AlSiO_4$) (Fig. 3a).

The increase in pyrolysis temperature promoted the appearance of peaks of identification of new substances in the swine manure biochar, differing from those observed in the raw material (Fig. 3b), especially at the highest temperatures (500–700 °C). The presences of quartz (4.26 and 3.34 Å), K-feldspar (4.17 and 3.34 Å), sylvite (KCl) (3.15 Å), dolomite ($CaMg(CO_3)_2$) (2.01 and 1.78 Å) and, lastly, calcite ($CaCO_3$) (3.04 and 3.86 Å) were identified in the biochar produced from swine manure. The peaks of sylvite (3.15 Å) are higher at the highest temperatures, such as 700 °C, which can be associated with higher concentrations of K_{total} (Table 2).

Compared to non-pyrolyzed wastes, the diffractograms of poultry litter (Fig. 3a) demonstrate that with the increase in pyrolysis temperature, there is greater formation of sylvite than in biochars made from swine manure, which can also be confirmed by the differences in soluble and total K contents in the biochars (Table 1 and 2). The peak of dolomite at 2.01 Å decreases with the increase in pyrolysis temperature until disappearing completely at 700 °C. As this peak disappears, new confirmatory peaks appear at temperatures of 600 and 700 °C (2.88 and 2.57 Å), which belong to nephelite ((Na, K) $AlSiO_4$). As for quartz and calcite, the increase in pyrolysis temperature leads to a reduction in the confirmatory peaks (4.26 and 3.86 Å, respectively), to the point of making them disappear (Fig. 3b).

The XRD pattern of the construction wood waste indicates the presence of calcite (3.86 and 3.04 Å) and dolomite (2.01 and 1.78 Å) (Fig. 3c). With the increase in pyrolysis temperature, it was observed that the height of the peak at 3.99 Å decreases, while the height of 3.04 Å increases, making it more compressed and less wide (confirmatory peaks of calcite). This behavior is in agreement with the highest contents of Ca_{total}, which increase with the increment in pyrolysis temperature (Table 2). The peak of dolomite at 2.02 Å remained constant as pyrolysis temperature increased, while the peak at 1.78 Å decreased, which might be related to the contents of Ca_{total} and Mg_{total} in the biochar. Magnesium presents constant contents with the increase in pyrolysis temperature, whereas Ca increases up to 600 °C and decreases at 700 °C (Table 2).

In biochars produced from tire, the high proportions of C found in both non-pyrolyzed wastes (Table S1) and biochars (Fig. 3d) were evident. According to the XRD patterns, this composition can be associated with graphite (3.36 and 2.03 Å), where the peak at 2.03 Å became increasingly longer with the increment in pyrolysis temperature (Fig. 3d). As for quartz (4.26, 3.34 and 2.46 Å), there was a reduction in peak intensity with temperature. The presence of anhydrite ($CaSO_4$) is confirmed in all spectra (2.85; 2.33 and 1.86 Å), where the increase in the peak at 1.86 Å is confirmed for temperatures higher than 300 °C and the peak 2.85 Å at 700 °C. It might have come from the dehydration of the gypsum ($CaSO_4.2H_2O$), identified in the non-pyrolyzed waste and at 300 °C by the peak at 2.87 Å (Fig. 3d). Pyrite (FeS_2) was observed from 400 °C with the peaks at 3.12 and 1.63 Å. In the case of these latter two minerals, the behavior might be related to increases in the total contents of Ca and S in temperatures higher than 300 °C (Table 2).

Biochars produced from PVC presented the highest reductions of peaks in the XRD spectra as pyrolysis temperature increased (Fig. 3e),

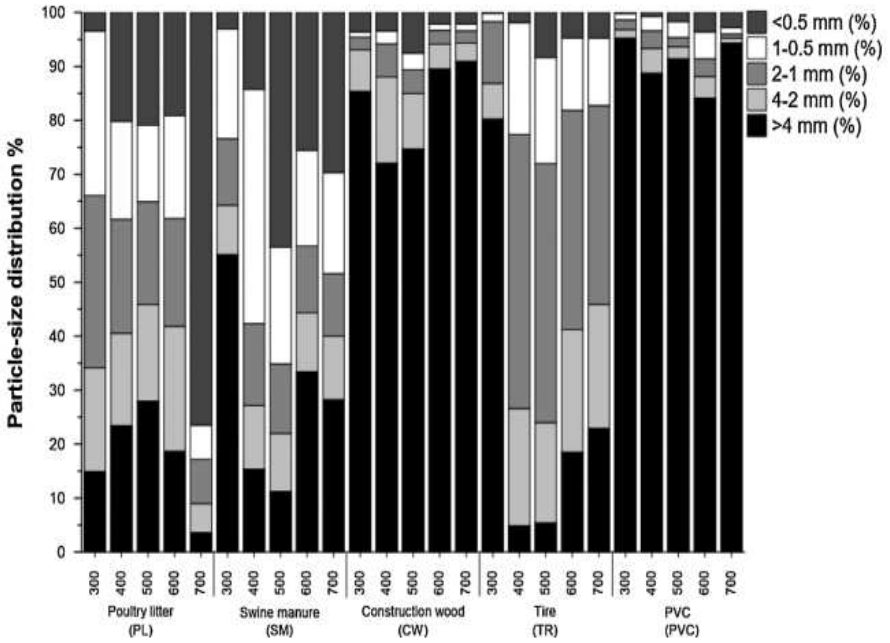

Fig. 1. Particle-size distribution of biochars produced from the agricultural wastes poultry litter (PL) and swine manure (SM) and from the industrial wastes construction wood (CW), tire (TR) and PVC (PVC), subjected to pyrolysis temperatures of 300, 400, 500, 600 and 700 °C.

even in comparison to the non-pyrolyzed material, indicating the reduction in the contents of biochar components with the increase of pyrolysis temperature [65]. Non-pyrolyzed PVC showed peaks of calcite (3.86; 2.10 and 2.29 Å), kainite ($MgSO_4KCl_3H_2O$) (3.02; 2.18 and 2.09 Å), gypsum ($CaSO_4.2H_2O$) (2.87 Å), quartz (2.46 Å) and graphite (2.03 and 1.80 Å). In the biochars produced from PVC, there was a reduction in the peaks of quartz, kainite and calcite, in addition to the appearance of anhydrite ($CaSO_4$) with the peak at 2.33 Å as pyrolysis temperature increased (Fig. 3e). The graphite peak at 2.03 Å became higher with the increment in pyrolysis temperature, results that agree with the behavior of the total elements in the PVC biochars at different temperatures (Table 2).

The evaluation of the occurrence and height of peaks and their association with minerals make it possible to confirm or not their presence, as well as their relative richness in comparison to the other evaluated situations. In the case of the present study, the occurrence can be determined and confirmed by the comparison between materials pyrolyzed at different temperatures and non-pyrolyzed materials [65].

In general, the presence of peaks in all XRD spectra indicated the occurrence of inorganic components in all samples [45]. It is possible to infer about the increase in the concentration of inorganic substances that constitute the different types of biochars due to increase in the length of these peaks with pyrolysis temperature. Higher peak height also indicates better crystallization of the identified substances [65]. The results indicate that the increase in the crystallinity of graphite minerals are recurrent in all evaluated biochars, which generates greater carbon stability [5].

Fourier-transform infrared spectrometry (FTIR) is an effective tool for studying the structure and properties of the compounds of raw materials and their biochars. The spectra of raw materials and biochars produced at different pyrolysis temperatures showed the most common peaks found in biochars, but with some exceptions (Fig. 4). The interpretations of the main peaks were based on the flowchart and tables for initial interpretation of the infrared spectra according to Barbosa. [42]. With the increase in pyrolysis temperature, significant changes in biochars were evident, which can be monitored with this non-destructive technique [66,67].

The spectral peak observed in the range from 3600 to 3200 cm^{-1} was attributed to the vibration of the O–H bond in the hydroxyl and carboxyl groups, expressed by a broad band that is characterized by the participation of intermolecular or intramolecular H bonds, as well as amides (1680 to 1630 cm^{-1}) and amines (1640 to 1550 cm^{-1}). The range between 3300 and 2800 cm^{-1} was attributed to the stretching band of C–H bond, representing the aliphatic group, typically methyl (CH_3) and methylene (CH_2). The groups with triple bonding such as alkynes (C≡C) and nitriles (C≡N) are found in ranges between 2250 and 2100 cm^{-1} and between 2260 and 2240 cm^{-1}, respectively.

The peaks for double bonds in aromatic chains are found in the ranges from 1650 to 1500 cm^{-1}. The angular deformations in the plane of the C–H bonds of the aromatic ring are in the angular range from 1290 to 1000 cm^{-1} and the hydrogen assemblies are outside the plane of the C–H bonds of the aromatic ring; they are in the wavelength range from 900 to 650 cm^{-1}. Finally, there are functional groups with double oxygen bond (C=O), confirmed by the presence of carboxyls (OH) from 650 to 1000 cm^{-1} [42,66,67].

The spectra of poultry litter and its respective biochars (Fig. 4a) showed that there were significant changes ($p < 0.05$) in the chemical and structural composition with increased pyrolysis temperature. The first change observed was the attenuation or disappearance of the band related to the presence of hydroxyls in the range of 3600 to 3200 cm^{-1} with the increase in pyrolysis temperature in non-pyrolyzed raw material and in the biochar produced at 300 °C. These results indicate that for temperature values higher than 300 °C, there is release of moisture and hydroxyl groups [8,67]. Likewise, there was an attenuation of the bands in the ranges from 3300 to 2800 cm^{-1} and from 1650 to 1500 cm^{-1}, corresponding to the methylene group (CH_2) and to the amide group (N–H), respectively. These compounds are of open and simpler chain, which makes hydrogen loss possible at temperatures higher than 400 °C. However, it was observed that the methylene group band decreased as pyrolysis temperature increased.

On the other hand, the stretching in wavenumbers from 2600 to 2100 cm^{-1}, corresponding to the alkyl (C≡C) and nitrile (C≡N) groups, is evident. The stretching of the alkyl group begins at pyrolysis temperature of 400 °C, while for nitrile it occurs at 600 °C [59]. These results are consistent with those obtained in the elemental composition (Table 3), which showed increases in the proportions of C and losses of H, N and O, but with sufficient contents, establishing the identified chemical structures.

Table 3
Elemental content of biochars produced from the agricultural wastes poultry litter (PL) and swine manure (SM) and from the industrial wastes construction wood (CW), tire (TR) and PVC plastic (PVC), subjected to pyrolysis temperatures of 300, 400, 500, 600 and 700 °C.

Temperature (ºC)	Biochar	C total	H total	N total	O total
		% (w:w)			
300	PL	47.2 ± 0.79	4.56 ± 0.22	3.82 ± 0.00	25.4 ± 0.47
	SM	38.3 ± 0.66	4.13 ± 0.83	3.16 ± 0.02	17.6 ± 0.08
	CW	70.6 ± 0.12	4.57 ± 0.21	0.27 ± 0.02	22.0 ± 0.13
	TR	75.1 ± 0.16	6.44 ± 0.69	0.42 ± 0.02	4.94 ± 0.82
	PVC	41.4 ± 0.35	6.97 ± 0.18	0.03 ± 0.00	19.1 ± 0.63
400	PL	49.0 ± 0.28	3.14 ± 0.32	3.21 ± 0.01	18.1 ± 0.41
	SM	33.8 ± 0.23	2.39 ± 0.23	2.23 ± 0.01	14.1 ± 0.22
	CW	75.1 ± 0.13	3.52 ± 0.28	0.10 ± 0.02	17.5 ± 0.07
	TR	74.1 ± 0.23	3.54 ± 0.40	0.07 ± 0.01	15.2 ± 0.09
	PVC	32.4 ± 0.29	4.72 ± 0.09	0.14 ± 0.04	24.7 ± 0.16
500	PL	54.1 ± 0.04	1.67 ± 0.42	2.78 ± 0.01	14.5 ± 0.08
	SM	32.6 ± 0.65	0.97 ± 0.07	1.70 ± 0.03	6.89 ± 0.32
	CW	70.6 ± 0.26	2.58 ± 0.14	0.04 ± 0.00	23.1 ± 0.07
	TR	61.4 ± 0.21	0.19 ± 0.02	0.30 ± 0.00	27.7 ± 0.12
	PVC	29.3 ± 0.24	5.68 ± 0.07	0.16 ± 0.00	18.6 ± 0.67
600	PL	48.0 ± 0.34	1.22 ± 0.06	2.02 ± 0.02	20.9 ± 0.35
	SM	39.4 ± 0.09	0.54 ± 0.04	1.49 ± 0.01	15.8 ± 1.39
	CW	93.6 ± 0.11	1.98 ± 0.02	0.00 ± 0.00	0.19 ± 0.04
	TR	66.6 ± 0.24	0.21 ± 0.06	0.09 ± 0.01	21.1 ± 0.03
	PVC	24.3 ± 0.45	4.86 ± 0.15	0.00 ± 0.00	21.3 ± 0.15
700	PL	55.8 ± 0.72	0.67 ± 0.00	1.67 ± 0.10	10.9 ± 0.15
	SM	36.4 ± 0.37	0.21 ± 0.09	0.90 ± 0.01	0.00 ± 0.00
	CW	78.4 ± 0.25	1.06 ± 0.09	0.34 ± 0.02	16.4 ± 0.07
	TR	71.9 ± 0.13	0.03 ± 0.00	0.00 ± 0.00	17.2 ± 1.02
	PVC	24.8 ± 0.01	6.97 ± 0.09	0.30 ± 0.01	16.7 ± 0.62

w:w: weight:weight determination. Values refer to the mean (n = 3) ± standard error of the mean.

The analysis of the spectra of swine manure biochars (Fig. 4b) indicated some characteristics in the FTIR spectrum similar to those of biochars produced from poultry litter (Fig. 4a). The OH and CH_2 groups of swine manure biochars decomposed more slowly than those of poultry litter biochars, evidenced by the differences in spectral intensity of the materials used for biochar production at pyrolysis temperature of 300 °C. Another similarity observed between both biochar groups was the increased intensity of the peaks of the functional groups alkyl (C≡C) and nitrile (C≡N). Spectral intensity was evident at pyrolysis temperatures from 600 to 700 °C and, in the case of C–H, there was a reduction in the spectral intensity of the waste for the biochar at 300 °C.

Peaks become more intense as temperatures increase, especially

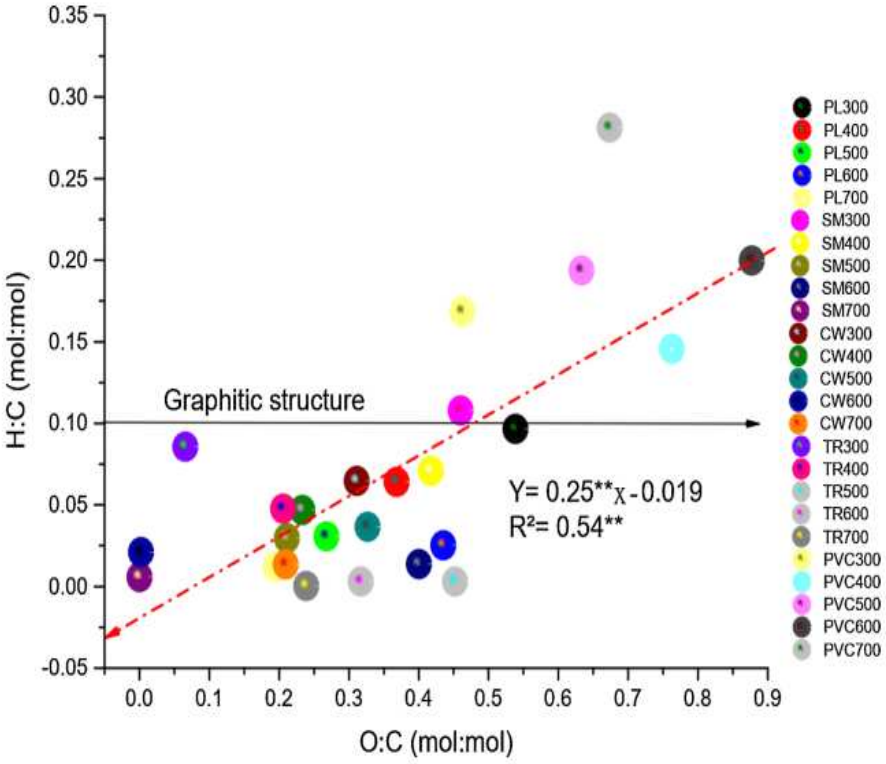

Fig. 2. H:C and O:C molecular ratios of biochars produced from the agricultural wastes poultry litter (PL) and swine manure (SM) and from the industrial wastes construction wood (CW), tire (TR) and PVC plastic (PVC), subjected to pyrolysis temperatures of 300, 400, 500, 600 and 700 °C. Abbreviations of different types of waste followed by subscripts indicating temperature values.

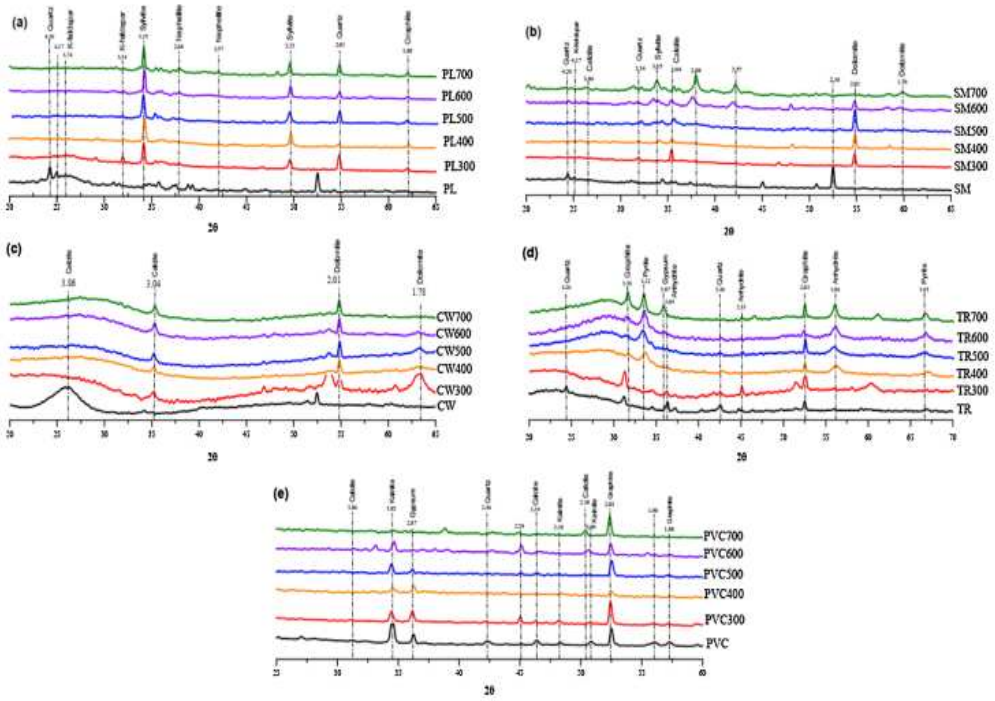

Fig. 3. X-ray diffractograms of wastes and biochars produced from the agricultural wastes (a) poultry litter (PL) and (b) swine manure (SM) and from the industrial wastes (c) construction wood, (d) tire (TR) and (e) PVC plastic (PVC) subjected to pyrolysis temperatures of 300, 400, 500, 600 and 700 °C.

between 400 and 700 °C. In different bands, in the range from 3300 to 2800 cm^{-1} attributable to the methyl group (CH_3), the reduction occurs from temperatures up to 300 °C. The range from 1850 to 1375 cm^{-1} presents the double bonds in aromatic chains (C═O; C═C and CH_2), which decreased with the increase in pyrolysis temperature, until the loss at temperature of 600 °C. The intensification of peaks in the ranges from 1000 to 530 cm^{-1}, corresponding to the alkyne (CH) and sulfone (SO_2) groups, respectively, was also observed with the increment in pyrolysis temperature, besides occurring in the non-pyrolyzed waste.

The spectra of construction wood biochars (Figure 5c) are very similar to those of biochars produced from poultry litter and swine manure (Fig. 4a and b, respectively), differing only in peak intensities as pyrolysis temperature increases, especially those belonging to the alkyl groups (C≡C), whose formation is less intense when compared with those of poultry litter biochars. Finally, in the range from 900 to 500 cm^{-1}, the peaks are not differentiable, evidencing a losses of oxygenated groups, remaining only structures with carbon rings [68].

The waste produced from tire and its biochars showed similarities regarding the presence of some functional groups at different pyrolysis temperatures, as observed for swine manure. In addition to these results being consistent with those found by Lian et al. [67], there was presence of aliphatic groups, typically methyl (CH_3) and methylene (CH_2), and double bonds in aromatic chains (C═O; C═C and CH_2). Such evidence indicates that these wastes were rapidly decomposed as pyrolysis temperature increased. The groups with triple bonding, such as alkynes (C≡C) and nitriles (C≡N), were identified and no changes were identified with pyrolysis temperature. The group containing sulfur (S═O) present in the tire samples was reduced in the biochars at temperatures above 300 °C (Fig. 4d).

The wastes and biochars of PVC showed characteristic peaks in the FTIR spectra (Fig. 4e). These peaks are associated with O–H bonds in hydroxyl and carboxyl groups, expressed by a broad band that elongates with the increase of temperature, followed by C–H bonds, aliphatic groups typically methyl (CH_3) and methylene (CH_2), which disappear after pyrolysis temperature of 400 °C.

Within the plane of aromatic rings it was possible to observe the peaks of the functional groups alkyl (C≡C) and nitrile (C≡N), whose intensity increased from temperatures up to 400 °C. In the range from 1850 to 1375 cm^{-1}, there were peaks typical of double bonds in aromatic chains (C═O), which appeared to be a fusion with those of the bonds outside the plane of aromatic chains of methyl (CH_3) and methylene (CH_2) [69]. This same range showed the presence of groups containing halogens (C-Cl) in the wastes, with total loss already at the beginning of the pyrolysis process (300 °C) [70].

The FTIR technique made it possible to understand the effects of pyrolysis temperatures. Enlargement, reduction or increase of peaks in FTIR spectra differentiate one spectrum from another, which can be associated with chemical and structural changes of the produced biochars. As observed, all biochars showed peaks relative to the chemical groups of higher and lower recalcitrance, such as aromatic and aliphatic groups, respectively. Thus, it is possible to note the increase in the visibility of peaks related to aromatic groups and the reduction of CH_3 and OH groups. These differences occurred according to the material used for the production of the biochars [70], except for those produced with tire, which presented spectra very similar to that of the raw material.

4. Conclusions

The results showed that both the parent biomass type and pyrolysis temperature caused changes in the characteristics of the biochars. The increase in pyrolysis temperature promoted reductions of yield of solids and volatile compounds and increases in pH in water and $K_{soluble}$ in all produced biochars. The pH of biochars derived from PL, SM and PVC was high, especially at 600 and 700 °C, due to the high ash content in its composition, indicating that it could be advantageous for acidic soil improvement. However, biochars derived from PVC had high electrical conductivity, which can increase soil salinity leading to undesirable impacts on the plant growth. In addition, with the exception of biochar from PL, the cation exchange capacity results confirmed that the biochar prepared at 500 °C is more suitable for soil nutrient retention. X-ray diffraction results revealed the presence of minerals such as sylvite and quartz in poultry litter biochar, sylvite and dolomite in swine

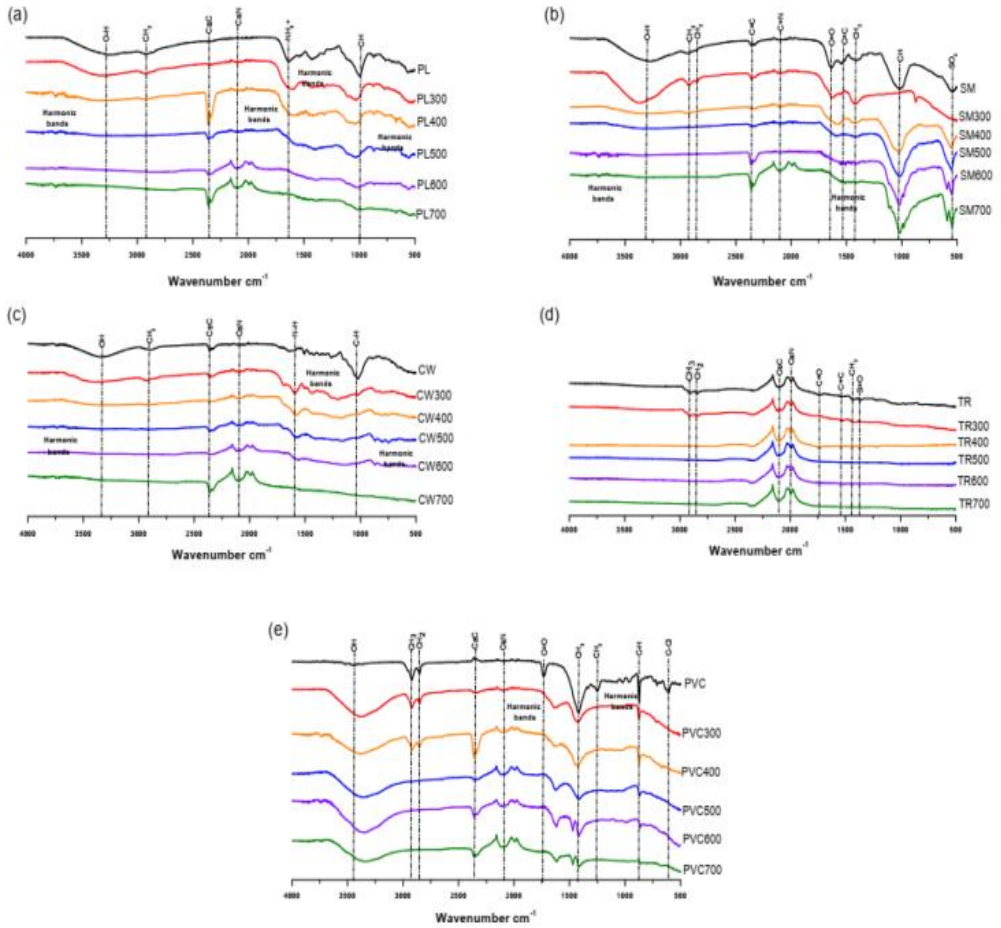

Fig. 4. FTIR spectra of non-pyrolyzed wastes and biochars produced from the agricultural wastes (a) poultry litter (PL) and (b) swine manure (SM) and from the industrial wastes (c) construction wood (CW), (d) tire (TR) and (e) PVC plastic (PVC) subjected to pyrolysis temperatures of 300, 400, 500, 600 and 700 °C.

manure biochar, calcite and dolomite in construction wood biochar, pyrite and anhydrite in tire biochar and kainite and gypsum in PVC biochar. In general, the heavy metal concentration is within the limit established by International Biochar Initiative guidelines, with the exception of biochar from PVC with lead content above the maximum allowed threshold. The results obtained enable the design of biochars for a desired purpose, which might be a solution for agronomic and environmental issues, taking into account the effects of pyrolysis temperature and the type of waste to be processed. Finally, the characterizations enable the identification of potentialities and limitations for the use of biochars.

Declaration of Competing Interest

The authors declare that they have no known competing financial interests or personal relationships that could have appeared to influence the work reported in this paper.

CRediT authorship contribution statement

José Alexander Rodriguez: Conceptualization, Formal analysis, Investigation, Writing - original draft. **José Ferreira Lustosa Filho:** Writing - review & editing. **Leônidas Carrijo Azevedo Melo:** Conceptualization, Writing - review & editing. **Igor Rodrigues de Assis:** Formal analysis. **Teógenes Senna de Oliveira:** Funding acquisition, Conceptualization, Supervision.

Acknowledgements

The authors are grateful to Dr. Jairo Tronto for the XRD analysis. The authors thank the Brazilian foundations: Brazilian National Council for Scientific and Technological Development (CNPq) and Coordination for the Improvement of Higher Education Personnel (CAPES) for scholarship.

Appendix A. Supplementary data

Supplementary material related to this article can be found, in the online version, at doi:https://doi.org/10.1016/j.jaap.2020.104839.

References

[1] F.S. Dalólio, J.N. da Silva, A.C.C. de Oliveira, I. de, F.F. Tinôco, R.C. Barbosa, Mde O. Resende, L.F.T. Albino, S.T. Coelho, Poultry litter as biomass energy: a review and future perspectives, Renewable Sustainable Energy Rev. 76 (2017) 941–949, https://doi.org/10.1016/j.rser.2017.03.104.

[2] I.B. do, M.A. e dos, R.N.R. Ibama, Relatório de pneumáticos: Resolução Conama n° 416/09: 2017 (ano- base 2016) // Diretoria de Qualidade Ambiental, Ibama, Brasíli (2017).

[3] J.S. de Faria, R. da, S.T. Manhães, F.S. da Luz, S.N. Monteiro, C.M.F. Vieira, Incorporation of unserviceable tire waste in red ceramic, J. Mater. Res. Technol. 8 (2019) 6041–6050, https://doi.org/10.1016/j.jmrt.2019.09.078.

[4] C.A. Correa, C.R. de Santi, A. Leclerc, Green-PVC with full recycled industrial waste and renewably sourced content, J. Clean. Prod. 229 (2019) 1397–1411, https://doi.org/10.1016/j.jclepro.2019.04.383.

[5] J. Lehmann, S. Joseph, Biochar for Environmental Management: Science, Technology and Implementation, 2 ed, Routledge, London, 2015.

[6] J.J. Manyà, Pyrolysis for biochar purposes: a review to establish current knowledge gaps and research needs, Environ. Sci. Technol. 46 (2012) 7939–7954, https://doi.org/10.1021/es301029g.

[7] D. Woolf, J.E. Amonette, F.A. Street-Perrott, J. Lehmann, S. Joseph, Sustainable biochar to mitigate global climate change, Nat. Commun. 1 (2010) 56, https://doi.org/10.1038/ncomms1053.

[8] T. Mimmo, P. Panzacchi, M. Baratieri, C.A. Davies, G. Tonon, Effect of pyrolysis temperature on miscanthus (Miscanthus × giganteus) biochar physical, chemical and functional properties, Biomass Bioenergy 62 (2014) 149–157, https://doi.org/10.1016/j.biombioe.2014.01.004.

[9] K.A. Spokas, Review of the stability of biochar in soils: predictability of O:C molar ratios, Carbon Manag. 1 (2010) 289–303, https://doi.org/10.4155/cmt.10.32.

[10] H. Wu, K. Yip, Z. Kong, C.-Z. Li, D. Liu, Y. Yu, X. Gao, Removal and recycling of inherent inorganic nutrient species in Mallee Biomass and derived biochars by water leaching, Ind. Eng. Chem. Res. 50 (2011) 12143–12151, https://doi.org/10.1021/ie200679n.

[11] S. Li, S. Harris, A. Anandhi, G. Chen, Predicting biochar properties and functions based on feedstock and pyrolysis temperature : a review and data syntheses, J. Clean. Prod. 215 (2019) 890–902, https://doi.org/10.1016/j.jclepro.2019.01.106.

[12] H. Lu, W. Zhang, S. Wang, L. Zhuang, Y. Yang, R. Qiu, Characterization of sewage sludge-derived biochars from different feedstocks and pyrolysis temperatures, J. Anal. Appl. Pyrolysis 102 (2013) 137–143, https://doi.org/10.1016/j.jaap.2013.03.004.

[13] P. Pariyar, K. Kumari, M.K. Jain, P.S. Jadhao, Evaluation of change in biochar properties derived from different feedstock and pyrolysis temperature for environmental and agricultural application, Sci. Total Environ. 105 (2020) 136433, , https://doi.org/10.1016/j.scitotenv.2019.136433.

[14] H. Zhang, C. Chen, E.M. Gray, S.E. Boyd, Effect of feedstock and pyrolysis temperature on properties of biochar governing end use efficacy, Biomass Bioenergy 105 (2017) 136–146, https://doi.org/10.1016/j.biombioe.2017.06.024.

[15] J. Heitkötter, B. Marschner, Interactive effects of biochar ageing in soils related to feedstock, pyrolysis temperature, and historic charcoal production, Geoderma 245–246 (2015) 56–64, https://doi.org/10.1016/j.geoderma.2015.01.012.

[16] S. Li, G. Chen, Thermogravimetric, thermochemical, and infrared spectral characterization of feedstocks and biochar derived at different pyrolysis temperatures, Waste Manag. 78 (2018) 198–207, https://doi.org/10.1016/j.wasman.2018.05.048.

[17] Z. Dai, P.C. Brookes, Y. He, J. Xu, Increased agronomic and environmental value provided by biochars with varied physiochemical properties derived from swine manure blended with rice straw, J. Agric. Food Chem. 62 (2014) 10623–10631, https://doi.org/10.1021/jf504106v.

[18] Z. Dai, X. Zhang, C. Tang, N. Muhammad, J. Wu, P.C. Brookes, J. Xu, Potential role of biochars in decreasing soil acidification - a critical review, Sci. Total Environ. 581–582 (2017) 601–611, https://doi.org/10.1016/j.scitotenv.2016.12.169.

[19] K.C. Uzoma, M. Inoue, H. Andry, A. Zahoor, E. Nishihara, Influence of biochar application on sandy soil hydraulic properties and nutrient retention, J. Food, Agric. Environ. 9 (2011) 1137–1143, https://doi.org/10.1234/4.2011.2517.

[20] A.I. Ferjani, M. Jeguirim, S. Jellali, L. Limousy, C. Courson, H. Akrout, N. Thevenin, L. Ruidavets, A. Muller, S. Bennici, The use of exhausted grape marc to produce biofuels and biofertilizers: effect of pyrolysis temperatures on biochars properties, Renewable Sustainable Energy Rev. 107 (2019) 425–433, https://doi.org/10.1016/j.rser.2019.03.034.

[21] J.M. Novak, W.J. Busscher, D.L. Laird, M. Ahmedna, D.W. Watts, M.A.S. Niandou, Impact of biochar amendment on fertility of a southeastern coastal plain soil, Soil Sci. 174 (2009) 105–112, https://doi.org/10.1097/SS.0b013e3181981d9a.

[22] L. Zhao, X. Cao, O. Mašek, A. Zimmerman, Heterogeneity of biochar properties as a function of feedstock sources and production temperatures, J. Hazard. Mater. 256–257 (2013) 1–9, https://doi.org/10.1016/j.jhazmat.2013.04.015.

[23] Abrelpe - Associação Brasileira de Empresas de Limpesa Pública e Resíduos Especiais, Estimativas Dos Custos Para Viabilizar a Universalização Da Destinação, São Paulo, 2015.

[24] Ipea, Plano nacional de resíduos sólidos: diagnóstico dos resíduos urbanos, agro-silvopastoris e a questão dos catadores, (2012).

[25] A.C.A. Orrico, N.D.S. Sunada, J. De Lucas Junior, M.A.P. Orrico Junior, A.W. Schwingel, Codigestão anaeróbia de dejetos de suínos e níveis de inclusão de óleo de descarte, Eng. Agric. 35 (2015) 657–664, https://doi.org/10.1590/1809-4430-Eng.Agríc.v35n4p657-664/2015.

[26] J.F. Lustosa Filho, E.S. Penido, P.P. Castro, C.A. Silva, L.C.A. Melo, Co-pyrolysis of poultry litter and phosphate and magnesium generates alternative slow-release fertilizer suitable for tropical soils, ACS Sustain. Chem. Eng. 5 (2017) 9043–9052, https://doi.org/10.1021/acssuschemeng.7b01935.

[27] A. Shaaban, S.-M. Se, M.F. Dimin, J.M. Juoi, M.H. Mohd Husin, N.M.M. Mitan, Influence of heating temperature and holding time on biochars derived from rubber wood sawdust via slow pyrolysis, J. Anal. Appl. Pyrolysis 107 (2014) 31–39, https://doi.org/10.1016/j.jaap.2014.01.021.

[28] X. Zhang, P. Zhang, X. Yuan, Y. Li, L. Han, Effect of pyrolysis temperature and correlation analysis on the yield and physicochemical properties of crop residue biochar, Bioresour. Technol. 296 (2020) 122318, , https://doi.org/10.1016/j.biortech.2019.122318.

[29] Astm Standard D3172-13, Standard Practice for Proximate Analysis of Coal and Coke, ASTM international, West Conshohocken, 2013, https://doi.org/10.1520/D3172-13.2.

[30] I.B.I. IBI, Standardized Product Definition and Product Testing Guidelines for Biochar That Is Used in Soil, International Biochar Initiative, (2015) http://www.biochar-international.org/sites/default/files/Guidelines_for_Biochar_That_Is_Used_in_Soil_Final.pdf.

[31] T.Q. Zorzeto, S.C.F. Dechen, M.F. de Abreu, F. Fernandes Júnior, Caracterização física de substratos para plantas, Bragantia 73 (2014) 300–311, https://doi.org/10.1590/1678-4499.0086.

[32] C.E. Brewer, V.J. Chuang, C.A. Masiello, H. Gonnermann, X. Gao, B. Dugan, L.E. Driver, P. Panzacchi, K. Zygourakis, C.A. Davies, New approaches to measuring biochar density and porosity, Biomass Bioenergy 66 (2014) 176–185, https://doi.org/10.1016/j.biombioe.2014.03.059.

[33] ASTM standard D1762-84, standard test method for chemical analysis of wood charcoal, ASTM international, West Conshohocken (2007), https://doi.org/10.1520/D1762-84R07.2.

[34] A. Enders, K. Hanley, T. Whitman, S. Joseph, J. Lehmann, Characterization of biochars to evaluate recalcitrance and agronomic performance, Bioresour. Technol. 114 (2012) 644–653, https://doi.org/10.1016/j.biortech.2012.03.022.

[35] K. Jindo, K. Suto, K. Matsumoto, C. García, T. Sonoki, M.A. Sanchez-Monedero, Chemical and biochemical characterisation of biochar-blended composts prepared from poultry manure, Bioresour. Technol. 110 (2012) 396–404, https://doi.org/10.1016/j.biortech.2012.01.120.

[36] M.I. Al-Wabel, A. Al-Omran, A.H. El-Naggar, M. Nadeem, A.R.A. Usman, Pyrolysis temperature induced changes in characteristics and chemical composition of biochar produced from conocarpus wastes, Bioresour. Technol. 131 (2013) 374–379, https://doi.org/10.1016/j.biortech.2012.12.165.

[37] G.E. Rayment, D.J. Lyon, Soil Chemical Methods - Australasia, CSIRO Publishing, Collingwood, Australia, 2010.

[38] W. Song, M. Guo, Quality variations of poultry litter biochar generated at different pyrolysis temperatures, J. Anal. Appl. Pyrolysis 94 (2012) 138–145, https://doi.org/10.1016/j.jaap.2011.11.018.

[39] N. Prakongkep, R.J. Gilkes, W. Wiriyakitnateekul, Forms and solubility of plant nutrient elements in tropical plant waste biochars, J. Plant Nutr. Soil Sci. 178 (2015) 732–740, https://doi.org/10.1002/jpln.201500001.

[40] A. Enders, J. Lehmann, Comparison of wet-digestion and dry-ashing methods for total elemental analysis of biochar, Commun. Soil Sci. Plant Anal. 43 (2012) 1042–1052, https://doi.org/10.1080/00103624.2012.656167.

[41] P.Y. Chen, Table of key lines in x ray powder diffraction patterns of minerals in clays and assocated rocks, Dep. Nat. Resour. Geol. Surv. Occas. Pap. 21 (1977) 77 internal-pdf://op21-1614768640/OP21.pdf..

[42] L.C.A. Barbosa, Espectroscopia no infravermelho na caracterização de compostos orgânicos, Editora UFV, Viçosa, (2011).

[43] IBM SPSS, IBM SPSS Statistics for Windows, (2013).

[44] Z. Dai, J. Meng, N. Muhammad, X. Liu, H. Wang, Y. He, P.C. Brookes, J. Xu, The potential feasibility for soil improvement, based on the properties of biochars pyrolyzed from different feedstocks, J. Soils Sediments 13 (2013) 989–1000, https://doi.org/10.1007/s11368-013-0698-y.

[45] X. Gai, H. Wang, J. Liu, L. Zhai, S. Liu, T. Ren, H. Liu, Effects of feedstock and pyrolysis temperature on biochar adsorption of ammonium and nitrate, PLoS One 9 (2014) e113888, https://doi.org/10.1371/journal.pone.0113888.

[46] M. Bernardo, S. Mendes, N. Lapa, M. Gonçalves, B. Mendes, F. Pinto, H. Lopes, Leaching behaviour and ecotoxicity evaluation of chars from the pyrolysis of forestry biomass and polymeric materials, Ecotoxicol. Environ. Saf. 107 (2014) 9–15, https://doi.org/10.1016/j.ecoenv.2014.05.007.

[47] O. Mašek, V. Budarin, M. Gronnow, K. Crombie, P. Brownsort, E. Fitzpatrick, P. Hurst, Microwave and slow pyrolysis biochar—comparison of physical and functional properties, J. Anal. Appl. Pyrolysis 100 (2013) 41–48, https://doi.org/10.1016/j.jaap.2012.11.015.

[48] A.T. Tag, G. Duman, S. Ucar, J. Yanik, Effects of feedstock type and pyrolysis temperature on potential applications of biochar, J. Anal. Appl. Pyrolysis 120 (2016) 200–206, https://doi.org/10.1016/j.jaap.2016.05.006.

[49] X. Wang, W. Zhou, G. Liang, D. Song, X. Zhang, Characteristics of maize biochar with different pyrolysis temperatures and its effects on organic carbon, nitrogen and enzymatic activities after addition to fluvo-aquic soil, Sci. Total Environ. 538 (2015) 137–144, https://doi.org/10.1016/j.scitotenv.2015.08.026.

[50] D. Angın, S. Şensöz, Effect of pyrolysis temperature on chemical and surface properties of biochar of rapeseed (Brassica napus L.), Int. J. Phytoremediation 16 (2014) 684–693, https://doi.org/10.1080/15226514.2013.856842.

[51] X. Cao, K.S. Ro, M. Chappell, Y. Li, J. Mao, Chemical structures of swine-manure chars produced under different carbonization conditions investigated by advanced solid-state 13 C nuclear magnetic resonance (NMR) spectroscopy †, Energy Fuels 25 (2011) 388–397, https://doi.org/10.1021/ef101342v.

[52] M. Tripathi, J.N. Sahu, P. Ganesan, Effect of process parameters on production of biochar from biomass waste through pyrolysis: a review, Renew. Sustain. Energy Rev. 55 (2016) 467–481, https://doi.org/10.1016/j.rser.2015.10.122.

[53] F. Bellandi, B. Fontal, M. Reyes, T. Suárez, R. Contreras, Elementos químicos y su periodicidad, Universidad de Los Andes, Facultad de Ciencias, Departamento de Química, Venezuela, 2005.

[54] P.J. Mitchell, T.S.L. Dalley, R.J. Helleur, Preliminary laboratory production and characterization of biochars from lignocellulosic municipal waste, J. Anal. Appl. Pyrolysis 99 (2013) 71–78, https://doi.org/10.1016/j.jaap.2012.10.025.

[55] K. Lorenz, R. Lal, Biochar application to soil for climate change mitigation by soil organic carbon sequestration, J. Plant Nutr. Soil Sci. 177 (2014) 651–670, https://doi.org/10.1002/jpln.201400058.

[56] F.A. Petter, B.E. Madari, Biochar: agronomic and environmental potential in Brazilian savannah soils, Rev. Bras. Eng. Agrícola e Ambient. 16 (2012) 761–768, https://doi.org/10.1590/S1415-43662012000700009.

[57] K.H. Kim, J.-Y. Kim, T.-S. Cho, J.W. Choi, Influence of pyrolysis temperature on physicochemical properties of biochar obtained from the fast pyrolysis of pitch pine (Pinus rigida), Bioresour. Technol. 118 (2012) 158–162, https://doi.org/10.1016/j.biortech.2012.04.094.

[58] P. He, Y. Liu, L. Shao, H. Zhang, F. Lü, Particle size dependence of the physico-chemical properties of biochar, Chemosphere 212 (2018) 385–392, https://doi.org/10.1016/j.chemosphere.2018.08.106.

[59] X. Zhang, H. Wang, L. He, K. Lu, A. Sarmah, J. Li, N.S. Bolan, J. Pei, H. Huang, Using biochar for remediation of soils contaminated with heavy metals and organic pollutants, Environ. Sci. Pollut. Res. 20 (2013) 8472–8483, https://doi.org/10.1007/s11356-013-1659-0.

[60] J. Zhou, B. Gui, Y. Qiao, J. Zhang, W. Wang, H. Yao, Y. Yu, M. Xu, Understanding the pyrolysis mechanism of polyvinylchloride (PVC) by characterizing the chars produced in a wire-mesh reactor, Fuel 166 (2016) 526–532.

[61] L. Xiao, E. Bi, B. Du, X. Zhao, C. Xing, Surface characterization of maize-straw-derived biochars and their sorption performance for MTBE and benzene, Environ. Earth Sci. 71 (2014) 5195–5205, https://doi.org/10.1007/s12665-013-2922-x.

[62] T.T.N. Nguyen, C.-Y. Xu, I. Tahmasbian, R. Che, Z. Xu, X. Zhou, H.M. Wallace, S.H. Bai, Effects of biochar on soil available inorganic nitrogen: A review and meta-analysis, Geoderma 288 (2017) 79–96, https://doi.org/10.1016/j.geoderma.2016.11.004.

[63] G.K. Gupta, P.K. Gupta, M.K. Mondal, Experimental process parameters optimization and in-depth product characterizations for teak sawdust pyrolysis, Waste Manag. 87 (2019) 499–511, https://doi.org/10.1016/j.wasman.2019.02.035.

[64] B. Acharya, A. Dutta, S. Mahmud, M. Tushar, M. Leon, Ash analysis of poultry litter, Willow and oats for combustion in boilers, J. Biomass to Biofuel. 1 (2014), https://doi.org/10.11159/jbb.2014.003.

[65] J.-H. Yuan, R.-K. Xu, H. Zhang, The forms of alkalis in the biochar produced from crop residues at different temperatures, Bioresour. Technol. 102 (2011) 3488–3497, https://doi.org/10.1016/j.biortech.2010.11.018.

[66] X. Dong, T. Guan, G. Li, Q. Lin, X. Zhao, Long-term effects of biochar amount on the content and composition of organic matter in soil aggregates under field conditions, J. Soils Sediments 16 (2016) 1481–1497, https://doi.org/10.1007/s11368-015-1338-5.

[67] Y. Liu, Z. He, M. Uchimiya, Comparison of biochar formation from various agricultural by-products using FTIR spectroscopy, Mod. Appl. Sci. 9 (2015) 246–253, https://doi.org/10.5539/mas.v9n4p246.

[68] R. Azargohar, S. Nanda, J.A. Kozinski, A.K. Dalai, R. Sutarto, Effects of temperature on the physicochemical characteristics of fast pyrolysis bio-chars derived from Canadian waste biomass, Fuel 125 (2014) 90–100, https://doi.org/10.1016/j.fuel.2014.01.083.

[69] Q. Wang, Z. Lai, J. Mu, D. Chu, X. Zang, Converting industrial waste cork to biochar as Cu (II) adsorbent via slow pyrolysis, Waste Manag. 105 (2020) 102–109, https://doi.org/10.1016/j.wasman.2020.01.041.

[70] R. Singh, D. Pant, Polyvinyl chloride degradation by hybrid (chemical and biological) modification, Polym. Degrad. Stab. 123 (2016) 80–87, https://doi.org/10.1016/j.polymdegradstab.2015.11.012.

CAPÍTULO 2

CO-PYROLYSIS OF AGRICULTURAL AND INDUSTRIAL WASTES CHANGES THE COMPOSITION AND STABILITY OF BIOCHARS AND CAN IMPROVE THEIR AGRICULTURAL AND ENVIRONMENTAL BENEFITS

Journal of Analytical and Applied Pyrolysis 155 (2021) 105036

Contents lists available at ScienceDirect

Journal of Analytical and Applied Pyrolysis

journal homepage: www.elsevier.com/locate/jaap

Co-pyrolysis of agricultural and industrial wastes changes the composition and stability of biochars and can improve their agricultural and environmental benefits

José Alexander Rodriguez [a,c], José Ferreira Lustosa Filho [a,*], Leônidas Carrijo Azevedo Melo [b], Igor Rodrigues de Assis [a], Teógenes Senna de Oliveira [a]

[a] Department of Soil, Federal University of Viçosa, 36570-900, Viçosa, MG, Brazil
[b] Soil Science Department, Federal University of Lavras, 37200-000, Lavras, MG, Brazil
[c] Faculty of Veterinary Medicine and Zootechnics, Autonomous University Foundation of the Americas, South Avenue 98-56, Pereira, R/da, Colombia

ARTICLE INFO

Keywords:
Pyrolysis
PVC
Tire
Construction wood
Poultry litter
Swine manure

ABSTRACT

Co-pyrolysis is an alternative process for waste management and pollution elimination, producing a solid material (biochar) useful for energy generation and soil improvement. The objective of this study was to assess the changes in the physicochemical characteristics, mineral composition, and functional groups of biochars derived from the co-pyrolysis of agricultural and industrial wastes produced by different pyrolysis temperatures and feedstocks. Ten different types of biochars were produced by co-pyrolysis of two agricultural wastes (poultry litter - PL and swine manure - SM) and three industrial wastes (construction wood - CW, tire - TR and PVC plastic - PVC) combined in proportions of 1:1 (w:w) at five temperatures (300, 400, 500, 600 and 700 °C). With the increase of pyrolysis temperatures from 300 to 500 °C, there were drastic reductions in biochar yield (79−48%) and volatile matter (43−17%) and increases in ash content (21–33 %), fixed carbon (30–45 %), cation exchange capacity (CEC) (16–68 $cmol_c\ kg^{-1}$) and concentration of nutrients and heavy metals. Between 500 and 700 °C these changes were much less pronounced. The biochars prepared with mixtures from PL and SM had high ash contents (44 %), relatively high CEC (37 $cmol_c\ kg^{-1}$), water holding capacity (WHC) (41 %), and alkalinity (10.0) and can enhance the nutrient supply and CEC in soils. All biochars had low H:C (0.06) and O:C (0.30) molar ratios, suggesting a potential for carbon sequestration in soils. Our study shows that the interaction or synergy between agricultural and industrial materials in co-pyrolysis improved certain properties of biochars fundamental to soil quality, such as reduction of electrical conductivity (EC), increase in WHC, neutralizing power, and stability, and enabling the release or concentration of macro and micronutrients. Therefore, co-pyrolysis of agricultural and industrial wastes to produce biochars would have both agricultural and environmental benefits.

1. Introduction

Inadequate disposal of solid wastes can result in environmental problems in urban, rural and industrial areas, and co-pyrolysis is a promise alternative process for waste management and reduction of potential environmental pollution. However, there is a need to improve the production process and a better understanding of the characteristics of resulted biochars to improve its potential future use. In Brazil, only 58.4 % (~41.6 billion ton $year^{-1}$) of urban wastes are appropriately managed [1] and the disposal of animal wastes is a critical environmental problem. For instance, the Brazilian animal wastes are estimated to be 1.704 billion ton $year^{-1}$, being 20 million ton $year^{-1}$ of swine manure and 28 million ton $year^{-1}$ of poultry manure [2], which poses a challenge for their adequate disposal. Therefore, it is necessary to create sustainable solutions aiming to reduce the environmental problems represented by waste stocks.

Biochar is a carbon-rich byproduct obtained from thermochemical conversion of biomass under low or absent oxygen [9]. The physicochemical properties of biochar are affected mainly by the feedstock and pyrolysis conditions such as heating rate, holding time and pyrolysis

* Corresponding author.
E-mail addresses: filhoze04@hotmail.com, jose.lustosa@ufv.br (J.F. Lustosa Filho).

https://doi.org/10.1016/j.jaap.2021.105036
Received 3 August 2020; Received in revised form 6 October 2020; Accepted 31 January 2021
Available online 4 February 2021

temperature [14–18]. An increase in pyrolysis temperatures increases volatile compounds loss, pore size, surface area and ash content, but decreases surface functional groups that generate cation exchange capacity [14,19,20]. Likewise, H/C and O/C molar ratios of biochar tend to decrease with increasing pyrolysis temperature [21]. Thus, biochar produced at high pyrolysis temperature increases persistence due to resistance to microbial and chemical decomposition in soil [22]. In contrast, low-temperature (<400 °C) biochar has higher yield, lower pH and contains easily decomposable substrates [22,23]. Feedstock type also has substantial impact on the compositional constituents and properties of biochar [22]. For example, biochars produced from poultry litter and swine manure are rich in phosphorus and calcium [24]. PVC plastic- and tire-derived biochars showed high WHC [25], while biochar derived from wood have high C concentration and low H/C ratio, which increases its potential for improving C storage in soils due to high aromatic character [26].

Co-pyrolysis is an alternative that uses two or more materials, whether agricultural or industrial wastes [3–5], to generate energy and serve as soil and water amendment [6–8]. This process can be conducted in total or partial absence of oxygen and transforms the feedstock into biochar (solid), bio-oil and combustible gases (CO, CO_2, H_2, CH_4 and other hydrocarbons) [9]. The combination of organic waste especially with plastics increases the calorific power of oils, resulting in benefits such as the reduction of ash contents and production costs [12,13]. Although there are many recent studies with biochars from several feedstocks to enhance their use in soil improvement and water decontamination [9], there is a lack of studies evaluating the agronomic potential and environmental uses of products resulted from co-pyrolysis [4].

Mixtures of common biomass (woods, manure, straws, peels, among others) and industrial wastes (plastics, tires and PVC) have been used in co-pyrolysis to improve the yield of pyrolysis products such as oil, coal and gases [27–29]. Energy is also generated by using the chemical and physical synergy that occurs between wastes with low and high calorific power [11,30]. However, the improvement in agronomic attributes of interest, such as WHC, EC, CEC, nutrient availability, acid-neutralizing power, among others, has not been considered in the evaluation of the co-pyrolysis process, as well as the solid products generated [31]. In a recent study, the pyrolysis of two agricultural wastes (poultry litter and swine manure) and three industrial wastes (construction wood, tire and PVC plastic) at different temperatures showed that biochars derived from tire or PVC plastic alone are not suitable materials to soil amendments due to their low nutrient content and high EC (PVC biochar), which can increase soil salinity and has lead content above the maximum allowed threshold [25]. Thus, there is a practical need to develop alternative pyrolysis technologies that can minimize potential environmental risks of heavy metals in biochars derived from PVC for soil application. On the other hand, biochars derived from agricultural wastes are rich in plant nutrients (e.g., P, Ca and Mg), have significant CEC, WHC and alkaline pH [25]. Therefore, the scientific contribution of this work is to combine agricultural wastes (poultry litter and swine manure) and industrial wastes (construction wood, tire and PVC plastic) in co-pyrolysis process for improving physicochemical properties of the derived biochars to alleviate the ecological risks of heavy metals, while improving agronomic and environmental performance in soil application.

Information about the physical and chemical properties of biochars produced in co-pyrolysis for agronomic uses are scarce and can be valuable for the management of solid wastes, which faces difficulties for adequate final disposal. Therefore, the objective of this study was to evaluate the effect of slow co-pyrolysis between agricultural and industrial wastes to improve the properties of the biochars produced and their potential for agronomic and environmental applications.

2. Material and methods

2.1. Selection of wastes used

The feedstocks were selected consulting state inventories of agricultural and industrial solid wastes from the National Solid Waste Plan and the Solid Waste Panorama Report [2,32]. We selected poultry litter and swine manure to represent animal wastes commonly used in agriculture and construction wood, tire and PVC plastic to represent industrial wastes generated in high amounts and misused in general. These feedstocks were also selected considering their high potential to cause negative impacts on the environment due to the large quantities generated and difficult final disposal. Besides that, the selection of feedstocks was based on materials with very different structural and chemical properties and representing feedstocks readily available in many regions of Brazil and worldwide. The agricultural residues are rich in nutrients and can be used as organic fertilizers; nonetheless, if applied *in natura*, they can act as vectors of animal diseases and might become a source of pollution [25]. Therefore, these residues must first go through a composting process or some other process capable of eliminating undesirable effects. The industrial wastes are generated in large quantities and are mostly discarded in landfills or disposed directly into the environment, which might lead to water and soil contamination due to the presence of toxic elements and pathogens [25,33]. Detailed information about the wastes used in this study and collection locations can be found in Rodriguez et al. [25]. The characteristics of these wastes are described in Table S1 in the supplementary material.

2.2. Production and characteristics of biochars

The wastes, hereinafter named feedstocks, were ground for separation on a 4-mm-mesh sieve. Then, the samples were placed in an oven at 65 °C for 48 h to dry, and finally the five wastes were mixed in the proportion of 1:1 (w:w) with the aid of a small agitator, obtaining 10 mixtures: poultry litter + swine manure, poultry litter + construction wood, poultry litter + tire, poultry litter + PVC plastic, swine manure + construction wood, swine manure + tire, swine manure + PVC plastic, construction wood + tire, construction wood + PVC plastic and tire + PVC plastic. The mixture ratio of feedstocks was selected based on preliminary experiments, and based on previous studies [34–36]. The mixtures were placed in hermetically closed stainless steel cylinders (10.6 cm diameter and 42 cm height) and placed in an adapted muffle furnace that allows the release of gases during pyrolysis and collection of bio-oil. A schematic figure of the pyrolysis system can be seen in Fig. S1. Pyrolysis was carried out at temperatures of 300, 400, 500, 600 and 700 °C, with a heating rate of 10 °C min^{-1} and one hour of holding time at the desired temperature [37]. Aiming to facilitate the presentation, biochars were termed PL (biochar from poultry litter), SM (biochar from swine manure), CW (biochar from construction wood), TR (biochar from tire) and PVC (biochar from PVC), followed by the corresponding pyrolysis temperature (e.g., PL + SM300, abbreviation for biochar produced from poultry litter + swine manure pyrolyzed at 300 °C).

The physical analyses were performed using 100 g of each biochar in triplicates to determine: (i) biochar yield by the difference between weights, according to ASTM Standard D3172 -13 [38]; (ii) mean weight diameter of particles determined from the particle distribution according to the International Biochar Initiative [39]; and (iii) WHC determined in a pressure chamber at 33 kPa for 72 h [40].

For the chemical analyses, biochar samples were ground and passed through a 60-mesh sieve (0.25 mm), oven-dried at 65 °C ± 2 °C for 48 h to remove moisture and standardize its content to <10 % [41], and the following attributes were measured: volatile matter content [42], modified by Enders et al. [43]; ash content [42]; fixed carbon content [38]; elemental composition in elemental analyzer (C, H, N and O) [44]; electrical conductivity (EC) and pH in water by potentiometry in 1:20 solution, after 12 -h rest and stirring of suspension [45]; neutralizing

power determined by the acid/base titrimetric method [46]; cation exchange capacity determined by the method of saturation with NH_4OAC (1.0 mol L^{-1}) and Phenate method using colorimetry [47]; contents of elements both soluble in water (Ca, K, P, Mg and S) [48] and total (Ca, K, P, Mg, S, Fe, Mn, Zn, Mo, B, Al, Cu, As, Pb, Cd, and Cr) [49]. After extraction, K was determined by flame photometry, Ca by atomic absorption spectroscopy and the other elements by inductively coupled plasma atomic emission spectroscopy (ICP-AES); identification of minerals of the crystalline phases were performed by X-ray powder diffractometry (XRD), using a PAN analytical device, X' Pert Powder model, with cobalt tube, nickel filter in the range from 4 to 50°2θ, scanning speed of 10°2θ and interpretation according to Chen [50]; and identification of functional groups by molecular absorption spectrophotometry in the infrared region with Fourier transform (FTIR) (Jasco FTIR 4100), using spectra obtained with 60 scans, with wavenumber from 4000 to 400 cm^{-1} and resolution of 4 cm^{-1}, in KBr tablets and interpretation according to Barbosa [51].

3. Results and discussion

3.1. Effects of temperature on the biochars in co-pyrolysis

Regardless of the feedstock, biochar yields gradually decreased from 70 to 88% to around 48 % with increasing pyrolysis temperature, with a drastic reduction in biochar yield between 300 °C and 500 °C (Fig. 1a). For instance, the yield of biochar from co-pyrolysis between construction wood and tire reduced from 88.1%–37.8% as the temperature increased from 300 to 500 °C. High pyrolysis temperature intensifies the carbonization of the biomass through rapid dehydrogenation, gasification, and condensation [52], reducing the production of solid biochar. However, when the pyrolysis temperature increased from 500 to 700 °C lower biochar yield variations (mean 5.4 %) were observed. Therefore, high-temperature pyrolysis (>500 °C) did not affect the yield, but resulted in changes in the physical and chemical properties of the biochars.

Mixtures of tire with PVC resulted in the highest yields, likely influenced by the higher individual yield of these wastes [25]. Although other researchers observed an increase of biochar yield during co-pyrolysis of biomass and PVC, the mechanism has not been adequately explained [27]. The study of co-pyrolysis of PVC with cellulose (40–60 % of total biomass) can improve our understanding of the interaction between PVC and biomass. Pyrolysis of cellulose occurs mainly by two competing reactions as proposed by Matsuzawa et al. [53]: (1) dehydration and charring, and (2) transglycosylation and levoglucosan formation. Hydrochloric acid derived from PVC induces the dehydration of cellulose and increases the production of aldehyde from cellulose. Under lower temperatures, the dehydration decreases H and O atoms in the cellulose molecule and the production of aldehyde is an indication of the cleavage of glycosidic units, which reduces the chance of depolymerization and amount of tar, like levoglucosan. Therefore, the lack of H atoms and cleavage of intra-ring leads to a higher amount of biochar [53].

The proximate analysis indicated a decrease in the volatile matter with the increase in pyrolysis temperature, whereas the reverse situation

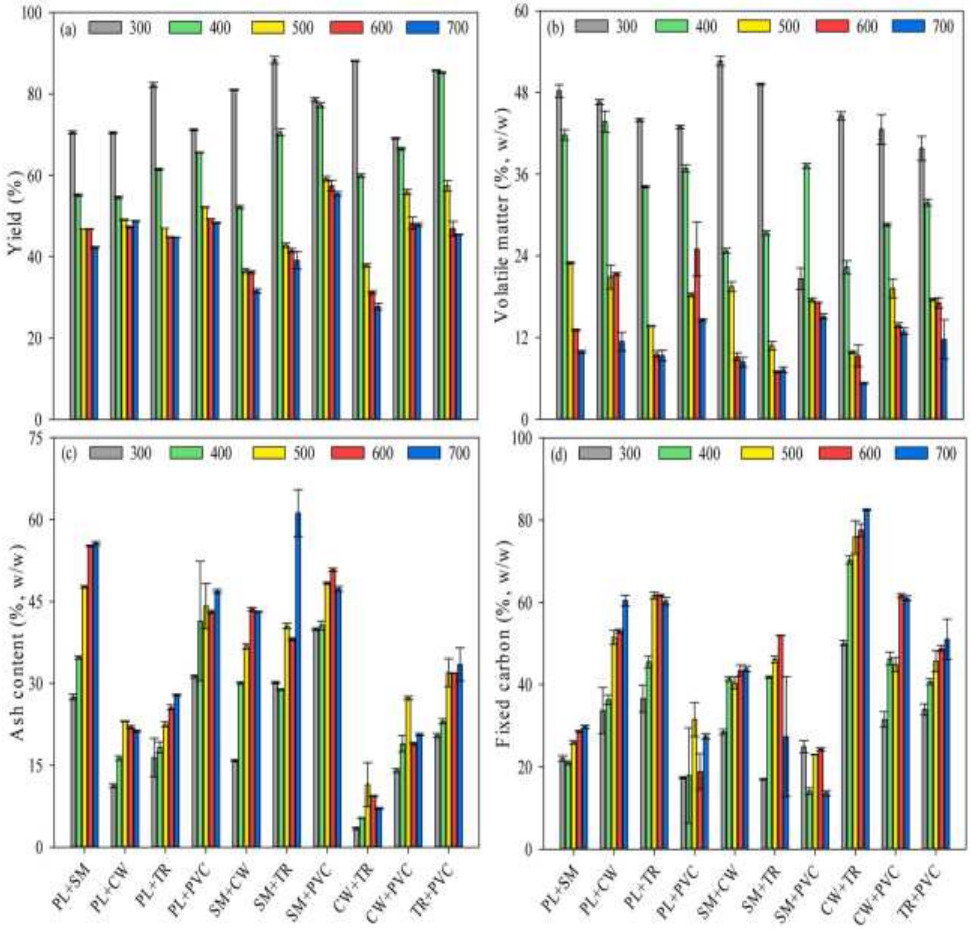

Fig. 1. Yield, volatile matter, ash and carbon fixed content (w/w) of biochars produced in co-pyrolysis of the agricultural wastes poultry litter (PL) and swine manure (SM) and the industrial wastes construction wood (CW), tire (TR) and PVC plastic (PVC), at temperatures of 300, 400, 500, 600 and 700 °C. Error bars represent the standard error of the mean (n = 3).

was observed for ash content and fixed carbon (Fig. 1b-d). Most volatile matter could be decomposed by pyrolysis at 500 °C, since no great changes were observed at higher temperatures, except for the biochars from mixtures of swine manure with poultry litter or tire (Fig. 1b). For the biochars in co-pyrolysis with tire, the volatile matter content decreased (on average) from 44.4%–8.4% when the temperature was increased from 300 to 700 °C. This range was narrower for PVC-derived biochars, with volatile matter content decreasing from 36.5%–13.6% within the same range of temperatures. This difference might be related to the high ash content of PVC [25], which can protect the organic fraction and structures of biochars during pyrolysis [54,55].

Biochars from mixtures between agricultural wastes or when these feedstocks were co-pyrolyzed with PVC showed higher ash content than the other biochars (Fig. 1c). This is due to large amounts of inorganic compounds (K, P, Ca, Mg and S) in poultry litter and swine manure (Table S1), which accumulated after removing volatile compounds. Conversely, the fixed carbon content was lower in biochars from mixtures with PVC, as found in other studies [17,56], while low-ash biochars (derived from tire in co-pyrolysis with construction wood and poultry litter) had around three-fold greater contents of fixed carbon, indicating its higher potential as a recalcitrant carbon sink in soil [21].

3.2. Physicochemical properties

The physicochemical properties of the biochar samples are reported in Fig. 2. Higher pyrolysis temperature increased the pH of most biochars (Fig. 2a). The biochar from co-pyrolysis between poultry litter and PVC showed the lowest pH range (4.5–8.5) compared with the other poultry litter biochars with values of pH ≥ 10.0. Biochar pH increased by 3.2 units, on average, with increasing pyrolysis temperature from 300 to 700 °C, mainly due to higher concentrations of mineral elements in the feedstocks, especially P, K, Ca and Mg [57]. Regardless of mineral

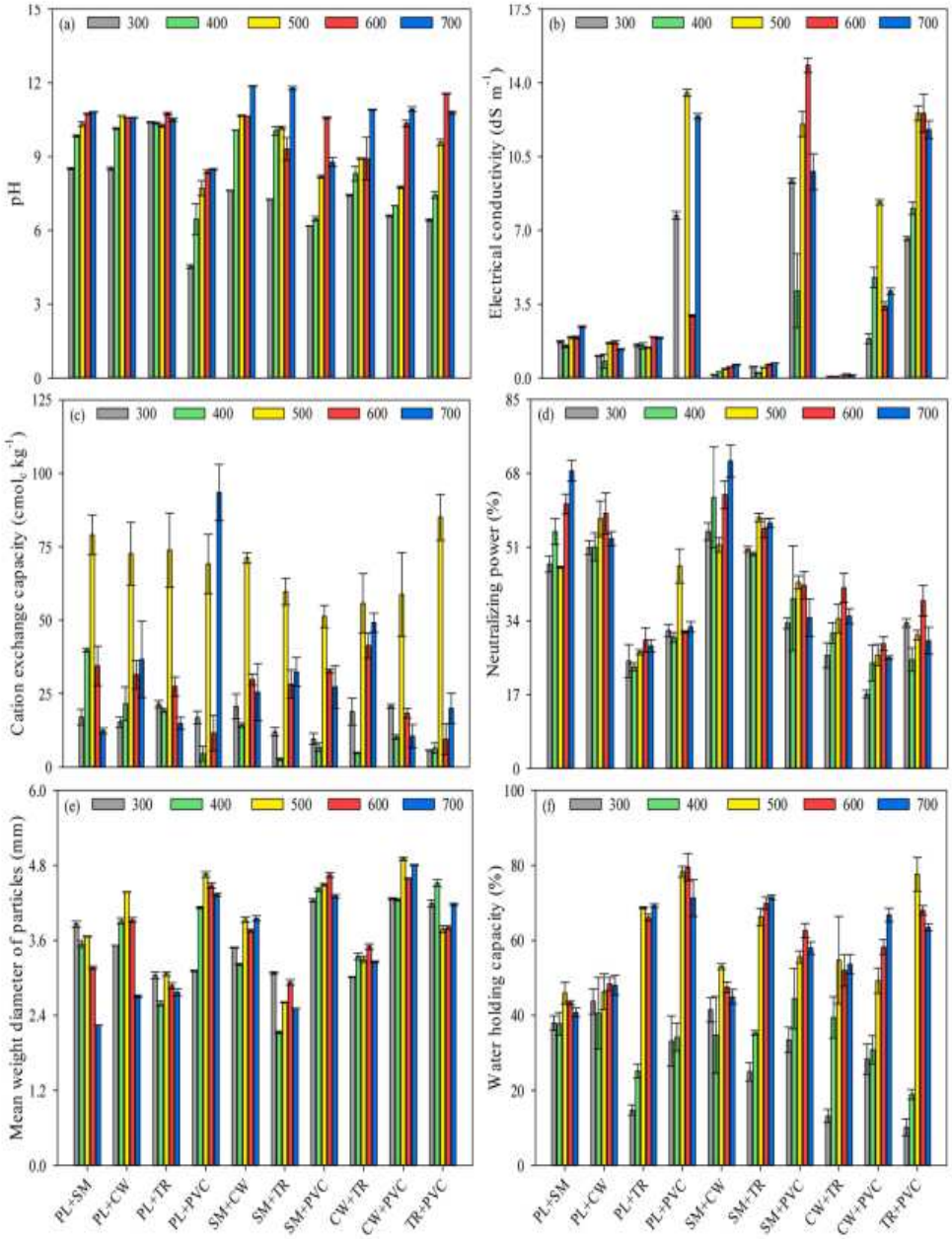

Fig. 2. Average values of pH, electrical conductivity, cation exchange capacity, acid-neutralizing power, mean weight diameter of particles and water holding capacity of biochars produced in co-pyrolysis of the agricultural wastes poultry litter (PL) and swine manure (SM) and the industrial wastes construction wood (CW), tire (TR) and PVC plastic (PVC), at temperatures of 300, 400, 500, 600 and 700 °C. Error bars represent the standard error of the mean (n = 3).

composition, pH values can also be influenced by the presence of acidic functional groups (e.g., carboxylic and phenolic functional groups) and the H/C ratio [58,59]. The alkaline nature of the relatively high pyrolysis temperature biochars (>400 °C) has both a liming effect in acidic soils and an induced immobilization of heavy metals in polluted soils [58,60]. However, the application of highly alkaline biochar may negatively affect sandy soils with low buffer capacity [61]. In this context, pyrolysis temperature is a useful tool to design biochar for specific purposes.

Electrical conductivity (EC) was mainly influenced by the feedstock used in biochar production (Fig. 2b), with the highest values in the co-pyrolysis of PVC with other feedstocks regardless of the pyrolysis temperature. The EC might indicate the salt content [62] as well as the soluble alkaline cations content of biochars [63]. Therefore, biochars produced from mixtures involving PVC should be applied carefully to soil to avoid salinity levels that adversely affect plant growth. It must be highlighted that co-pyrolysis of PVC plastic with other feedstocks has drastically reduced the EC of, biochar produced from pure PVC (165 dS m^{-1} at 700 °C) [25] to a maximum of 14.8 dS m^{-1} 600 °C, biochar from co-pyrolysis of this feedstock with swine manure.

CEC is the capacity of a given media to adsorb and exchange positively charged species such as Ca^{2+}, Mg^{2+}, K^{+} and Na^{+}. Biochar CEC values in this study ranged from 2.7–93.5 $cmol_c$ kg^{-1} and increased when pyrolysis temperature varied from 300 to 500 °C. The only exception was for biochar from co-pyrolysis between poultry litter and PVC, whose value was higher at 700 °C (Fig. 2c). Biochar CEC is determined by both surface area and oxygenated functional groups, such as carboxylic, phenolic, and lactonic [64,65]. According to Carrier et al. [66], biochar produced at temperatures up to 480 °C allows the retention of some acidic oxygenated functional groups such as phenolic and carboxyl groups. Therefore, this explains higher CEC at 500 °C observed in the present study. Similarly, Gai et al. [67] found that the CEC of biochars prepared from wheat-straw, corn-straw and peanut-shell at 500 °C was higher than those at 300 °C and 700 °C.

Biochars from co-pyrolysis involving poultry litter showed the highest average values of CEC and this is likely due to the content of alkali elements (K, Ca, Mg, and P), which promote the formation of O-containing functional groups on biochar surface during pyrolysis [47,68,69]. However, these functional groups are lost at pyrolysis temperatures of 600 and 700 °C. Intensely weathered soils are dominated by kaolinite and iron and aluminum (hydr)oxides in the clay fraction, resulting in low CEC and high dependence on the organic carbon content for increase of CEC [70]. Thus, the application of biochar in these soils might effectively increase the CEC [71] and enable nutrient retention (e.g., K^{+} and $NH4^{+}$) in the root zone and prevent leaching. These biochars could also be used for rehabilitation of mining-affected areas that normally involve re-establishment of vegetation in sterile wastes and tailings, generally physically, chemically and biologically deficient [72]. Therefore, biochar addition could increase the soil organic matter content and nutrient availability, which facilitates the development and establishment of plants [73].

The neutralizing power increased up to the temperature of 600 °C for most biochars (Fig. 2d), with the highest values ranging from 46.4%–70.8% for biochars from the co-pyrolysis of poultry litter, swine manure and construction wood. The neutralizing power of biochar is the capacity of a material to accept protons, being dependent on the kinetics of the reactions of H^{+} released by the compounds of the feedstocks along the processes of thermal transformation. This process occurs faster in organic wastes and, thus, the use of poultry litter, swine manure and construction wood results in biochars with higher alkalinity [74]. Also, the high neutralizing power of organic waste biochars can be attributed to the presence of carbonates (calcite and dolomite) as observed in the XRD spectra (Fig. 5). Therefore, the neutralizing power should be considered when biochar is used to neutralize soil acidity [26].

The mean weight diameter of biochars' particles had a narrow variation (3.51–3.88 mm) with increase in pyrolysis temperature (Fig. 2e), similar to the results found when the feedstocks were individually pyrolyzed [25]. This result supports the evidence that changes in biochar particle size are not always associated with thermal transformations of the wastes used for their production. Biochars produced from mixtures with PVC had the highest values of mean weight diameter of particles, while the lowest values occurred for the biochars produced from tire with other feedstocks. Similarly for CEC, the WHC of biochars increased when pyrolysis temperature was increased from 300 to 500 °C (Fig. 2f). Biochars from co-pyrolysis of agricultural wastes (poultry litter and swine manure) with PVC plastic and tire showed greater WHC, with average values ranging from 48.9 to 59.3%. The high WHC of these biochars may be explained by the existence of oxygen-containing functional groups (C═O, COOH, and OH—) that tend to bond with water molecules [75]. Therefore, biochar could be a competent amendment to soils, especially for sandy loam soils, with high sand deposits and low value (21 %) of WHC [76].

3.3. Total and water-extractable contents of nutrients and heavy metals

The total and water-soluble content of inorganic minerals (i.e., Ca, K, P, Mg and S) in the biochars are presented in Fig. 3. The total contents of S and K increased with the increase in pyrolysis temperature, and the average contents of Ca (45.1−35.6 g kg^{-1}), P (31.0−29.4 g kg^{-1}) and Mg (6.10−5.81 g kg^{-1}) slightly reduced when the temperature increased from 600 to 700 °C. The positive relationship between the increase in total contents of S and K and temperature is probably due to the loss of C, H, O, and N during the pyrolysis process, thereby resulting in a relative increase in concentrations of these nutrients [77].

In general, biochars produced from waste mixtures in co-pyrolysis reflected the composition of the feedstocks (Table S1). Biochars derived from mixing agricultural wastes had higher contents of P, K and Mg when compared to the other mixtures due to the originally high concentrations of these elements in the feedstocks. In addition, biochars from co-pyrolysis between agricultural wastes and tire showed high contents of S and those in co-pyrolysis with construction wood or PVC showed high contents of Ca. Considering the mean of all biochars, the increase in pyrolysis temperature decreased the water extractability of Mg (29.3−14.1%), P (7.29−0.58%) and S (42.1−25.4%) and increased that of Ca (12.0–26.8 %) and K (22.4–32.6 %).

Less than 3%, on average, of the total P in the biochars was water-extractable, and the proportion decreased with increasing temperature (Fig. 3b). The formation of insoluble metal phosphate minerals such as calcium pyrophosphate ($Ca_2P_2O_7$) and magnesium pyrophosphate ($Mg_2P_2O_7$) might be the main reason for the reduced P solubility in the biochars [78,79]. The lower proportion of water-soluble Ca and Mg in the co-pyrolysis biochar among agricultural residues (rich in Ca, Mg and P) evidences the formation of water-insoluble P compounds during pyrolysis. Therefore, this biochar when applied to soil can act as a slow-release source of these nutrients.

The concentration of micronutrients (Zn, Fe, Mn, B and Mo) in the biochars revealed that Zn, Fe, and Mn were abundant in all samples (Table S2), and in most biochars there was an increase in Zn, Fe, Mn and B with the increase in pyrolysis temperature. However, in some cases, at the highest temperatures (600−700 °C) these elements were reduced or remained unchanged. A plausible explanation for this behavior is that these elements might be lost by volatilization at higher temperatures [80,81]. The concentration of heavy metal varied among the various biochars (Table S3), but practically in all materials, the individual metal concentrations were below the permissible values for biochars, according to International Biochar Initiative guidelines [39]. The only exception was for biochars produced from mixtures containing PVC, in which Pb content was above the maximum allowed threshold due to the high concentration (1400 mg kg^{-1} at 600 °C) in this biochar [25].

In general, biochars derived from waste mixtures in co-pyrolysis reflect the composition of the feedstocks, in terms of solubility of macro and micronutrients, and composition of the total elements, which

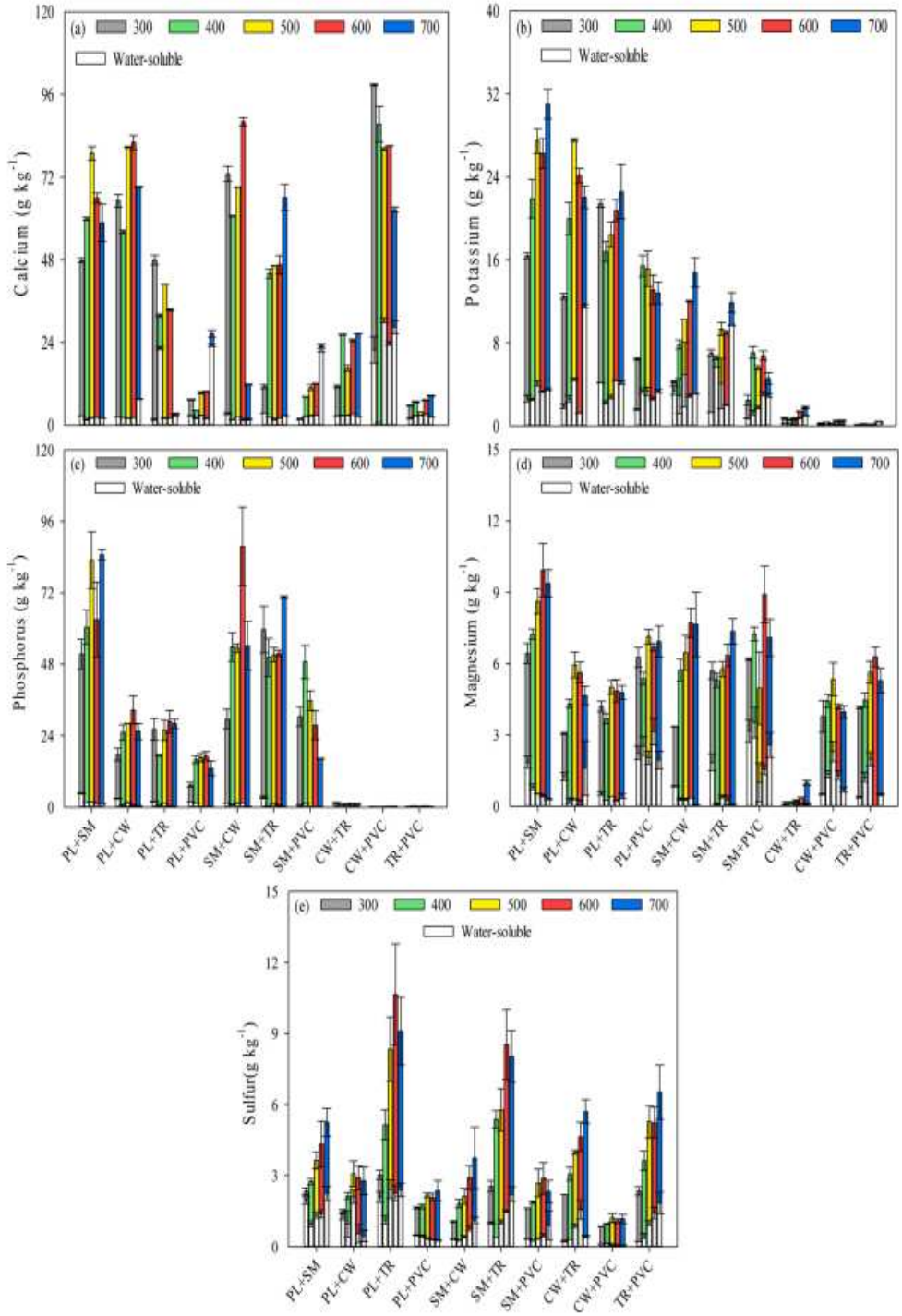

Fig. 3. Averages of total and water-soluble contents of calcium, potassium, phosphorus, magnesium and sulfur of biochars produced in co-pyrolysis of the agricultural wastes poultry litter (PL) and swine manure (SM) and the industrial wastes construction wood (CW), tire (TR) and PVC plastic (PVC), at temperatures of 300, 400, 500, 600 and 700 °C. Error bars represent the standard error of the mean (n = 2).

are concentrated or lost by the effect of pyrolysis temperature [9,67,82, 83]. This effect is related to the degree of feedstock's stability [43] and co-pyrolysis process, and it may be influenced by the synergy that occurs in the different mixtures and by the pyrolysis temperature. Thermal transformations will depend on the different mixtures of feedstocks, and adjustments can be made in the characteristics of the biochars or feedstocks involved in the process and the pyrolysis temperatures [7,84]

3.4. Stability and thermal transformations of biochars

Biochar stability can be inferred based on the degree of carbonization of the pyrolyzed material through elemental ratios of C, H and O [43, 60], using van Krevelen's diagram (Fig. 4). The diagrams enable the evaluation of thermal transformations of the feedstocks, and the interaction of the mixtures between wastes in the co-pyrolysis process.

Increasing the pyrolysis temperature decreased the N, O and H contents of biochars (Table S4). Regardless of the feedstocks used in co-pyrolysis, noticeable changes in elemental composition primarily

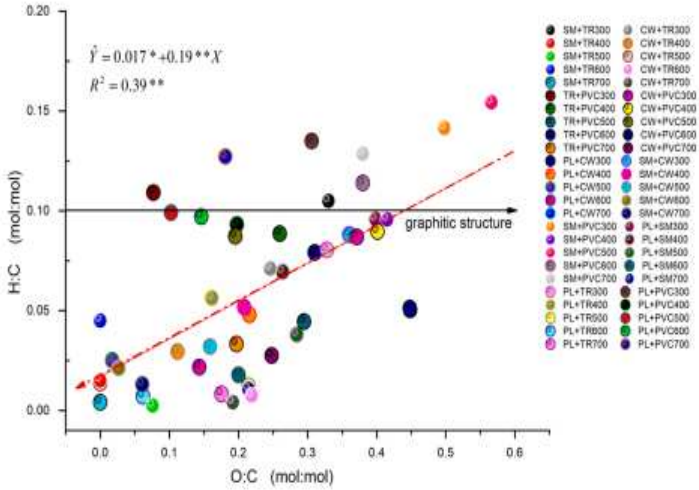

Fig. 4. Molecular ratios H/C and O/C of biochars produced in co-pyrolysis of the agricultural wastes poultry litter (PL) and swine manure (SM) and the industrial wastes construction wood (CW), tire (TR) and PVC plastic (PVC), subjected to pyrolysis temperatures of 300, 400, 500, 600 and 700 °C. Abbreviations of different types of waste followed by subscripts indicate temperature values.

occurred below 500 °C, which can be explained by the aggressive deoxygenation and dehydration reactions during pyrolysis, as reported in other studies [85,86]. The percent content of C in biochar tends to increase at higher pyrolysis temperatures. In the present study, this was observed in all biochars, except in mixtures involving PVC, in which the C content reduced after 400 or 500 °C (Table S4). This is because at temperatures below 450 °C there is great weight loss due to the dehydrochlorination of the PVC plastic, while at higher temperatures (>500 °C) the release of hydrocarbon plays an important role, causing a significant decrease in the C content [87].

The H:C molar ratio decreased faster than that of O:C with increasing temperatures, indicating that H is more easily lost at lower pyrolysis temperatures than O, as observed in our previous study when the feedstocks were individually pyrolyzed [25]. The H:C ratios of all biochars were equal to or lower than 0.15, which indicates high stability or recalcitrance [18,43]. Therefore, co-pyrolysis is a useful tool to improve the stability and properties of the materials, leading to reductions in the molecular ratios H:C and O:C, compared to biochars produced with feedstocks separately [25]. Therefore, the co-pyrolysis enables the design of ideal biochar and enhances its use through higher stability and recalcitrance [43,88].

3.5. X-ray diffraction characterization

It was possible to differentiate crystalline mineral phases between individual biochars and those in co-pyrolysis, revealing crystallinity peaks at different positions [6,89,90]. Also, differences in crystallinity caused by the temperatures could be observed (Fig. 5).

XRD peaks indicating the presence of the following minerals were identified: Quartz (SiO_2) (4.26; 2.02 and 1.80 Å), Sylvite (KCl) (3.12; 2.20 and 1.80 Å), Calcite ($CaCO_3$) (3.86; 2.29 and 2.10 Å), magnesium pyrophosphate ($Mg_2P_2O_7$) (3.04 Å), calcium pyrophosphate ($Ca_2P_2O_7$) (3.34 Å), Dolomite ($CaMg(CO_3)_2$) (2.20 and 2.02 Å), Nephelite ($(Na, K)AlSiO_4$) (4.19 and 2.57 Å), K-feldspar ($KAlSi_3O_8$) (4.26; 4.17 and 3.34 Å), Gypsum ($CaSO_4.2H_2O$) (4.26 and 2.87 Å), Pyrite (FeS_2) (2.20 and 1.63 Å), Graphite (2.10; 2.02 and 1.80 Å), Kainite ($MgSO_4KCl_3H_2O$) (2.18 and 2.10 Å) and Anhydrite (2.87; 2.33 and 1.86 Å). These minerals occurred in all feedstocks and biochars produced in co-pyrolysis, regardless of temperature.

The increase in co-pyrolysis temperature can lead to larger or smaller peaks of some minerals, which indicate an increase or decrease in their quantities (Quartz, Calcite, Dolomite, Sylvite, K-feldspar and Kainite) or even their formation (Gypsum, Nephelite, Anhydrite, Pyrite and Graphite). The increase and decrease of peaks or even the formation of new peaks are consistent with the behavior of the total contents of some elements [37,91], such as Si (not determined), Ca, Mg, K, S and Al (Table S1 and Fig. 3). With the increase of pyrolysis temperature, the peaks of certain minerals disappeared, such as those of K-feldspar (biochars of poultry litter + construction wood and swine manure + PVC plastic), Quartz (biochars construction wood + PVC plastic and tire + PVC plastic) and Graphite (biochar of wine manure + construction wood).

In general, the peaks found in the feedstocks were also present in the corresponding biochars [11,30,92], which confirms the presence of inorganic compounds in the produced biochars [67]. The appearance of graphitic material with increasing temperature and a higher C concentration evidenced the greater stability of biochars [9,90]. Conversely, the increase in these mineral peak sizes suggests increased content with the increment in pyrolysis temperature [90,91], and it may also be associated with the concentration of total elements [91], which can be observed in Fig. 3 and Table S3.

3.6. Functional groups in biochars - FTIR analysis

The transformations that occurred in the feedstocks with the increase in pyrolysis temperature can also be evaluated by FTIR analysis [82,93]. The spectra showed the same bands found in the feedstocks and the individual biochars [25], with differences in the stretching of contrasting functional groups, which is a consequence of changes in the chemical structure of the biochars due to the effect of thermal transformation.

The spectra of biochars indicates that changes in temperature affected several functional groups (Fig. 6). There was elongation, decrease or disappearance of the band related to the functional groups hydroxyl (H), methyl (CH_3) and methylene (CH_2) in the ranges from 3500 to 2800 cm^{-1}; alkyl (CC), nitrile (CN≡≡) and carboxylic acids (C=O) in the range from 2600 to 1600 cm^{-1}; amine (NH— and NH_3), groups containing sulfur (S=O) and aromatic chains (C=C, CO= and CH_2) in bands between 1700 to 1400 cm^{-1}; alkenes (C–H), halogens (C-Cl) and sulfone (SO_2) in the range from 1800 to 500 cm^{-1}; as well as outside the plane of the aromatic chains.

Most of the biochars evaluated showed increments and deformations in the groups alkene (CH) and sulfone (SO_2) in the bands from 1000 to 530 cm^{-1} when temperature increased from 300 to 600 °C, disappearing at 700 °C. On the other hand, a stretching was observed at wavelengths from 2600 to 1300 cm^{-1}, corresponding to the groups alkyl (C≡C), nitrile (CN≡), carboxylic acids (C=O), amine (NH—) and aromatic

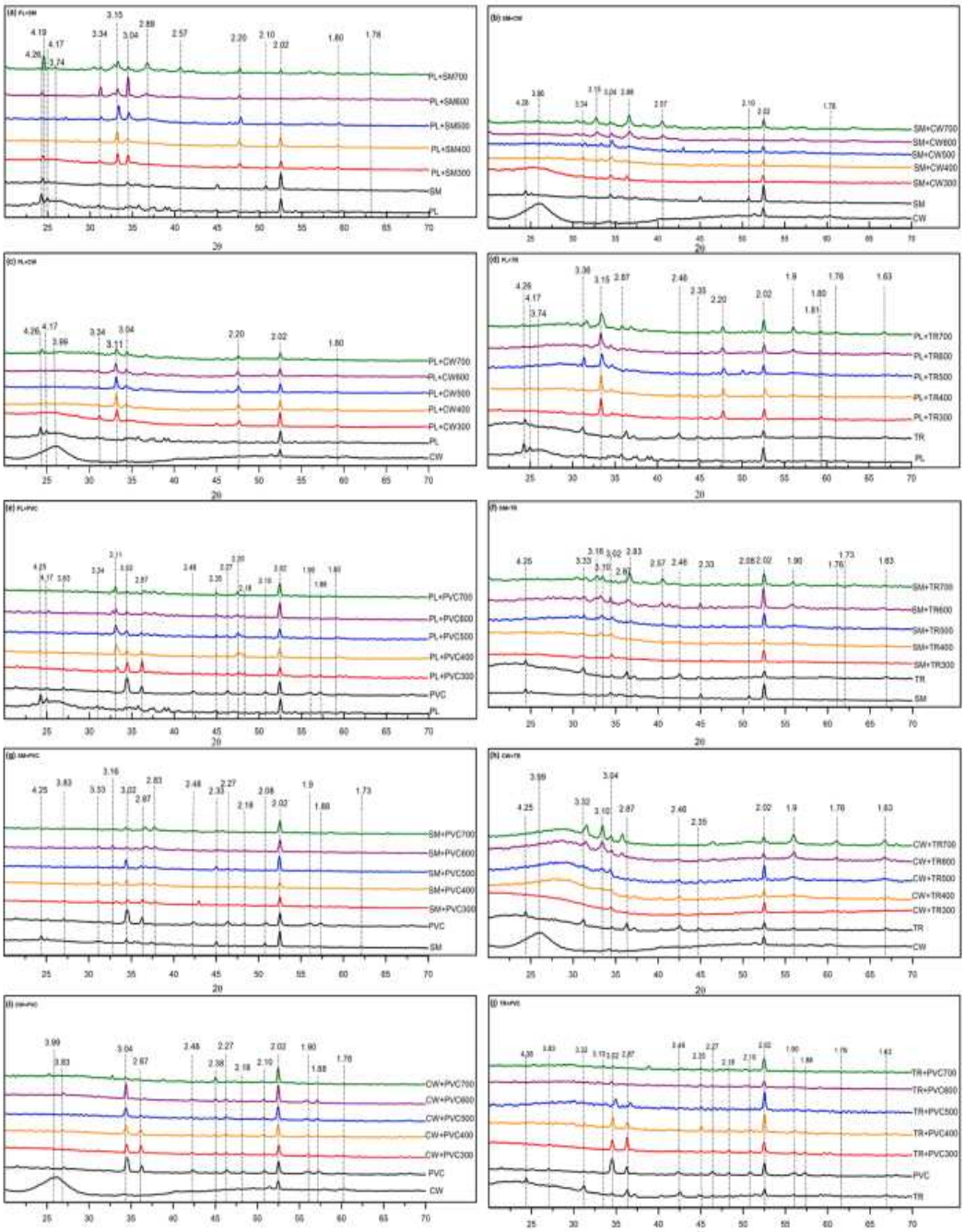

Fig. 5. X-ray diffractograms of biochars produced in co-pyrolysis of the agricultural wastes poultry litter (PL) and swine manure (SM) and the industrial wastes construction wood (CW), tire (TR) and PVC plastic (PVC), at temperatures of 300, 400, 500, 600 and 700 °C.

compounds (C═C) with the temperatures from 400 °C. We also found a reduction in the bands in the range from 3,000–2,800 cm^{-1}, corresponding to the groups methyl (CH_3) and methylene (CH_2), inside and outside the plane of aromatic chains. Groups amide (NH_3) and the double bonds in aromatic chains (C═C and CH_2) in the bands from 1650 to 1400 cm^{-1} from 500 °C showed this similar pattern (Fig. 6).

In bands between 1700 and 1400 cm^{-1}, the biochars showed a reduction in groups of double bonds in aromatic chains (C═O; CC═ and CH_2), amide (NH_3) and stretching of N—H bond of amines (NH_3 and N—H) in the range from 1600 to 1500 cm^{-1}. The group containing sulfur (S═O) showed attenuation of the bands in the range from 2,000–1,300 cm^{-1}, indicating their rapid decomposition as the pyrolysis temperature increased. The groups alkyne (C≡C), nitrile (CN≡), carboxylic acids (C═O), aromatic compounds (C═C) and methylene (CH_2) are outside the plane of the aromatic chains in the range from 2500 to 1400 cm^{-1}, and the groups alkene (C–H), halogens (C-Cl) and sulfone (SO_2) showed a deformation with reduction of peaks compared to those of the feedstocks evaluated (Fig. 5a and b).

The reduction of moisture loss caused by pyrolysis led to decrease of the groups hydroxyl (O—H), methyl (CH_3) and methylene (CH_2) in the range from 3500 to 2800 cm^{-1}, along with the group methylene (CH_2) (outside the aromatic chains), alkene at 1200 cm^{-1}, and alkene (CH) at 1000 cm^{-1}, except for biochars with mixtures of PVC, which showed stretching of the hydroxyl group (OH) in the band from 3500 to 3000 cm^{-1}. This functional group appears in PL, SM and CW wastes and not in PVC wastes, demonstrating a great influence of PVC synergy with the protection of the hydroxyl group (OH) during the co-pyrolysis process. The peak observed at 1620 cm^{-1} in the PL biochars is characteristic of

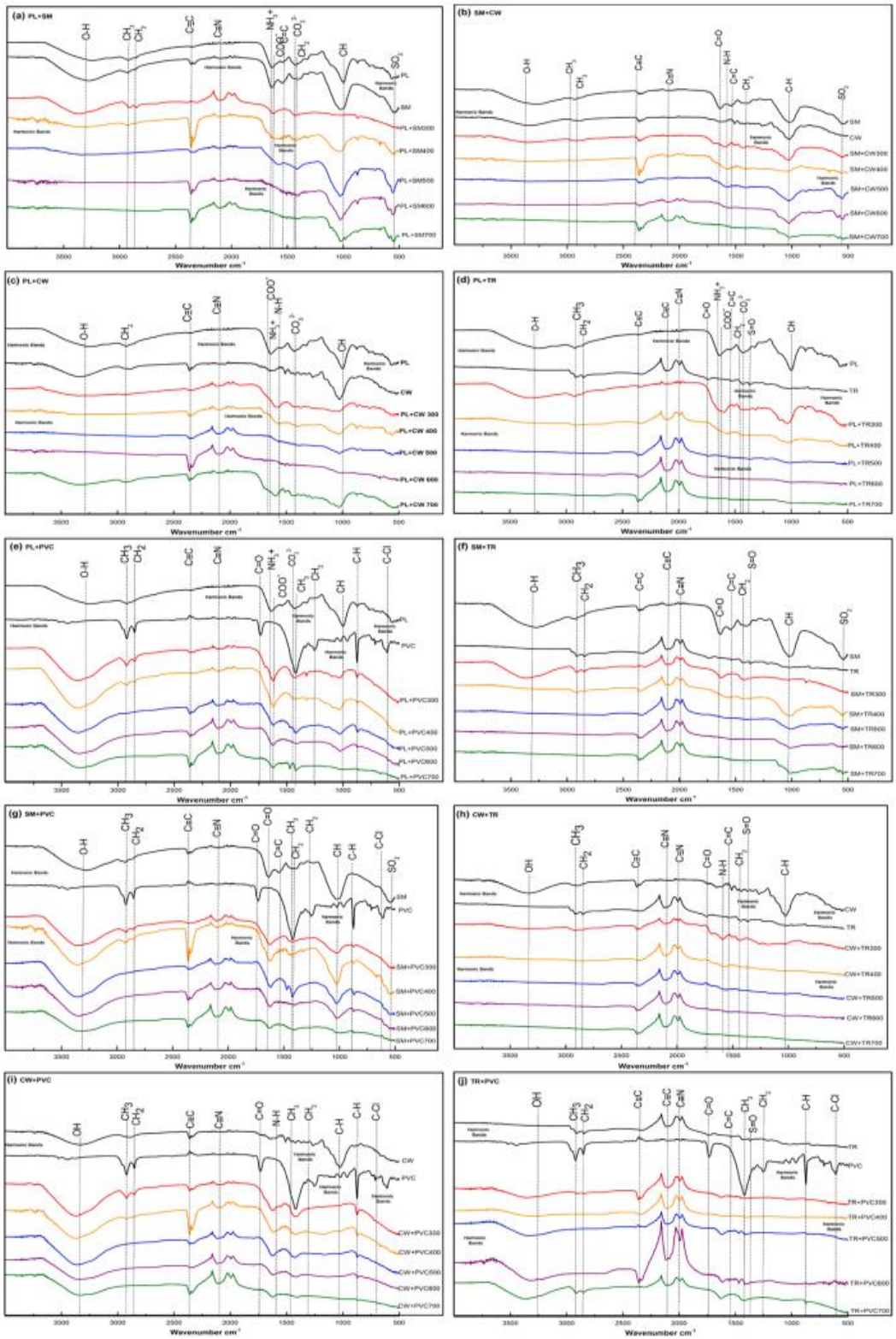

Fig. 6. FTIR spectra of biochars produced in co-pyrolysis of the agricultural wastes poultry litter (PL) and swine manure (SM) and the industrial wastes construction wood (CW), tire (TR) and PVC plastic (PVC), at temperatures of 300, 400, 500, 600 and 700 °C.

aromatic compounds, COO-, ketones, and NH—, and also a peak at 1435 cm^{-1} can be attributed to carbonyl or carbonates (CO_3^{2-}).

Biochars containing mixtures with tire showed reductions in most peaks when compared with peaks in the feedstock of tire. In poultry litter, swine manure, construction wood, tire and PVC there were no peaks of hydroxyl (OH), methyl (CH_3), methylene (CH_2), carboxylic acids (C═O), aromatic compounds (C═C), amine (NH—) and group containing sulfur (S═O), indicating total consumption of these functional groups due to co-pyrolysis process and non-protection by the effect of synergy between materials. Finally, there was deformation of the groups of alkynes (C≡C) and nitrile (CN≡) with the increase in pyrolysis temperature (Fig. 6). The thermal transformations in the biochars

may have occurred because of the release of moisture due to the increase in temperature, resulting in the loss of hydrogen in the case of hydroxyls (H), considered to be compounds of an open and simple chain [83,93]. This condition enables losses of hydrogen in the heating of the co-pyrolysis process, especially above 300 °C, as well as the appearance of aromatic and aliphatic groups, which are related to biochar stability and activity, respectively [94].

The stretching of alkyl (C≡C) and nitrile (CN≡) groups is considered a consequence of the concentration and loss of C, H, N and O, as well as the composition of the feedstocks and their thermal transformation [43, 95,96]. The wastes used and their biochars showed similarities regarding the presence of some functional groups at different pyrolysis temperatures (Fig. 6). The FTIR technique allowed us to observe changes that occurred in the pyrolysis process of the mixtures of materials [82]. The biochars evaluated can be compared regarding the influence that one material has on the other, considering the synergy of co-pyrolysis between feedstocks [11], maintaining or enhancing their properties.

Improving our understanding about the feedstocks and thermal transformations that may occur with different mixtures during co-pyrolysis could help to predict biochar characteristics and design it specifically according to the feedstock and pyrolysis temperature [7,84]. This could promote the effective use of co-pyrolysis as a tool to improve the agronomic and environmental potential of agricultural and industrial solid wastes in generating products to improve the chemical, physical and biological soil characteristics.

Feedstocks and pyrolysis temperature greatly influenced the characteristics of the biochars produced via co-pyrolysis. The use of agricultural wastes in co-pyrolysis process with industrial wastes alleviated the potential environmental risks of heavy metals and drastically reduced the EC in PVC-derived biochars, while improving other physicochemical properties and nutrient content of all biochars derived from industrial wastes. Thus, the co-pyrolysis process of agricultural biomass and industrial waste becomes relevant as it resulted in enhanced biochars and reduces waste disposal problems. In addition, these biochars showed potential to be used for heavy metal remediation, soil acidity correction and fertilization, as well as carbon sequestration.

4. Conclusions

The results of this study indicate that the interaction or synergy between agricultural and industrial materials in co-pyrolysis improves certain properties of biochar that can improve soil quality. Although the co-pyrolysis of PVC with agricultural wastes is effective for reducing high EC, increasing ash content, CEC and WHC of biochars (compared to pure PVC biochar), the major limitation of these biochars is the Pb content above the maximum allowed threshold. Therefore, for wider application of these biochars, especially for crop production, long-term studies about the release and mobility of this toxic element are needed.

The main transformations occur with pyrolysis temperature between 300 and 500 °C due to dehydration of feedstocks and increase in stable carbon forms more resistant to thermal transformations. Biochars produced at 500 °C show high CEC, WHC, alkalinity and high contents of essential elements for plants and could be ideal for use as soil amendment, mainly those produced by mixing agricultural wastes due to their high nutrient content. All biochars have the potential for increasing C storage in soils due their high stability as the aromatic character increases with the pyrolysis temperature, except for biochar mixtures involving PVC.

CRediT authorship contribution statement

José Alexander Rodriguez: Conceptualization, Formal analysis, Investigation, Writing - original draft. **José Ferreira Lustosa Filho:** Writing - review & editing. **Leônidas Carrijo Azevedo Melo:** Conceptualization, Writing - review & editing. **Igor Rodrigues de Assis:** Formal analysis. **Teógenes Senna de Oliveira:** Funding acquisition, Conceptualization, Supervision.

Declaration of Competing Interest

The authors declare that they have no known competing financial interests or personal relationships that could have appeared to influence the work reported in this paper.

Acknowledgements

The authors are grateful to Dr. Jairo Tronto for the XRD analysis. The authors thank the Brazilian agencies Conselho Nacional de Desenvolvimento Científico e Tecnológico (CNPq) and Coordenação de Aperfeiçoamento de Pessoal de Nível Superior (CAPES) for the financial support.

Appendix A. Supplementary data

Supplementary material related to this article can be found, in the online version, at doi:https://doi.org/10.1016/j.jaap.2021.105036.

References

[1] Abrelpe - Associação Brasileira de Empresas de Limpesa Pública e Resíduos Especiais, Panorama dos resíduos sólidos no Brasil, São Paulo, 2014.
[2] Ipea, Plano nacional de resíduos sólidos: diagnóstico dos resíduos urbanos, agrosilvopastoris e a questão dos catadores, 2012.
[3] O.A. Fakayode, E.A.A. Aboagarib, C. Zhou, H. Ma, Co-pyrolysis of lignocellulosic and macroalgae biomasses for the production of biochar – a review, Bioresour. Technol. 297 (2020), 122408, https://doi.org/10.1016/j.biortech.2019.122408.
[4] H. Hassan, J.K. Lim, B.H. Hameed, Recent progress on biomass co-pyrolysis conversion into high-quality bio-oil, Bioresour. Technol. 221 (2016) 645–655, https://doi.org/10.1016/j.biortech.2016.09.026.
[5] Y. Xu, X. Zeng, G. Luo, B. Zhang, P. Xu, M. Xu, H. Yao, Chlorine-Char composite synthesized by co-pyrolysis of biomass wastes and polyvinyl chloride for elemental mercury removal, Fuel 183 (2016) 73–79, https://doi.org/10.1016/j.fuel.2016.06.024.
[6] A. Dewangan, D. Pradhan, R.K. Singh, Co-pyrolysis of sugarcane bagasse and low-density polyethylene: influence of plastic on pyrolysis product yield, Fuel 185 (2016) 508–516, https://doi.org/10.1016/j.fuel.2016.08.011.
[7] J.J. Manyà, M.A. Ortigosa, S. Laguarta, J.A. Manso, Experimental study on the effect of pyrolysis pressure, peak temperature, and particle size on the potential stability of vine shoots-derived biochar, Fuel 133 (2014) 163–172, https://doi.org/10.1016/j.fuel.2014.05.019.
[8] M. Uchimiya, I.M. Lima, K.T. Klasson, L.H. Wartelle, Contaminant immobilization and nutrient release by biochar soil amendment: roles of natural organic matter, Chemosphere 80 (2010) 935–940, https://doi.org/10.1016/j.chemosphere.2010.05.020.
[9] J. Lehmann, S. Joseph, Biochar for Environmental Management: Science, Technology and Implementation, 2 ed, Routledge, London, 2015.
[11] F. Abnisa, W.M.A. Wan Daud, A review on co-pyrolysis of biomass: an optional technique to obtain a high-grade pyrolysis oil, Energy Convers. Manage. 87 (2014) 71–85, https://doi.org/10.1016/j.enconman.2014.07.007.
[12] O. Bičáková, P. Straka, Co-pyrolysis of waste tire/coal mixtures for smokeless fuel, maltenes and hydrogen-rich gas production, Energy Convers. Manage. 116 (2016) 203–213, https://doi.org/10.1016/j.enconman.2016.02.069.
[13] J. Xu, Z. Bai, J. Bai, L. Kong, D. Lv, Y. Han, X. Dai, W. Li, Physico-chemical structure and combustion properties of chars derived from co-pyrolysis of lignite with direct coal liquefaction residue, Fuel 187 (2017) 103–110, https://doi.org/10.1016/j.fuel.2016.09.028.
[14] F.N.D. Mukome, X. Zhang, L.C.R. Silva, J. Six, S.J. Parikh, Use of chemical and physical characteristics to investigate trends in biochar feedstocks, J. Agric. Food Chem. 61 (2013) 2196–2204, https://doi.org/10.1021/jf3049142.
[15] S. Li, S. Harris, A. Anandhi, G. Chen, Predicting biochar properties and functions based on feedstock and pyrolysis temperature : a review and data syntheses, J. Clean. Prod. 215 (2019) 890–902, https://doi.org/10.1016/j.jclepro.2019.01.106.
[16] H. Lu, W. Zhang, S. Wang, L. Zhuang, Y. Yang, R. Qiu, Characterization of sewage sludge-derived biochars from different feedstocks and pyrolysis temperatures, J. Anal. Appl. Pyrolysis 102 (2013) 137–143, https://doi.org/10.1016/j.jaap.2013.03.004.
[17] P. Pariyar, K. Kumari, M.K. Jain, P.S. Jadhao, Evaluation of change in biochar properties derived from different feedstock and pyrolysis temperature for environmental and agricultural application, Sci. Total Environ. 105 (2020), 136433, https://doi.org/10.1016/j.scitotenv.2019.136433.
[18] H. Zhang, C. Chen, E.M. Gray, S.E. Boyd, Effect of feedstock and pyrolysis temperature on properties of biochar governing end use efficacy, Biomass Bioenergy 105 (2017) 136–146, https://doi.org/10.1016/j.biombioe.2017.06.024.

[19] M. Hassan, Y. Liu, R. Naidu, S.J. Parikh, J. Du, F. Qi, I.R. Willett, Influences of feedstock sources and pyrolysis temperature on the properties of biochar and functionality as adsorbents: a meta-analysis, Sci. Total Environ. 744 (2020), 140714, https://doi.org/10.1016/j.scitotenv.2020.140714.

[20] K. Weber, P. Quicker, Properties of biochar, Fuel 217 (2018) 240–261, https://doi.org/10.1016/j.fuel.2017.12.054.

[21] M. Uchimiya, D.I. Bannon, L.H. Wartelle, Retention of heavy metals by carboxyl functional groups of, J. Agric. Food Chem. 60 (2012) 1798–1809, https://doi.org/10.1021/jf2047898.

[22] S. Li, G. Chen, Thermogravimetric, thermochemical, and infrared spectral characterization of feedstocks and biochar derived at different pyrolysis temperatures, Waste Manag. 78 (2018) 198–207, https://doi.org/10.1016/j.wasman.2018.05.048.

[23] K. Intani, S. Latif, Z. Cao, J. Müller, Characterisation of biochar from maize residues produced in a self-purging pyrolysis reactor, Bioresour. Technol. 265 (2018) 224–235, https://doi.org/10.1016/j.biortech.2018.05.103.

[24] R. Subedi, N. Taupe, S. Pelissetti, L. Petruzzelli, C. Bertora, J.J. Leahy, C. Grignani, Greenhouse gas emissions and soil properties following amendment with manure-derived biochars: influence of pyrolysis temperature and feedstock type, J. Environ. Manage. 166 (2016) 73–83, https://doi.org/10.1016/j.jenvman.2015.10.007.

[25] J.A. Rodríguez, J.F. Lustosa Filho, L.C.A. Melo, I.R. de Assis, T.S. de Oliveira, Influence of pyrolysis temperature and feedstock on the properties of biochars produced from agricultural and industrial wastes, J. Anal. Appl. Pyrolysis 149 (2020), 104839, https://doi.org/10.1016/j.jaap.2020.104839.

[26] R.R. Domingues, P.F. Trugilho, C.A. Silva, I.C.N.A. de Melo, L.C.A. Melo, Z. M. Magriotis, M.A. Sánchez-Monedero, Properties of biochar derived from wood and high-nutrient biomasses with the aim of agronomic and environmental benefits, PLoS One 12 (2017), e0176884, https://doi.org/10.1371/journal.pone.0176884.

[27] P. Lu, Q. Huang, A.C. (Thanos) Bourtsalas, Y. Chi, J. Yan, Synergistic effects on char and oil produced by the co-pyrolysis of pine wood, polyethylene and polyvinyl chloride, Fuel 230 (2018) 359–367, https://doi.org/10.1016/j.fuel.2018.05.072.

[28] G. Özsin, A.E. Pütün, TGA/MS/FT-IR study for kinetic evaluation and evolved gas analysis of a biomass/PVC co-pyrolysis process, Energy Convers. Manage. 182 (2019) 143–153, https://doi.org/10.1016/j.enconman.2018.12.060.

[29] L. Wang, M. Chai, R. Liu, J. Cai, Synergetic effects during co-pyrolysis of biomass and waste tire: a study on product distribution and reaction kinetics, Bioresour. Technol. 268 (2018) 363–370, https://doi.org/10.1016/j.biortech.2018.07.153.

[30] M. Bernardo, S. Mendes, N. Lapa, M. Gonçalves, B. Mendes, F. Pinto, H. Lopes, Leaching behaviour and ecotoxicity evaluation of chars from the pyrolysis of forestry biomass and polymeric materials, Ecotoxicol. Environ. Saf. 107 (2014) 9–15, https://doi.org/10.1016/j.ecoenv.2014.05.007.

[31] S.D.A. Sharuddin, F. Abnisa, W.M.A. Wan Daud, M.K. Aroua, A review on pyrolysis of plastic wastes, Energy Convers. Manage. 115 (2016) 308–326, https://doi.org/10.1016/j.enconman.2016.02.037.

[32] Abrelpe - Associação Brasileira de Empresas de Limpesa Pública e Resíduos Especiais, Estimativas Dos Custos Para Viabilizar a Universalização Da Destinação, São Paulo, 2015.

[33] A.C.A. Orrico, N.D.S. Sunada, J. De Lucas Junior, M.A.P. Orrico Junior, A. W. Schwingel, Codigestão anaeróbia de dejetos de suínos e níveis de inclusão de óleo de descarte, Eng. Agric. 35 (2015) 657–664, https://doi.org/10.1590/1809-4430-Eng.Agríc.v35n4p657-664/2015.

[34] Z. Qiu, Y. Zhai, S. Li, X. Liu, X. Liu, B. Wang, Y. Liu, C. Li, Y. Hu, Catalytic co-pyrolysis of sewage sludge and rice husk over biochar catalyst: bio-oil upgrading and catalytic mechanism, Waste Manag. 114 (2020) 225–233, https://doi.org/10.1016/j.wasman.2020.07.013.

[35] J. Zhang, J. Jin, M. Wang, R. Naidu, Y. Liu, Y.B. Man, X. Liang, M.H. Wong, P. Christie, Y. Zhang, C. Song, S. Shan, Co-pyrolysis of sewage sludge and rice husk/ bamboo sawdust for biochar with high aromaticity and low metal mobility, Environ. Res. 191 (2020), 110034, https://doi.org/10.1016/j.envres.2020.110034.

[36] H. jun Huang, T. Yang, F. ying Lai, G. qiang Wu, Co-pyrolysis of sewage sludge and sawdust/rice straw for the production of biochar, J. Anal. Appl. Pyrolysis 125 (2017) 61–68, https://doi.org/10.1016/j.jaap.2017.04.018.

[37] A. Shaaban, S.-M. Se, M.F. Dimin, J.M. Juoi, M.H. Mohd Husin, N.M.M. Mitan, Influence of heating temperature and holding time on biochars derived from rubber wood sawdust via slow pyrolysis, J. Anal. Appl. Pyrolysis 107 (2014) 31–39, https://doi.org/10.1016/j.jaap.2014.01.021.

[38] ASTM Standard D3172-13, Standard Practice for Proximate Analysis of Coal and Coke, ASTM International, West Conshohocken, 2013, https://doi.org/10.1520/D3172-13.2.

[39] I.B.I. IBI, Standardized Product Definition and Product Testing Guidelines for Biochar That Is Used in Soil, International Biochar Initiative, 2015. http://www.biochar-international.org/sites/default/files/Guidelines_for_Biochar_That_Is_Used_in_Soil_Final.pdf.

[40] T.Q. Zorzeto, S.C.F. Dechen, M.F. de Abreu, F. Fernandes Júnior, Caracterização física de substratos para plantas, Bragantia 73 (2014) 300–311, https://doi.org/10.1590/1678-4499.0086.

[41] C.E. Brewer, V.J. Chuang, C.A. Masiello, H. Gonnermann, X. Gao, B. Dugan, L. E. Driver, P. Panzacchi, K. Zygourakis, C.A. Davies, New approaches to measuring biochar density and porosity, Biomass Bioenergy 66 (2014) 176–185, https://doi.org/10.1016/j.biombioe.2014.03.059.

[42] ASTM Standard D1762-84, Standard Test Method for Chemical Analysis of Wood Charcoal, ASTM International, West Conshohocken, 2007, https://doi.org/10.1520/D1762-84R07.2.

[43] A. Enders, K. Hanley, T. Whitman, S. Joseph, J. Lehmann, Characterization of biochars to evaluate recalcitrance and agronomic performance, Bioresour. Technol. 114 (2012) 644–653, https://doi.org/10.1016/j.biortech.2012.03.022.

[44] K. Jindo, K. Suto, K. Matsumoto, C. García, T. Sonoki, M.A. Sanchez-Monedero, Chemical and biochemical characterisation of biochar-blended composts prepared from poultry manure, Bioresour. Technol. 110 (2012) 396–404, https://doi.org/10.1016/j.biortech.2012.01.120.

[45] M.I. Al-Wabel, A. Al-Omran, A.H. El-Naggar, M. Nadeem, A.R.A. Usman, Pyrolysis temperature induced changes in characteristics and chemical composition of biochar produced from conocarpus wastes, Bioresour. Technol. 131 (2013) 374–379, https://doi.org/10.1016/j.biortech.2012.12.165.

[46] G.E. Rayment, D.J. Lyon, Soil Chemical Methods - Australasia, CSIRO Publishing, Collingwood, Australia, 2010.

[47] W. Song, M. Guo, Quality variations of poultry litter biochar generated at different pyrolysis temperatures, J. Anal. Appl. Pyrolysis 94 (2012) 138–145, https://doi.org/10.1016/j.jaap.2011.11.018.

[48] N. Prakongkep, R.J. Gilkes, W. Wiriyakitnateekul, Forms and solubility of plant nutrient elements in tropical plant waste biochars, J. Plant Nutr. Soil Sci. 178 (2015) 732–740, https://doi.org/10.1002/jpln.201500001.

[49] A. Enders, J. Lehmann, Comparison of wet-digestion and dry-ashing methods for total elemental analysis of biochar, Commun. Soil Sci. Plant Anal. 43 (2012) 1042–1052, https://doi.org/10.1080/00103624.2012.656167.

[50] P.Y. Chen, Table of key lines in x ray powder diffraction patterns of minerals in clays and assocated rocks, Dep. Nat. Resour. Geol. Surv. Occas. Pap. 21 (1977) 77, internal-pdf://op21-1614768640/OP21.pdf.

[51] L.C.A. Barbosa, Espectroscopia no infravermelho na caracterização de compostos orgânicos, Editora UFV, Viçosa, 2011.

[52] S. Li, G. Chen, Thermogravimetric, thermochemical, and infrared spectral characterization of feedstocks and biochar derived at different pyrolysis temperatures, Waste Manag. 78 (2018) 198–207, https://doi.org/10.1016/j.wasman.2018.05.048.

[53] Y. Matsuzawa, M. Ayabe, J. Nishino, Acceleration of cellulose co-pyrolysis with polymer, Polym. Degrad. Stab. 71 (2001) 435–444, https://doi.org/10.1016/S0141-3910(00)00195-6.

[54] M. Xu, C. Sheng, Influences of the Heat-Treatment Temperature and Inorganic Matter on Combustion Characteristics of Cornstalk Biochars, 2012, pp. 209–218.

[55] Y. Yang, K. Sun, L. Han, J. Jin, H. Sun, Y. Yang, B. Xing, Chemosphere Effect of minerals on the stability of biochar, Chemosphere 204 (2018) 310–317, https://doi.org/10.1016/j.chemosphere.2018.04.057.

[56] J.H. Windeatt, A.B. Ross, P.T. Williams, P.M. Forster, M.A. Nahil, S. Singh, Characteristics of biochars from crop residues: potential for carbon sequestration and soil amendment, J. Environ. Manage. 146 (2014) 189–197, https://doi.org/10.1016/j.jenvman.2014.08.003.

[57] J. Jin, Y. Li, J. Zhang, S. Wu, Y. Cao, P. Liang, J. Zhang, M.H. Wong, M. Wang, S. Shan, P. Christie, Influence of pyrolysis temperature on properties and environmental safety of heavy metals in biochars derived from municipal sewage sludge, J. Hazard. Mater. 320 (2016) 417–426, https://doi.org/10.1016/j.jhazmat.2016.08.050.

[58] S. Taherymoosavi, S. Joseph, B. Pace, P. Munroe, A comparison between the characteristics of single- and mixed-feedstock biochars generated from wheat straw and basalt, J. Anal. Appl. Pyrolysis 129 (2018) 123–133, https://doi.org/10.1016/j.jaap.2017.11.020.

[59] L. Fryda, R. Visser, Biochar for soil improvement: evaluation of biochar from gasification and slow pyrolysis, Agriculture 5 (2015) 1076–1115, https://doi.org/10.3390/agriculture5041076.

[60] A.T. Tag, G. Duman, S. Ucar, J. Yanik, Effects of feedstock type and pyrolysis temperature on potential applications of biochar, J. Anal. Appl. Pyrolysis 120 (2016) 200–206, https://doi.org/10.1016/j.jaap.2016.05.006.

[61] J.M. Novak, W.J. Busscher, D.L. Laird, M. Ahmedna, D.W. Watts, M.A.S. Niandou, Impact of biochar amendment on fertility of a southeastern coastal plain soil, Soil Sci. 174 (2009) 105–112, https://doi.org/10.1097/SS.0b013e3181981d9a.

[62] M. Irfan, Q. Chen, Y. Yue, R. Pang, Q. Lin, X. Zhao, H. Chen, Co-production of biochar, bio-oil and syngas from halophyte grass (Achnatherum splendens L.) under three different pyrolysis temperatures, Bioresour. Technol. 211 (2016) 457–463, https://doi.org/10.1016/j.biortech.2016.03.077.

[63] X. Zhang, P. Zhang, X. Yuan, Y. Li, L. Han, Effect of pyrolysis temperature and correlation analysis on the yield and physicochemical properties of crop residue biochar, Bioresour. Technol. 296 (2020), 122318, https://doi.org/10.1016/j.biortech.2019.122318.

[64] D. Huang, L. Yang, J.H. Ko, Q. Xu, Comparison of the methane-oxidizing capacity of landfill cover soil amended with biochar produced using different pyrolysis temperatures, Sci. Total Environ. 693 (2019), 133594, https://doi.org/10.1016/j.scitotenv.2019.133594.

[65] W. Suliman, J.B. Harsh, N.I. Abu-Lail, A.M. Fortuna, I. Dallmeyer, M. Garcia-Perez, Influence of feedstock source and pyrolysis temperature on biochar bulk and surface properties, Biomass Bioenergy 84 (2016) 37–48, https://doi.org/10.1016/j.biombioe.2015.11.010.

[66] M. Carrier, A.G. Hardie, Ü. Uras, J. Görgens, J. Knoetze, Production of char from vacuum pyrolysis of South-African sugar cane bagasse and its characterization as activated carbon and biochar, J. Anal. Appl. Pyrolysis 96 (2012) 24–32, https://doi.org/10.1016/j.jaap.2012.02.016.

[67] X. Gai, H. Wang, J. Liu, L. Zhai, S. Liu, T. Ren, H. Liu, Effects of feedstock and pyrolysis temperature on biochar adsorption of ammonium and nitrate, PLoS One 9 (2014), e113888, https://doi.org/10.1371/journal.pone.0113888.

[68] E. Mészáros, E. Jakab, G. Várhegyi, J. Bourke, M. Manley-Harris, T. Nunoura, M. J. Antal, Do all carbonized charcoals have the same chemical structure? 1.

Implications of thermogravimetry-mass spectrometry measurements, Ind. Eng. Chem. Res. 46 (2007) 5943–5953, https://doi.org/10.1021/ie0615842.
[69] P. Cely, G. Gascó, J. Paz-Ferreiro, A. Méndez, Agronomic properties of biochars from different manure wastes, J. Anal. Appl. Pyrolysis 111 (2015) 173–182, https://doi.org/10.1016/j.jaap.2014.11.014.
[70] A.S. Lopes, L.R. Guilherme, L.R. Guimarães Guilherme, A career perspective on soil management in the cerrado region of Brazil, Adv. Agron. 137 (2016) 1–72, https://doi.org/10.1016/bs.agron.2015.12.004.
[71] R.R. Domingues, M.A. Sánchez-Monedero, K.A. Spokas, L.C.A. Melo, P.F. Trugilho, M.N. Valenciano, C.A. Silva, Enhancing Cation Exchange Capacity of Weathered Soils Using Biochar: Feedstock, Pyrolysis Conditions and Addition Rate, Agronomy 10 (2020) 824, https://doi.org/10.3390/agronomy10060824.
[72] J.R. Silva, M. Gastauer, S.J. Ramos, S.K. Mitre, A.E. Furtini Neto, J.O. Siqueira, C. F. Caldeira, Initial growth of Fabaceae species: combined effects of topsoil and fertilizer application for mineland revegetation, Flora 246–247 (2018) 109–117, https://doi.org/10.1016/j.flora.2018.08.001.
[73] G. Fellet, L. Marchiol, G. Delle Vedove, A. Peressotti, Application of biochar on mine tailings: effects and perspectives for land reclamation, Chemosphere 83 (2011) 1262–1267, https://doi.org/10.1016/j.chemosphere.2011.03.053.
[74] G. Xu, L.L. Wei, J.N. Sun, H.B. Shao, S.X. Chang, What is more important for enhancing nutrient bioavailability with biochar application into a sandy soil: Direct or indirect mechanism? Ecol. Eng. 52 (2013) 119–124, https://doi.org/10.1016/j.ecoleng.2012.12.091.
[75] S. Kizito, H. Luo, J. Lu, H. Bah, R. Dong, S. Wu, Role of nutrient-enriched biochar as a soil amendment during maize growth: exploring practical alternatives to recycle agricultural residuals and to reduce chemical fertilizer demand, Sustainability 11 (2019) 3211, https://doi.org/10.3390/su11113211.
[76] N. Brady, R. Weil, The Nature and Properties of Soils, 13th ed, Prentice Hall, Upper Saddle River, NJ, 2002.
[77] K. Wang, N. Peng, G. Lu, Z. Dang, Effects of Pyrolysis Temperature and Holding Time on Physicochemical Properties of Swine-Manure-Derived Biochar, Waste Biomass Valorization 11 (2020) 613–624, https://doi.org/10.1007/s12649-018-0435-2.
[78] T. Qian, X. Zhang, J. Hu, H. Jiang, Effects of environmental conditions on the release of phosphorus from biochar, Chemosphere 93 (2013) 2069–2075, https://doi.org/10.1016/j.chemosphere.2013.07.041.
[79] J.F. Lustosa Filho, E.S. Penido, P.P. Castro, C.A. Silva, L.C.A. Melo, Co-pyrolysis of poultry litter and phosphate and magnesium generates alternative slow-release fertilizer suitable for tropical soils, ACS Sustain. Chem. Eng. 5 (2017) 9043–9052, https://doi.org/10.1021/acssuschemeng.7b01935.
[80] H.L. Scott, D. Atkinson, C.J. Ponsonby, Biochar an improver of nutrient and soil water availability – what is the evidence? CAB Rev. Perspect. Agric. Vet. Sci. Nutr. Nat. Resour. 9 (2014) 1–19.
[81] S. Chandra, J. Bhattacharya, In fl uence of temperature and duration of pyrolysis on the property heterogeneity of rice straw biochar and optimization of pyrolysis conditions for its application in soils, J. Clean. Prod. 215 (2019) 1123–1139, https://doi.org/10.1016/j.jclepro.2019.01.079.
[82] X. Dong, T. Guan, G. Li, Q. Lin, X. Zhao, Long-term effects of biochar amount on the content and composition of organic matter in soil aggregates under field conditions, J. Soils Sediments 16 (2016) 1481–1497, https://doi.org/10.1007/s11368-015-1338-5.
[83] T. Mimmo, P. Panzacchi, M. Baratieri, C.A. Davies, G. Tonon, Effect of pyrolysis temperature on miscanthus (Miscanthus × giganteus) biochar physical, chemical and functional properties, Biomass Bioenergy 62 (2014) 149–157, https://doi.org/10.1016/j.biombioe.2014.01.004.
[84] D. Angın, S. Şensöz, Effect of pyrolysis temperature on chemical and surface properties of biochar of rapeseed (Brassica napus L.), Int. J. Phytoremediation 16 (2014) 684–693, https://doi.org/10.1080/15226514.2013.856842.
[85] S. Wang, H. Zhang, H. Huang, R. Xiao, R. Li, Z. Zhang, Influence of temperature and residence time on characteristics of biochars derived from agricultural residues: a comprehensive evaluation, Process Saf. Environ. Prot. 139 (2020) 218–229, https://doi.org/10.1016/j.psep.2020.03.028.
[86] A. Nzihou, B. Stanmore, N. Lyczko, D.P. Minh, The catalytic effect of inherent and adsorbed metals on the fast/flash pyrolysis of biomass: a review, Energy 170 (2019) 326–337, https://doi.org/10.1016/j.energy.2018.12.174.
[87] J. Zhou, B. Gui, Y. Qiao, J. Zhang, W. Wang, H. Yao, Y. Yu, M. Xu, Understanding the pyrolysis mechanism of polyvinylchloride (PVC) by characterizing the chars produced in a wire-mesh reactor, Fuel 166 (2016) 526–532.
[88] C.E. Brewer, R. Unger, K. Schmidt-Rohr, R.C. Brown, Criteria to select biochars for field studies based on biochar chemical properties, Bioenergy Res. 4 (2011) 312–323, https://doi.org/10.1007/s12155-011-9133-7.
[89] S. Fang, Z. Yu, Y. Lin, Y. Lin, Y. Fan, Y. Liao, X. Ma, A study on experimental characteristic of co-pyrolysis of municipal solid waste and paper mill sludge with additives, Appl. Therm. Eng. 111 (2017) 292–300, https://doi.org/10.1016/j.applthermaleng.2016.09.102.
[90] J.-H. Yuan, R.-K. Xu, H. Zhang, The forms of alkalis in the biochar produced from crop residues at different temperatures, Bioresour. Technol. 102 (2011) 3488–3497, https://doi.org/10.1016/j.biortech.2010.11.018.
[91] B. Acharya, A. Dutta, S. Mahmud, M. Tushar, M. Leon, Ash analysis of poultry litter, Willow and oats for combustion in boilers, J. Biomass Biofuel. 1 (2014), https://doi.org/10.11159/jbb.2014.003.
[92] S.-Y. Oh, J.-G. Son, P.C. Chiu, Biochar-mediated reductive transformation of nitro herbicides and explosives, Environ. Toxicol. Chem. 32 (2013) 501–508, https://doi.org/10.1002/etc.2087.
[93] Y. Liu, Z. He, M. Uchimiya, Comparison of biochar formation from various agricultural by-products using FTIR spectroscopy, Mod. Appl. Sci. 9 (2015) 246–253, https://doi.org/10.5539/mas.v9n4p246.
[94] R. Singh, D. Pant, Polyvinyl chloride degradation by hybrid (chemical and biological) modification, Polym. Degrad. Stab. 123 (2016) 80–87, https://doi.org/10.1016/j.polymdegradstab.2015.11.012.
[95] L. Beesley, E. Moreno-Jiménez, J.L. Gomez-Eyles, E. Harris, B. Robinson, T. Sizmur, A review of biochars' potential role in the remediation, revegetation and restoration of contaminated soils, Environ. Pollut. 159 (2011) 3269–3282, https://doi.org/10.1016/j.envpol.2011.07.023.
[96] F. Lian, F. Huang, W. Chen, B. Xing, L. Zhu, Sorption of apolar and polar organic contaminants by waste tire rubber and its chars in single- and bi-solute systems, Environ. Pollut. 159 (2011) 850–857, https://doi.org/10.1016/j.envpol.2011.01.002.

CAPÍTULO 3

CLASSIFYING THE POTENTIAL OF BIOCHARS FROM AGRICULTURAL AND INDUSTRIAL WASTE FOR THE RECOVERY OF Fe AND Mn MINING TAILINGS

José Alexander Rodrigueza, c, José Ferreira Lustosa Filhoa*, Leônidas Carrijo Azevedo Melob, Igor Rodrigues de Assisa, Teógenes Senna de Oliveiraa

a Department of Soil, Federal University of Viçosa, 36570-900 Viçosa, MG, Brazil
b Soil Science Department, Federal University of Lavras, 37200-900, Lavras, MG, Brazil
c Faculty of Veterinary Medicine and Zootechnics, Autonomous University Foundation of the Americas, South Avenue 98-56, Pereira, R/da, Colombia
* Corresponding authors:
E-mail addresses: filhoze04@hotmail.com; Phone: (31) 3612 3033; Fax: (31) 3612 4540.

Abstract

Various agricultural and industrial wastes have been used for biochar production. However, a consistent stratification method for agronomic and environmental purposes for biochar use is still missing. The objective was to propose and evaluate a stratification method based on physical and chemical properties. A set of biochar samples was produced by pyrolysis and co-pyrolysis from two agricultural wastes (poultry litter - PL and swine manure - SM) and three industrial wastes (construction wood - CW, tire - TR and PVC plastic - PVC) at a wide range of pyrolysis temperatures (300-700 °C). The stratification proposed considered the following criteria in order: (i) construction of a biochar viability indicator (IVB); (ii) classification of the potential of biochars based on fixed carbon, ash and volatile matter; (iii) joint use of the biochar quality criteria and those established in the literature (e.g. International Biochar Initiative - IBI); and (iv) the restrictive conditions of the environment where biochar could be applied aiming at the development of plants, in this case, we used mining tailings. Using the proposed stratification method, PL+CW pyrolyzed at 300 °C was chosen for the recovery of Fe and Mn mining tailings, due to its intermediate fertility level and very low risk of environmental pollution. The proposed method allowed the identification of restrictions for biochar use, and most importantly highlighted the potential of the most viable biochars for conditioning the mining tailings, which are difficult for plant growth. However, despite being useful and efficient in the selection of the biochar, the proposed methods are still dependent on the physicochemical characteristics of the biochars.

Keywords: Pyrolysis, co-pyrolysis, immediate analysis, principal components.

1. Introduction

The fast growth of the human population and its consumption habits produces high quantities of solid waste, which can cause environmental problems in urban, rural and industrial areas (Kebede et al., 2021). The potential environmental problems with the inadequate disposal and accumulation leads to the need to create sustainable solutions for their management and reuse (Kebede et al., 2021; Manríquez-Altamirano et al., 2020).

Pyrolysis and co-pyrolysis can be an alternative for the reuse of agricultural or industrial wastes by transforming them into a value-added material as biochar (Chew et al., 2021; Hassan et al., 2016). Biochar is the solid by-product of biomass thermochemical conversion under limited supply of oxygen (Lehmann and Joseph, 2015), that when applied to soil has many beneficial functions, including: carbon sequestration (Majumder et al., 2019; Mimmo et al., 2014), adsorption of organic and inorganic contaminants (Shaaban and Abid, 2021), water retention, cation exchange capacity and nutrient cycling (Dai et al., 2020; Mukherjee et al., 2011), reduction of nutrient leaching (Schulz et al., 2013) and improved soil structure and drainage, and interactions with microbial communities (Jeffery et al., 2011; Wang et al., 2021).

The physical and chemical properties of biochar is greatly influenced by the nature and physical state of the feedstock, as well as by the production conditions, specifically pyrolysis temperature, amount of oxygen and residence time (Li et al., 2019; Lu et al., 2013; Pariyar et al., 2020; Rodriguez et al., 2020; Zhang et al., 2017). These conditions leads to a high diversity of biochars from the same materials, affecting the intensity and type of functions to be exerted and the dependence of the interactions with soil in its conditioning (Marta Camps-Arbestain et al., 2015).

Due to the high variability in biochar characteristics, a classification system is needed such that express the main positive or negative aspects for specific uses of biochar and stablish criteria to improve agricultural or environmental soil functions. There are methodologies of classification that considers specific properties of biochar, especially by using fast and easy identification properties, such as the proximate analysis (ash, volatile and fixed carbon content) (Enders et al., 2012). Furthermore, it is possible to identify the biochar by the main chemical and physical limiting soil conditions to be conditioned (Marta Camps-Arbestain et al., 2015). Multivariate methods are considered an alternative when a number of biochars properties is available. These methods have a vast application in different areas and considers the integration

and reduction of variables, which differentiate groups of biochar and create appropriate indexes for a defined purpose (Templeton, 2011), which allow some anticipation of biochar conditioning effects in soil.

Classification methods can also be useful for biochar production aiming to design the characteristics for specific purposes. For instance, degraded soils such as those impacted by mining activities require specific biochar characteristics to improve their quality and allow revegetation (Penido et al., 2019; Puga et al., 2015). We hypothesized that the biochar stratification methods developed through four successive methods, considering the characteristics of the biochars produced and the restrictions for plant growth in Fe and Mn mining tailings could be adopted as a useful predictive system. An intended outcome is a biochar classification systems framework that can provide initial guidance for producers/researchers regarding the choice of feedstocks and pyrolysis temperature and specific purposes. The objective was to propose and evaluate classification methods for biochar of a diverse set of characteristics. It is expected that regardless the type of material used for biochar production, that choices and/or interpretations of its quality and uses are more efficient, especially of residues of difficult final destination.

2. Material and methods

2.1. Selection of wastes used

The feedstocks used for biochar production were selected by consulting state inventories of agricultural and industrial solid wastes in Brazil according to the 2012 National Solid Waste Plan and the 2015 Solid Waste Panorama Report (Abrelpe, 2015; Ipea, 2012). Two agricultural wastes (poultry litter and swine manure) were selected to represent animal wastes commonly used in agriculture and three industrial solid wastes (construction wood, tire and PVC plastic) to represent wastes generated in high amounts and misused in general. Besides that, we aimed to select feedstocks with contrasting physical and chemical attributes. In addition, these five different biomasses were chosen because of their locally and global quantitative significance. Agricultural residues are rich in nutrients and can be used as organic fertilizers. However, if applied in natura, they can act as vectors of animal diseases and might become a source of pollution (Ayilara et al., 2020; Nor Faiza et al., 2019). Therefore, they must first go through composting process or some other process capable of eliminating undesirable effects (Ayilara et al., 2020). Industrial wastes are generated in large quantities and mostly are discarded in

public landfills or disposed directly into the environment, which might lead to water and soil contamination due to the presence of toxic elements and pathogens (Abdel-Shafy and Mansour, 2018). Detailed information about the wastes used in this study and collection locations can be found elsewhere (Rodriguez et al., 2020). The characteristics of these wastes are described in Table S1 in the supplementary material.

2.2. Production and characteristics of biochars

The feedstocks were ground, sieved in 4-mm and dried at 65 ºC for 48 h in an oven. Each feedstock was pyrolyzed individually or co-pyrolyzed in homogenous mixtures that were prepared as the following: poultry litter (PL) + swine manure (SM), poultry litter (PL) + construction wood (CW), poultry litter (PL) + tire (TR), poultry litter (PL) + PVC, swine manure (SM) + construction wood (CW), swine manure (SM) + tire (TR), swine manure (SM) + PVC, construction wood (CW) + tire (TR), construction wood (CW) + PVC and tire (TR) + PVC. The feedstocks or their mixtures were placed in hermetically closed stainless steel cylinders (10.6 cm diameter and 42 cm height) and placed in an adapted muffle furnace that allows the release of gases during pyrolysis and collection of bio-oil. Details of the pyrolysis system can be found in Lustosa Filho et al. (2017). Pyrolysis was carried out at temperatures of 300, 400, 500, 600 and 700 °C, with a heating rate of 10 °C min-1 and one h of holding time at the desired temperature (Shaaban et al., 2014). A total of 75 samples was prepared (25 from individual feedstocks and 50 from the mixtures). The biochar samples were presented as the initials of the feedstocks followed by the corresponding pyrolysis temperature (e.g., PL+SM300, abbreviation for biochar produced from poultry litter + swine manure pyrolyzed at 300 °C).

The physical analyses were performed using 100 g of each biochar in triplicates to determine: (i) biochars yield were calculated based on a mass balance using following equation: $\text{Yield} = \frac{\text{Mbiochar}}{\text{Mfeedstock}} \text{x } 100\%$, where Mbiochar and Mfeedstock are the mass (g) of biochar and original feedstocks, respectively; (ii) mean weight diameter of particles determined from the distribution of particles according to the International Biochar Initiative (IBI, 2015); and (iii) water holding capacity determined in a pressure chamber at 33 kPa for 72 h (Zorzeto et al., 2014). For the chemical analyses, biochar samples were ground and passed through a 60-mesh sieve (0.25 mm), oven-dried at 65 °C ± 2 °C for 48 h to remove moisture and standardize its content to <10% (Brewer et al., 2014), and the following attributes were measured: volatile

matter content (ASTM, 2007), modified by Enders et al. (2012); ash content (ASTM, 2007); fixed carbon content (ASTM, 2013); C, H, N and O in elemental analyzer (Jindo et al., 2012); electrical conductivity and pH in water by potentiometry in 1:20 solution, after resting for 12-h and stirring of suspension (Al-Wabel et al., 2013); neutralizing power determined by the acid/base titrimetric method (Rayment and Lyon, 2010); cation exchange capacity determined by the method of saturation with NH4OAC (1.0 mol L-1) and NH4+ measured colorimetrically (Song and Guo, 2012); contents of elements both soluble in water (Ca, K, P, Mg and S) (Prakongkep et al., 2015) and total (Ca, K, P, Mg, S, Fe, Mn, Zn, Mo, B, Al, Cu, As, Pb, Cd, and Cr) (Enders and Lehmann, 2012). After extraction, K was determined by flame photometry, Ca by atomic absorption spectroscopy and the other elements by inductively coupled plasma atomic emission spectroscopy (ICP-AES).

2.3. Stratification of biochars

The selection of biochar followed four successive methods, considering the characteristics of the biochars produced and the restrictions for plant growth on soil/substrate (i.e. Fe and Mn mining tailings).

Firstly, it was considered the "classification by the intrinsic characteristics of the biochars" through a biochar viability indicator (BVI), generated from determined characteristics and multivariate statistical methods. Biochars with higher BVI values were then considered in the second method of "biochar classification by proximate analysis", which relates the biochar properties with the content of fixed carbon, ash and volatile matter (Enders et al., 2012; Lu et al., 2014). The stratification of the biochar agricultural and environmental potential was done in a triangle using pre-established limits by Enders et al. (2012) and Trompowsky et al. (2005).Then, the biochar was further selected by quality criteria proposed by Camps-Arbestain et al. (2015) and by the International Biochar Iniative (IBI, 2015). Finally, the biochar was classified by the "restrictive properties of soils/substrates" to be corrected. The details of each classification method are explained below.

2.3.1. Classification by the intrinsic characteristics of the biochars

The results of the biochar characterisation were submitted to analysis of variance (ANOVA) to determine any significant differences ($p < 0.05$) between the biochars produced by pyrolysis and by co-pyrolysis at different temperatures (total of 75 biochars). Attributes not influenced by the temperature were not further considered in the classification system. The data

were transformed into percentiles to follow a normal distribution and the inverse of normal distribution created variables with normally distributed scores, resulting in the probability of a uniform distribution (Templeton, 2011).

The only components selected for interpretation were those that presented eigenvalues >1.0, since they explain total data variation more than as a single variable. These data were submitted to orthogonal rotation of the variances where the sum was the maximum possible (varimax rotation) to maximize the relationship between interdependent variables, which facilitates interpretation. For the retained factors, the attributes were sought for each factor that presented a cumulative variance percentage ≥70% in the module (Li, 2016), making up a part of the group of variables to be considered in determining biochar quality according to the requirements to be improved, i.e. soil property and/or function. These attributes were again submitted to factor analysis to assign their relative weightings (Wi) for further calculation of the biochar viability index (BVI). Thus, variables considered redundant or of low representability were avoided for calculation of the BVI (Cavicchia et al., 2021).

The degree of importance is the weighting that represents each factor in the viability of the biochar. To assign weightings (Wi) to each indicator of biochar quality in the BVI, eigenvalues >1.0 and the respective rotated factor loadings of the selected attributes were used for the calculation of the relative weightings in the BVI, according to the equation: $Wi = \sum_{j=1}^{n}(R_{ij}^2 F_j) / \sum_{i=1}^{n}\left[\sum_{j=1}^{n}(R_{ij}^2 F_j)\right]$; where Wi is the relative weighting of variable (i) in the BVI; Rij is the rotated factor loading of attribute i in fator j; Fj is the eigenvalue of factor j; i is the index of the selected attribute and j is the index of the retained factor with an eigenvalue > 1,0. The BVI was then calculated from the sum of the score of each indicator (Pi), using the weighting of this indicator in assessing the viability of the biochar (Wi), as per the equation: $BVI = \sum_{i=1}^{n} P_i W_i;$ where BVI is the biochar viability index, Pi is the score of the ith factor, Wi is the relative weighting of the ith factor, and i are the indices of the variables ranging from 0 to 1.0.

Due to the high variability in biochar characteristics, in order to calculate the BVI, the variables were standardised by their degree of importance according to the loading factor and transformed into indicator scores ranging from 0 to 1.0 (Bhardwaj et al., 2011). The values for each indicator were ranked in ascending or descending order depending on whether the greatest value was considered harmful or beneficial to the requirements of the soils/substrates for

recovery. For indicators of the 'more is better' type, the highest value was given a score of 1.0 and, for 'less is better' indicators, the lowest value received a score of 1.0.

The BVI results for the biochars were submitted to non-hierarchical grouping analysis in order to separate them into different groups representing the properties obtained in producing the biochars. The K-means technique was used to compare the mean values of the BVI for each biochar. This technique uses a properly identified sequence of BVIs, comparing the pair distances and identifying the centroids, and prioritises the importance of the BVI, which allowed the construction of hierarchical levels pre-selected by the researcher (Wang et al., 2007). There were three pre-selected groups, identified as highly viable, moderately viable and non-viable.

2.3.2. Biochar classification by proximate analysis

The biochars identified as highly viable obtained through the BVI were further selected by proximate analysis (fixed carbon, ash and volatile matter), which are "easy to obtain" complementary properties. A combination of the proportions of volatile matter of ≤ 30%, ash ≤ 20% and fixed carbon ≥ 50% define the ideal biochar zone for environmental purposes (Environmental Potential Zone), as they characterise biochars of high stability, and high reactivity, and with a low proportion of volatile aromatic compounds, besides being photo- and thermo-oxidants (Trompowsky et al., 2005). The second zone comprised biochars with greater agronomic potential and lower stability, which has greater proportion of volatile matter (≥ 30%) that favours mineralisation and nutrients availability (Tag et al., 2016), while fixed carbon ≥ 40% confer a high reactivity on the surface of the biochar (Schulz et al., 2013), that favours adsorption of organic and inorganic contaminants (Kasozi et al., 2010).

The third zone characterises environmental restrictions due to the high ash content that might contain trace elements, which affects potential ecological risk factors directly (Bernardo et al., 2014). This zone was delimited by the proportional content of volatile matter ≤ 30%, fixed carbon ≤ 50% and ash ≥ 70%.

Finally, the fourth zone was delimited by the proportions of ash between ≥ 30% and ≤ 70%, volatile matter ≥ 30% and fixed carbon ≤ 40% and defined as having agronomic restrictions. The biochars of this zone have low stability and reactivity, such as low CEC (Mimmo et al., 2014). The high proportions of ash may represent a risk of toxicity of some

elements to plants, since it contains large amounts of certain elements which may hinder plant development (Bernardo et al., 2014; Tag et al., 2016).

2.3.3. Agronomic and environmental classification of the biochars

The third proposal for classification of biochars applied methods of identifying their potential conditions as established by Camps-Arbestain et al. (2015) and the International Biochar Initiative (IBI, 2015), and is based on (i) the direct or indirect effects that biochar application can have on soils/substrates; and (ii) on the limits of micronutrients, heavy metals and other elements that could cause environmental toxicity, hazardous or salinity.

Concentrations of these elements in the biochars should meet the following (IBI, 2015): Cu < 6,000 mg kg-1, Mo < 75 mg kg-1, Ni < 420 mg kg-1, Zn < 7,800 mg kg-1, As < 100 mg kg-1, Cd < 39 mg kg-1, Cr < 1,200 mg kg-1, Co < 100 mg kg-1, Pb < 300 mg kg-1, and Se < 200 mg kg-1, in order to avoid toxicity and Na < 1,200 mg kg-1 to avoid salinity. Both proposals use the characteristics of the biochars grouped into four aspects/categories: (i) stability, (ii) nutritional (iii) neutralizing and (iv) texture, classifying them into four classes: highly viable, moderately viable, low viable and non-viable.

Carbon stability was determined from the ratio between the organic carbon content (Corg) and H, characterised as highly stable when H:Corg ≤ 0.4 and stable when Corg ≥ 0.4 and < 0.7 (Tag et al., 2016). Stability indexes were obtained by multiplying the Corg content by H:Corg ratio and establishing the following: class 1 (BC < 30%), class 2 (30% ≤ BC < 40%), class 3 (40% ≤ BC < 50%) and class 4 (50% ≤ BC < 60%).

The nutritional classes of the biochar were determined from the soluble nutrient content, considering that the nutritional potential is influenced by the type of raw material and the pyrolysis conditions (Kloss et al., 2015). The total nutrient content is supposed not to be an adequate index of nutritional potential of the biochars, because the release of the total content of the nutrients will depend on the medium, the nature of the chemical compounds contained in the biochar and its stability, which may be longer than 100 years (Camps-Arbestain et al., 2015; Enders et al., 2012; Lin et al., 2013).

The classification of biochars by plant nutritional potential, besides considering solubility, also needs to consider the crop or the soil requirements for conditioning. The nutritional classes depend on the number of nutrients that meet the need of the crop on which the biochar will be used for, as follows: class 1: availability of at least one nutrient; class 2:

availability of at least two nutrients; class 3: availability of at least three nutrients; and class 4: availability of at least four nutrients. Camps-Arbestain et al. (2015) considered as a reference the nutritional requirements of the maize crop, and in this study we propose to modify the nutritional needs depending on the crop one wish to cultivate and identify which nutrients best meets the nutritional requirements.

Neutralizing power (NP) is expressed as a percentage of CaCO3 equivalent, recognised as an approximate measure of the neutralizing capacity of acidity by the biochar (Rayment and Lyon, 2010). The classification bands for NP were: class 0: NP < 1%; class 1: 1% ≤ PN < 10%; class 2: 10% ≤ PN < 20%; and class 3: PN ≥ 20%.

The textural class of the biochar particles was determined by calculating the weighted mean diameter (WMD), grouping the biochar particles according to percentage and size, as follows: Powder: > 50% of the biochar particles with a diameter ≤ 2mm (class 1); Mixture: > 50% of the biochar particles with a diameter between 2 and 3 mm (class 2); Stable: > 50% of the biochar particles with a diameter between 3 and 4 mm (class 3); and Aggregate: > 50% of the biochar particles with a diameter ≥ 4 mm (class 4). Knowledge and classification of the diameter of biochar particles is important because the larger the particle diameter the greater the water storage capacity and the availability of water to plants, as well as the drainage (Mukherjee and Zimmerman, 2013).

2.3.4. Classification of the biochars by the restrictive properties of soils/substrates

The last method considers the restrictive conditions of the environment where it will be applied and its suitability/conditioning for the development of plants. The biochars are evaluated with the aid of a radar-type graph, allowing one to observe the different attributes as a reference for the identification of biochars with potential to reduce the restrictions and/or limitations of the soil/substrates to be corrected. In order to evaluate the application of this method in highly degraded mining tailings, residues from Fe and Mn mining of Carajás Mineral Province were used, which are located in the Carajás National Forest, Parauapebas, in the State of Para (Table 1).

Both tailings show high chemical and physical limitations for the revegetation process, such as very low levels of several nutrients, lack of structure, fine texture, low permeability, low water retention capacity and the presence of toxic concentrations of elements such as Fe and Mn (Table 1).

Table 1. Physical and chemical characteristics of residues from Fe and Mn mining from the Carajás Mineral Province, Parauapebas, Brazil

	pH	K	P	Ca^{2+}	Mg^{2+}	Al^{3+}	H+Al	CEC	Fe	Mn	S	Zn	WRC	Texture
		mg dm^{-3}		----------cmolc dm^{-3}----------					---------mg dm^{-3}--------				%	
Fe Residue	6.1	3.0	3.0	0.2	0.1	0.0	0.6	0.9	39.2	60.0	16.3	1.5	18.0	Silt Loam
Mn Residue	5.3	8.0	0.3	0.0	0.0	0.0	2.5	2.6	21.4	463.7	44.7	1.7	32.0	Clay Loam

pH in water; exchangeable Ca^{2+}, Mg^{2+} and Al^{3+}; available P, K, S, Fe, Mn and Zn; H+Al: potential acidity; CEC: Cation exchange capacity; WRC: water retention capacity.

The analysis of variance (ANOVA) to determine significant differences between the biochars and the subsequent application of multivariate methods (principal component analysis and non-hierarchical grouping) for the classification of biochars was performed using the SPSS 22 software (IBM, 2013).

3.3. Results and discussion

3.1. Classification by the intrinsic characteristics of the biochars

The characteristics of the biochars showed significant differences ($p < 0.05$) influenced by the pyrolysis temperature and feedstocks. The only exception was the total selenium content, which did not show significant differences and, therefore, was excluded from the principal component analysis (PCA). This analysis generated nine components with eigenvalues greater than 1.0, using 38 selected variables, which explained 80% of the total variance and identified the attributes that presented rotated factor loadings ≥ 0.70 for the elaboration of part of the BVI (Table S2). Only 22 out of the 38 variables were used in the PCA, which became part of the group of variables to be considered in determining the quality and classification of the biochars. These same 22 variables were again submitted to PCA to obtain the relative weights (Wi), with six components explaining approximately 83% of the variation, meeting the criterion for a cumulative variance greater than 70% (Figueiredo Filho and da Silva Júnior, 2010) (Table 2).

The characteristics that presented both the highest rotated factor loading and a high potential for expressing biochar quality were considered for calculating the BVI (Table 2). Thus, the Pbtotal content was identified for the first factor, with a factor load of 0.96 and a commonality of 0.97, and representing a high potential for contamination risk (Bernardo et al., 2014) being ranked as “less is better” when calculating the BVI.

Volatile matter and biochar yield showed a factor load of 0.90, which indicate stability (Enders et al., 2012; Leng et al., 2019). The Mototal content had a rotational factor load of 0.89, and represents an essential micronutrient for enzymatic metabolism, and plays a key role in a variety of different biochemical processes (Manuel et al., 2018; Williams and Fraústo da Silva, 2002).

Table 2. Rotated factor loadings and commonalities (Com) of the functions and groups of indicators making up the biochar viability index, using the characteristics of biochars produced at different temperatures

Biochar Characteristics	Factor						Com	Wi
	1	2	3	4	5	6		
Pb_{total}	0.96	0.06	-0.06	0.11	-0.13	0.01	0.97	0.09
Cu_{total}	0.94	0.08	0.06	0.15	-0.12	0.08	0.93	0.09
Al_{total}	0.92	0.00	0.20	0.20	-0.14	0.08	0.95	0.08
Cd_{total}	0.79	0.21	0.10	0.05	-0.10	-0.04	0.70	0.06
Volatile matter	-0.06	0.90	0.08	-0.06	0.05	-0.20	0.83	0.07
Biochar yield	0.07	0.90	-0.01	0.10	-0.10	-0.01	0.87	0.07
Hydrogen	0.22	0.78	-0.16	0.18	-0.23	-0.25	0.83	0.06
pH	-0.32	-0.72	0.15	0.13	0.18	0.10	0.70	0.05
As_{total}	-0.03	0.51	-0.07	-0.13	-0.06	0.37	0.91	0.02
Mo_{total}	0.01	0.00	0.89	0.04	0.13	0.14	0.92	0.05
Fe_{total}	0.03	-0.07	0.86	0.28	-0.02	0.15	0.84	0.04
B_{total}	0.02	-0.07	0.85	-0.03	0.07	-0.11	0.84	0.04
Mn_{total}	0.23	-0.02	0.80	0.13	-0.01	0.11	0.84	0.04
Ash content	0.10	-0.20	0.10	0.92	0.09	0.06	0.74	0.04
Carbon	-0.18	-0.09	0.00	-0.90	-0.05	0.14	0.72	0.04
Mg_{total}	0.13	-0.12	0.25	0.86	0.27	0.01	0.92	0.03
Fixed carbon	-0.14	-0.51	-0.16	-0.76	-0.12	0.12	0.87	0.03
$K_{soluvel}$	-0.13	-0.10	-0.18	0.12	0.92	0.00	0.91	0.02
Na_{total}	-0.20	-0.11	0.12	0.16	0.86	-0.07	0.91	0.02
K_{total}	-0.17	-0.15	0.44	0.16	0.80	-0.07	0.87	0.02
Zn_{total}	0.22	-0.06	0.12	-0.12	-0.21	0.86	0.86	0.02
S_{total}	-0.12	-0.42	0.20	0.05	0.15	0.77	0.42	0.01
Eigenvalues	5.25	4.94	3.21	2.39	1.34	1.23	-	-
% explained variance	23.84	22.44	14.61	10.86	6.10	5.60	-	-
Cumulative percentage	23.84	46.28	60.89	71.75	77.84	83.44	-	-

Wi: relative weightings of each indicator.

Finally, in the sixth factor we have the contents of Zntotal with a rotational factor load of 0.86. Zinc is considered as an essential micronutrient for plants, hence its availability in biochar is beneficial to crop production.

The ash content showed the highest factor load rotated in factor four (0.92), and it is related with the presence of functional groups from the thermal transformation of materials

(Joseph et al., 2010; Lorenz and Lal, 2014; Mukome et al., 2013). In the fifth factor, Ksoluble content was identified with a rotational factor load of 0.92. Therefore, K bioavailability can be significantly improved of these biochars addition to soil. In this sense, substituting and/or supplementing K through alternative sources has great prospects in developing countries like Brazil, where imported K fertilizers are comparatively expensive (Galembeck et al., 2019).

The six attributes identified with the BVI were again submitted to factor analysis and allowed the calculation of the relative weighting for each indicator (Wi) as a function of their eigenvalues and the explicability of the indicator by the retained factor (Table 3).

The attributes with the highest Wi in the BVI were those associated with the group of 'potential stability' (volatile matter and biochar yield), while the lowest was that associated with potential contamination risk (Pbtotal). These weightings are consistent with the importance given by the characteristics shown by the biochar (Lehmann and Joseph, 2015).

Table 3. Rotated factor loadings and commonalities (Com), and relative weighting of the indicator (Wi) for calculating the Biochar Viability Indicators (BVI)

BVI Indicator	Factor loading				Com	Wi
	1	2	3	4		
Volatile matter	0.93				0.90	0.24
Biochar yield	0.93				0.87	0.23
Water-soluble K ($K_{soluble}$)		-0.76			0.63	0.12
Total Zn (Zn_{total})		0.69			0.63	0.10
Ash content			0.85		0.84	0.11
Total Pb (Pb_{total})			0.62		0.82	0.06
Total Mo (Mo_{total})				0.94	0.90	0.13
Eigenvalues	1.927	1.510	1.112	1.051		
Percentage explained variance	27.53	21.58	15.89	15.02		
Cumulative percentage	27.53	49.11	65.00	80.02		

The Biochar Viability Index (BVI) with the seven selected attributes is given by the equation:

BVI = 0.24*volatile matter + 0.23*c – 0.12*Ksoluble + 0.10*Zntotal + 0.11*ash content + 0.06*Pbtotal + 0.13*Mototal

The attributes selected for the BVI were ranked and those with highest values (biochar yield, Ksoluble, Zntotal, ash content e Mototal) are indicators of biochar quality, and were classified as 'more is better', so that the highest value was scored 1.0. Conversely, volatile matter and Pbtotal are considered indicators of low quality, and were classified as 'less is better', with the lowest value receiving a score of 1.0. The final BVI indicates that biochars are

persistent and of low mineralisation rate, and a source of nutrients (Lehmann and Joseph, 2015). Ash and volatile content allows a fast and efficient estimation of the stability and quality of different types of biochar (Aller et al., 2017; Enders et al., 2012).

The BVI value obtained for each biochar was significantly different ($p < 0.05$) among the biochars (Table S3) and suggests that assigning weightings to the biochar attributes by using PCA was efficient to elaborate the BVI, which can be used as a tool to evaluate the potential of biochars as a soil/substrate conditioner.

Table 4. Classification of biochars produced from the agricultural wastes poultry litter (PL) and swine manure (SM) and from the industrial wastes construction wood (CW), tire (TR) and PVC plastic (PVC), subjected to pyrolysis temperatures of 300, 400, 500, 600 and 700 °C, according to quality-indicator factor loadings by means of hierarchical grouping analysis

Group 1 Highly Viable				Group 2 Moderately Viable				Group 3 Non-viable	
Biochar	BVI	Biochar	BVI	Biochar	BVI	Biochar	BVI	Biochar	BVI
SM600	0.50	TR600	0.43	SM500	0.38	TR+PVC600	0.30	CW+PVC400	0.23
PL+TR400	0.50	SM+PVC600	0.43	SM+CW700	0.38	SM+CW300	0.30	CW+PVC300	0.21
TR+PVC700	0.49	PL+SM700	0.42	PL+SM500	0.38	CW+TR500	0.28	PL+SM300	0.21
PL600	0.49	PL+CW300	0.42	SM+CW400	0.38	SM+CW500	0.28	SM400	0.20
PL+SM600	0.48	PL+CW400	0.42	SM+TR700	0.37	PL+PVC300	0.27	PL+TR300	0.14
CW+PVC500	0.48	PL+PVC700	0.42	PVC400	0.37	CW+TR300	0.26	TR+PVC300	0.11
CW+TR400	0.47	PL+PVC500	0.41	SM+PVC300	0.37				
PL+CW600	0.47	SM+PVC500	0.41	PVC600	0.37				
PL+TR600	0.47	PL+TR500	0.41	PVC700	0.36				
SM700	0.47	TR+PVC400	0.41	SM+PVC400	0.36				
PL+TR700	0.46	CW+TR600	0.40	SM+TR400	0.35				
CW600	0.46	CW+TR700	0.40	PL500	0.35				
SM+PVC700	0.46	PVC300	0.40	TR400	0.35				
CW500	0.46	PL+CW700	0.39	SM+CW600	0.34				
CW+PVC600	0.45	TR+PVC500	0.39	PL+SM400	0.33				
PL+PVC400	0.44	SM+TR600	0.39	TR300	0.33				
CW700	0.44	TR700	0.39	CW400	0.33				
CW+PVC700	0.44	PL700	0.39	SM300	0.33				
PL+PVC600	0.44	PL+CW500	0.39	TR500	0.33				
PL300	0.44	PVC500	0.39	CW300	0.31				
SM+TR300	0.43	PL400	0.38	SM+TR500	0.30				

The classification obtained with the non-hierarchical grouping analysis generated a highly heterogeneous group of biochars that was divided into three groups (Table 4). The first group (highly viable) had 42 biochars, most of them resulting from the co-pyrolysis of the feedstock and produced under higher pyrolysis temperatures. The second group (moderately

viable) was composed of 27 biochars from agricultural waste and mixtures. The third group (non-viable) was composed of 6 pyrolyzed biochars produced at low pyrolysis temperatures i.e., ≤ 400 ºC (CW+PVC400, CW+PVC300, PL+SM300 SM400, PL+TR300 and TR+PVC300).

The results indicate that those biochars produced from industrial and agricultural wastes by co-pyrolysis showed the highest BVIs, especially at higher pyrolysis temperatures, which showed attributes associated with C stability (ash and volatiles) and biochar yield. These attributes had the highest Wi (Table 3), which is reasonable considering that the stability of biochars is one of their most interesting properties, especially when the objective is soil conditioning aiming a reduction in CO_2 emission, contaminant adsorption, and a reduction in nutrient leaching (Ahmad et al., 2017). These results are consistent with those observed in biochars from co-pyrolysis, demonstrating the synergistic character of co-pyrolysis in improving the properties of biochars, especially when agricultural and industrial residues are involved (Rodriguez et al., 2021).

Classification of the biochars according to factor loadings may have an influence on the formation of hierarchical groups using the Wi of the indicators. The variables ash and volatiles had greater weight in forming the 'potential stability' group. Although the biochar stability is an important characteristics for its use in soil due to the mitigation of climate change by C sequestration and beneficial agronomic effects on the soil in the long-term (Enders et al., 2012; Zhang et al., 2019), other attributes might also be important in the selection or classification of biochar.

It is worth mentioning that the ash content and volatile matter might lead to phytotoxicity of some of these elements (e.g. Na) (Enders et al., 2012). Thus, it is important to take into account that the restrictions and potentials depend on the use and type of environment where the biochar is applied.

3.2. Biochar classification by proximate analysis

The 42 biochars with the highest BVI obtained by the intrinsic characteristics of the biochars were re-classified by method proximate analysis, and reduced to 10 potential biochars (SM700, CW700, TR700, PVC500, PL + CW300, PL + CW600, PL + CW700, PL + TR700, PL + PVC600, CW + PVC600), mostly biochars of mixtures between PL with CW and PVC at temperatures of 600 and 700 ºC. These biochars present the lowest volatile matter and the

highest fixed carbon, characteristics that can contribute high stability and reactivity to the soil (Figure 1). The biochars with agronomic potential were 5 (CW500, PL400, PL + CW500, PL + TR500, PL + PVC400) produced mainly with PL and CW at temperatures of 400 and 500 ºC, which have an intermediate range of ash content and low stability, favoring the nutritional supply to the soil (Lu et al., 2014).

No classification standard was found for the different biochars produced either in pyrolysis or co-pyrolysis. The co-pyrolysis causes interactions between feedstocks during the pyrolysis process (Rodriguez et al., 2021), producing biochars with better properties than individual pyrolyzed materials (Rodriguez et al., 2020). Thus, it is necessary to identify the biochars that suits best for an intended use, whether by chemical, physical or biological functions as discussed below.

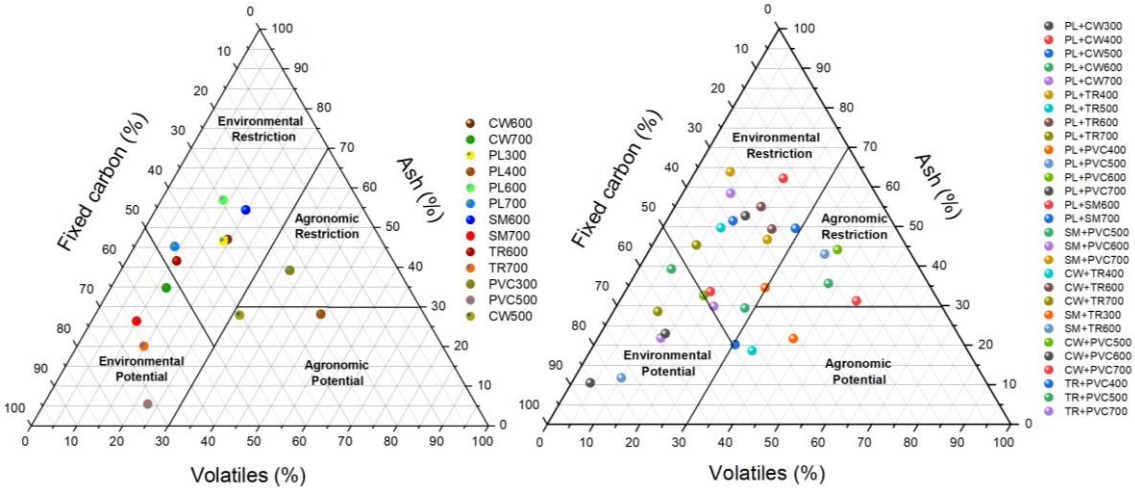

Figure 1. Classification of biochars produced by the pyrolysis and co-pyrolysis from the agricultural wastes poultry litter (PL) and swine manure (SM) and from the industrial wastes construction wood (CW), tire (TR) and PVC plastic (PVC), subjected to pyrolysis temperatures of 300, 400, 500, 600 and 700 °C, indicated by the increase in size of the geometric figures.

3.3. Agronomic and environmental stratification of the biochars

The biochars were classified according to the potential for soil revegetation following the stratification of agronomic and environmental potentials. Fifteen biochars with potential for soil recovery were obtained according to the biochar properties and their soil effect aiming to increase the positive effects and decrease negative ones (Camps-Arbestain et al., 2015, IBI, 2015) (Figure 2).

MATRIZ FOR BIOCHAR CLASSIFICATION FOR Camps-Arbestain CRITERIA (2015)

Nutricional requirements of the crop	P	K	S	Mg
	4.4	4.6	1.5	2.1

Biochar	Nutrient content (g/kg)				H/C	WMD	NP
	$P_{soluble}$	$K_{soluble}$	$S_{soluble}$	$Mg_{soluble}$			
PL+CW 300	2.830	19.147	1.27	1.248	0.08	3.52	50.90

MATRIX FOR BIOCHAR CLASSIFICATION FOR TOXIC ELEMENT CONTENT IBI (2015)

Biochar	Total micronutrient content (mg kg^{-1})						
PL+CW 300	B	Cu	Fe	Mn	Mo	Ni	Zn
	19	66	709	75	2	12	70
	Total trace-element content (mg kg^{-1})						Na_{total} (mg kg^{-1})
	As	Cd	Co	Cr	Pb	Se	
	1	0	1	66	0	2	2195

Toxicity classification		
Toxic	Dangerous	Saline
Non-toxic	Non-dangerous	Saline

Figure 2. Matrix for the classification of biochars according to the criteria of the Camps-Arbestain et al. (2015) and IBI (2015).

In the matrix of biochar classification (Tables S4 and S5), three non-viable biochars (PL+PVC400, PVC500 and CW+PVC600) were identified due to their high Cr and Pb contents. The biochar from the co-pyrolysis between poultry litter and construction wood at 500 ºC, showed high viability in soil recovery due to its high fertility and stability. On the other hand, 11 biochars were classified as moderately viable in soil recovery, mainly because they have adequate properties to increase the CEC and reduce soil acidity. However, these biochars presented restrictions for salinity due to the Na contents, with the exception of the biochars of CW500, CW700 and TR700 (Tables S4 and S4).

The criteria used enabled the knowledge of the biochar characteristics identified by proximate analysis, which further reduces the spectrum of the possibilities of biochars to be

used as a conditioner in the mining substrate. The chemical and physical properties of the Fe and Mn mining tailings combined with 12 biochars that showed viability in the criteria matrix were evaluated.

3.4. Classification of the biochars by the restrictive properties of soils/substrates

The key factor in this method is the restrictive or limiting characteristics of the soil/substrate for plant growth. The Fe and Mn tailings present a lack of particle cohesion and consequent high erodibility and low fertility (Table 1). Such properties requires biochars that provide nutrients (N, P, S, K and Mg), high weighted mean diameter index as a biological activity factor (Lehmann and Joseph, 2015), moderate neutralization power, low electric conductivity (EC), determined by the Na content as an indicator of salinity, and low levels of Fe, Mn and Zn as indicators of toxicity. In addition, low levels of trace elements such as Pb and Cr as indicators of environmental risk (IBI, 2015) and, finally, the stability represented by the high ash levels (Enders et al., 2012).

Thus, the attributes required for biochar to improve the restrictions of Fe and Mn tailings that limit plant development were identified, and with the support of a radar type chart is presented with pre-established limits (Figure 3). This is the last step in the selection of the "ideal biochar" to be used as a conditioner in the recovery of the Fe and Mn substrate. Thus, the 12 biochars were categorized with the characteristics closest to the needs of the Fe and Mn substrate to be revegetated (Figure 3).

The PL+CW300 biochar showed the best characteristics as conditioner for the Fe and Mn mining substrate among the 12 biochars. The contents of Pb and Cr, as well as high contents of Na where the main restrictive characteristics among the tested biochars.

It is important to note that biochars not considered in this classification may have environmental or agronomic potential for use in other conditions. Therefore, the restriction of this study is associated with the requirements Fe and Mn mining tailings.

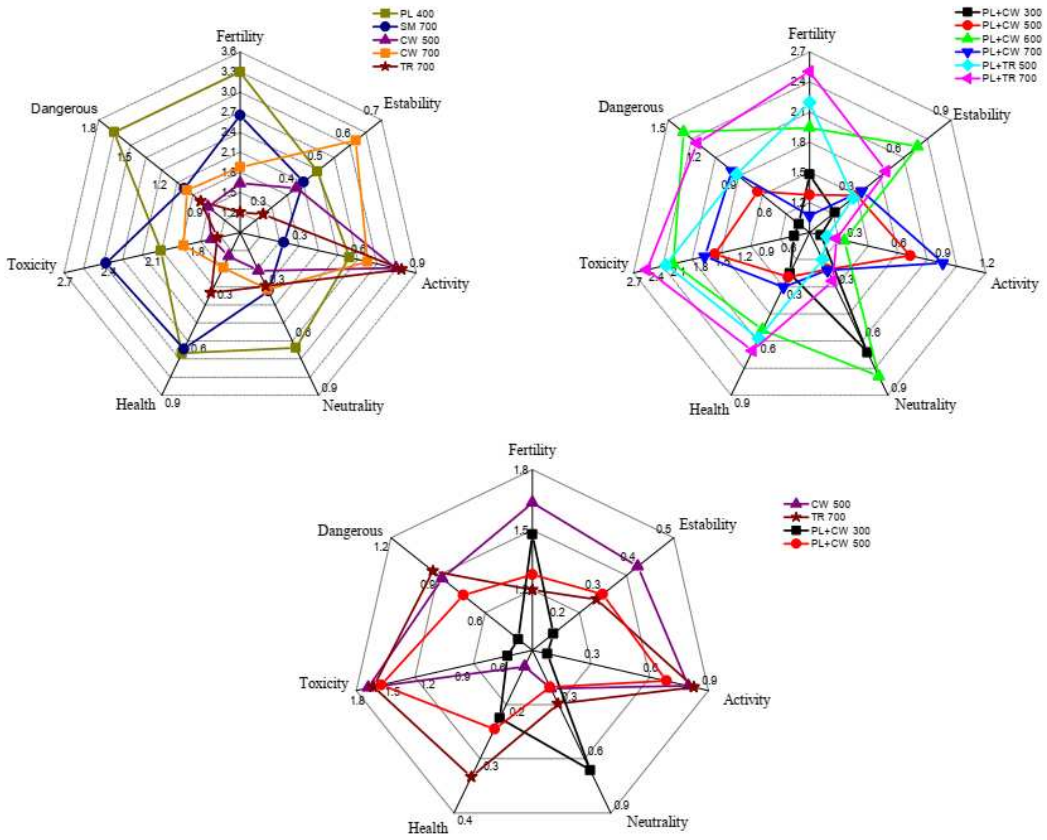

Figure 3. Comparison of the restrictive characteristics of the Fe and Mn mining substrate in the selection of the biochar.

4. Conclusions

The sequence of methods proposed in this study proved to be very efficient to stratify and classify the different biochars according to the potential shown by the physical and chemical characteristics and the limitations of the soil/substrate to be conditioned. The multivariate methods allowed the identification of the variables that present the greatest variability and classify the biochars according to the biochar viability indicator (BVI) and making the selection and interpretation of biochar more efficient. Proximate analysis (ash, fixed carbon and volatile matter) is an efficient tool for the classification of biochars, as it uses only three variables of rapid and low-cost evaluation. The combination of the criteria according to Camps-Arbestain et al. (2015) and IBI (2015) in the classification matrix of biochars allows evaluating the agronomic potential as well as the environmental restrictions according to the soil/substrate to be used. Finally, the use of a radar chart clearly indicated the biochar with the greatest potential for the recovery of Fe and Mn mining tailings, in this case the PL+CW300

biochar. Despite the methods proposed being useful and efficient in the selection of an appropriate biochar for specific uses, the dependency of physicochemical characteristics of the biochars might limit its broad application.

Acknowledgements

The authors wish to thank the Coordenação de Apeerfeiçoamento de Pessoal de Nível Superior (CAPES) and Conselho Nacional de Desenvolvimento Científico e Tecnológico (CNPq) from Braziliam Government, for the award of scholarships and research grants.

5. References

Abdel-Shafy, H.I., Mansour, M.S.M., 2018. Solid waste issue: Sources, composition, disposal, recycling, and valorization. Egypt. J. Pet. 27, 1275–1290. https://doi.org/10.1016/j.ejpe.2018.07.003

Abrelpe - Associação Brasileira de Empresas de Limpesa Pública e Resíduos Especiais, 2015. Estimativas Dos Custos Para Viabilizar a Universalização Da Destinação. São Paulo.

Ahmad, M., Lee, S.S., Lee, S.E., Al-Wabel, M.I., Tsang, D.C.W., Ok, Y.S., 2017. Biochar-induced changes in soil properties affected immobilization/mobilization of metals/metalloids in contaminated soils. J. Soils Sediments 17, 717–730. https://doi.org/10.1007/s11368-015-1339-4

Al-Wabel, M.I., Al-Omran, A., El-Naggar, A.H., Nadeem, M., Usman, A.R.A., 2013. Pyrolysis temperature induced changes in characteristics and chemical composition of biochar produced from conocarpus wastes. Bioresour. Technol. 131, 374–379. https://doi.org/10.1016/j.biortech.2012.12.165

Aller, D., Bakshi, S., Laird, D.A., 2017. Modified method for proximate analysis of biochars. J. Anal. Appl. Pyrolysis 124, 335–342. https://doi.org/10.1016/j.jaap.2017.01.012

ASTM Standard D1762 -84, 2007. Standard Test Method for Chemical Analysis of Wood Charcoal. ASTM International, West Conshohocken. https://doi.org/10.1520/D1762-84R07.2

ASTM Standard D3172 -13, 2013. Standard Practice for Proximate Analysis of Coal and Coke. ASTM International, West Conshohocken. https://doi.org/10.1520/D3172-13.2

Ayilara, M., Olanrewaju, O., Babalola, O., Odeyemi, O., 2020. Waste Management through Composting: Challenges and Potentials. Sustainability 12, 4456. https://doi.org/10.3390/su12114456

Bernardo, M., Mendes, S., Lapa, N., Gonçalves, M., Mendes, B., Pinto, F., Lopes, H., 2014. Leaching behaviour and ecotoxicity evaluation of chars from the pyrolysis of forestry biomass and polymeric materials. Ecotoxicol. Environ. Saf. 107, 9–15. https://doi.org/10.1016/j.ecoenv.2014.05.007

Bhardwaj, A.K., Jasrotia, P., Hamilton, S.K., Robertson, G.P., 2011. Ecological management of intensively cropped agro-ecosystems improves soil quality with sustained productivity. Agric. Ecosyst. Environ. 140, 419–429. https://doi.org/10.1016/j.agee.2011.01.005

Brewer, C.E., Chuang, V.J., Masiello, C.A., Gonnermann, H., Gao, X., Dugan, B., Driver, L.E., Panzacchi, P., Zygourakis, K., Davies, C.A., 2014. New approaches to measuring biochar density and porosity. Biomass and Bioenergy 66, 176–185. https://doi.org/10.1016/j.biombioe.2014.03.059

Camps-Arbestain, Marta, Amonette, J.E., Singh, B., Wang, T., Schmidt, H.P., 2015. A biochar classification system and associated test methods, in: Biochar for Environmental Management: Science, Technology and Implementation. p. 165.

Camps-Arbestain, M., Amonette, J.E., Singh, B., Wang, T., Schmidt, H.P., 2015. A biochar classification system and associated test methods, in: Lehmann, J., Joseph, S. (Eds.), Biochar for Environmental Management: Science, Technology and Implementation. aylor and Francis, London, pp. 165–194.

Cavicchia, C., Sarnacchiaro, P., Vichi, M., 2021. A composite indicator for the waste management in the EU via Hierarchical Disjoint Non-Negative Factor Analysis. Socioecon. Plann. Sci. 73, 100832. https://doi.org/10.1016/j.seps.2020.100832

Chew, K.W., Chia, S.R., Chia, W.Y., Cheah, W.Y., Munawaroh, H.S.H., Ong, W.J., 2021. Abatement of hazardous materials and biomass waste via pyrolysis and co-pyrolysis for environmental sustainability and circular economy. Environ. Pollut. 278, 116836. https://doi.org/10.1016/j.envpol.2021.116836

Dai, Y., Zheng, H., Jiang, Z., Xing, B., 2020. Combined effects of biochar properties and soil conditions on plant growth: A meta-analysis. Sci. Total Environ. 713, 136635. https://doi.org/10.1016/j.scitotenv.2020.136635

Enders, A., Hanley, K., Whitman, T., Joseph, S., Lehmann, J., 2012. Characterization of biochars to evaluate recalcitrance and agronomic performance. Bioresour. Technol. 114, 644–653. https://doi.org/10.1016/j.biortech.2012.03.022

Enders, A., Lehmann, J., 2012. Comparison of Wet-Digestion and Dry-Ashing Methods for Total Elemental Analysis of Biochar. Commun. Soil Sci. Plant Anal. 43, 1042–1052. https://doi.org/10.1080/00103624.2012.656167

Figueiredo Filho, D.B., da Silva Júnior, J.A., 2010. Visão além do alcance: Uma introdução à análise fatorial. Opiniao Publica 16, 160–185. https://doi.org/10.1590/S0104-62762010000100007

Galembeck, F., Galembeck, A., Santos, L.P. dos, 2019. NPK: essentials for sustainability. Quim. Nova 42, 1199–1207. https://doi.org/10.21577/0100-4042.20170441

Hassan, H., Lim, J.K., Hameed, B.H., 2016. Recent progress on biomass co-pyrolysis conversion into high-quality bio-oil. Bioresour. Technol. 221, 645–655. https://doi.org/10.1016/j.biortech.2016.09.026

IBI, I.B.I., 2015. Standardized Product Definition and Product Testing Guidelines for Biochar That Is Used in Soil. International Biochar Initiative.

IBM SPSS., 2013. IBM SPSS Statistics for Windows.

Ipea, 2012. Plano nacional de resíduos sólidos: diagnóstico dos resíduos urbanos, agrosilvopastoris e a questão dos catadores.

Jeffery, S., Verheijen, F.G.A., van der Velde, M., Bastos, A.C., 2011. A quantitative review of the effects of biochar application to soils on crop productivity using meta-analysis. Agric. Ecosyst. Environ. 144, 175–187. https://doi.org/10.1016/j.agee.2011.08.015

Jindo, K., Suto, K., Matsumoto, K., García, C., Sonoki, T., Sanchez-Monedero, M.A., 2012. Chemical and biochemical characterisation of biochar-blended composts prepared from poultry manure.

Bioresour. Technol. 110, 396–404. https://doi.org/10.1016/j.biortech.2012.01.120

Joseph, S.D., Camps-Arbestain, M., Lin, Y., Munroe, P., Chia, C.H., Hook, J., Van Zwieten, L., Kimber, S., Cowie, A., Singh, B.P., Lehmann, J., Foidl, N., Smernik, R.J., Amonette, J.E., 2010. An investigation into the reactions of biochar in soil. Aust. J. Soil Res. 48, 501–515. https://doi.org/10.1071/SR10009

Kasozi, G.N., Zimmerman, A.R., Nkedi-Kizza, P., Gao, B., 2010. Catechol and humic acid sorption onto a range of laboratory-produced black carbons (biochars). Environ. Sci. Technol. 44, 6189–6195. https://doi.org/10.1021/es1014423

Kebede, Y.S., Alene, M.M., Endalemaw, N.T., 2021. Urban landfill investigation for managing the negative impact of solid waste on environment using geospatial technique. A case study of Assosa town, Ethiopia. Environ. Challenges 4, 100103. https://doi.org/10.1016/j.envc.2021.100103

Kloss, S., Zehetner, F., Buecker, J., Oburger, E., Wenzel, W.W., Enders, A., Lehmann, J., Soja, G., 2015. Trace element biogeochemistry in the soil-water-plant system of a temperate agricultural soil amended with different biochars. Environ. Sci. Pollut. Res. 22, 4513–4526. https://doi.org/10.1007/s11356-014-3685-y

Lehmann, J., Joseph, S., 2015. Biochar for Environmental Management: Science, Technology and Implementation, 2 ed. ed. London: Routledge.

Leng, L., Huang, H., Li, H., Li, J., Zhou, W., 2019. Biochar stability assessment methods: A review. Sci. Total Environ. 647, 210–222. https://doi.org/10.1016/j.scitotenv.2018.07.402

Li, H., 2016. Accurate and efficient classification based on common principal components analysis for multivariate time series. Neurocomputing 171, 744–753. https://doi.org/10.1016/j.neucom.2015.07.010

Li, S., Harris, S., Anandhi, A., Chen, G., 2019. Predicting biochar properties and functions based on feedstock and pyrolysis temperature : A review and data syntheses. J. Clean. Prod. 215, 890–902. https://doi.org/10.1016/j.jclepro.2019.01.106

Lin, Y., Munroe, P., Joseph, S., Ziolkowski, A., van Zwieten, L., Kimber, S., Rust, J., 2013. Chemical and structural analysis of enhanced biochars: Thermally treated mixtures of biochar, chicken litter, clay and minerals. Chemosphere 91, 35–40. https://doi.org/10.1016/j.chemosphere.2012.11.063

Lorenz, K., Lal, R., 2014. Biochar application to soil for climate change mitigation by soil organic carbon sequestration. J. Plant Nutr. Soil Sci. 177, 651–670. https://doi.org/10.1002/jpln.201400058

Lu, H., Zhang, W., Wang, S., Zhuang, L., Yang, Y., Qiu, R., 2013. Characterization of sewage sludge-derived biochars from different feedstocks and pyrolysis temperatures. J. Anal. Appl. Pyrolysis 102, 137–143. https://doi.org/10.1016/j.jaap.2013.03.004

Lu, W., Ding, W., Zhang, J., Li, Y., Luo, J., Bolan, N., Xie, Z., 2014. Biochar suppressed the decomposition of organic carbon in a cultivated sandy loam soil: A negative priming effect. Soil Biol. Biochem. 76, 12–21. https://doi.org/10.1016/j.soilbio.2014.04.029

Lustosa Filho, J.F., Penido, E.S., Castro, P.P., Silva, C.A., Melo, L.C.A., 2017. Co-Pyrolysis of Poultry Litter and Phosphate and Magnesium Generates Alternative Slow-Release Fertilizer Suitable for Tropical Soils. ACS Sustain. Chem. Eng. 5, 9043–9052. https://doi.org/10.1021/acssuschemeng.7b01935

Majumder, S., Neogi, S., Dutta, T., Powel, M.A., Banik, P., 2019. The impact of biochar on soil carbon sequestration: Meta-analytical approach to evaluating environmental and economic

advantages. J. Environ. Manage. 250, 109466. https://doi.org/10.1016/j.jenvman.2019.109466

Manríquez-Altamirano, A., Sierra-Pérez, J., Muñoz, P., Gabarrell, X., 2020. Analysis of urban agriculture solid waste in the frame of circular economy: Case study of tomato crop in integrated rooftop greenhouse. Sci. Total Environ. 734, 139375. https://doi.org/10.1016/j.scitotenv.2020.139375

Manuel, T.-J., Alejandro, C.-A., Angel, L., Aurora, G., Emilio, F., 2018. Roles of Molybdenum in Plants and Improvement of Its Acquisition and Use Efficiency, in: Plant Micronutrient Use Efficiency. Elsevier, pp. 137–159. https://doi.org/10.1016/B978-0-12-812104-7.00009-5

Marschner, P., 2012. Marschner's Mineral Nutrition of Higher Plants, 3rd edn. ed. Elsevier, Amsterdam. https://doi.org/10.1016/C2009-0-63043-9

Mimmo, T., Panzacchi, P., Baratieri, M., Davies, C.A., Tonon, G., 2014. Effect of pyrolysis temperature on miscanthus (Miscanthus × giganteus) biochar physical, chemical and functional properties. Biomass and Bioenergy 62, 149–157. https://doi.org/10.1016/j.biombioe.2014.01.004

Mukherjee, A., Zimmerman, A.R., 2013. Organic carbon and nutrient release from a range of laboratory-produced biochars and biochar-soil mixtures. Geoderma 193–194, 122–130. https://doi.org/10.1016/j.geoderma.2012.10.002

Mukherjee, A., Zimmerman, A.R., Harris, W., 2011. Surface chemistry variations among a series of laboratory-produced biochars. Geoderma 163, 247–255. https://doi.org/10.1016/j.geoderma.2011.04.021

Mukome, F.N.D., Zhang, X., Silva, L.C.R., Six, J., Parikh, S.J., 2013. Use of chemical and physical characteristics to investigate trends in biochar feedstocks. J. Agric. Food Chem. 61, 2196–2204. https://doi.org/10.1021/jf3049142

Nor Faiza, M.., Hassan, N.A., Farhan, M.., Edre, M.A., Rus, R.., 2019. Solid Waste: its Implication for Health and Risk of Vector Borne Diseases. J. Wastes Biomass Manag. 1, 14–17. https://doi.org/10.26480/jwbm.02.2019.14.17

Pariyar, P., Kumari, K., Jain, M.K., Jadhao, P.S., 2020. Evaluation of change in biochar properties derived from different feedstock and pyrolysis temperature for environmental and agricultural application. Sci. Total Environ. 105, 136433. https://doi.org/10.1016/j.scitotenv.2019.136433

Penido, E.S., Martins, G.C., Mendes, T.B.M., Melo, L.C.A., do Rosário Guimarães, I., Guilherme, L.R.G., 2019. Combining biochar and sewage sludge for immobilization of heavy metals in mining soils. Ecotoxicol. Environ. Saf. 172, 326–333. https://doi.org/10.1016/j.ecoenv.2019.01.110

Prakongkep, N., Gilkes, R.J., Wiriyakitnateekul, W., 2015. Forms and solubility of plant nutrient elements in tropical plant waste biochars. J. Plant Nutr. Soil Sci. 178, 732–740. https://doi.org/10.1002/jpln.201500001

Puga, A.P., Abreu, C.A., Melo, L.C.A., Beesley, L., 2015. Biochar application to a contaminated soil reduces the availability and plant uptake of zinc, lead and cadmium. J. Environ. Manage. 159, 86–93. https://doi.org/10.1016/j.jenvman.2015.05.036

Rayment, G.E., Lyon, D.J., 2010. Soil Chemical Methods - Australasia. CSIRO Publishing: Collingwood, Australia.

Rodriguez, J.A., Lustosa Filho, J.F., Melo, L.C.A., de Assis, I.R., de Oliveira, T.S., 2021. Co-pyrolysis of agricultural and industrial wastes changes the composition and stability of biochars and can improve their agricultural and environmental benefits. J. Anal. Appl. Pyrolysis 155, 105036. https://doi.org/10.1016/j.jaap.2021.105036

Rodriguez, J.A., Lustosa Filho, J.F., Melo, L.C.A., de Assis, I.R., de Oliveira, T.S., 2020. Influence of pyrolysis temperature and feedstock on the properties of biochars produced from agricultural and industrial wastes. J. Anal. Appl. Pyrolysis 149, 104839. https://doi.org/10.1016/j.jaap.2020.104839

Schulz, H., Dunst, G., Glaser, B., 2013. Positive effects of composted biochar on plant growth and soil fertility. Agron. Sustain. Dev. 33, 817–827. https://doi.org/10.1007/s13593-013-0150-0

Shaaban, A., Se, S.-M., Dimin, M.F., Juoi, J.M., Mohd Husin, M.H., Mitan, N.M.M., 2014. Influence of heating temperature and holding time on biochars derived from rubber wood sawdust via slow pyrolysis. J. Anal. Appl. Pyrolysis 107, 31–39. https://doi.org/10.1016/j.jaap.2014.01.021

Shaaban, M., Abid, M., 2021. Biochar as a sorbent for organic and inorganic pollutants, in: Núñez-Delgado, A. (Ed.), Sorbents Materials for Controlling Environmental Pollution. Elsevier, pp. 189–208. https://doi.org/10.1016/B978-0-12-820042-1.00001-8

Song, W., Guo, M., 2012. Quality variations of poultry litter biochar generated at different pyrolysis temperatures. J. Anal. Appl. Pyrolysis 94, 138–145. https://doi.org/10.1016/j.jaap.2011.11.018

Tag, A.T., Duman, G., Ucar, S., Yanik, J., 2016. Effects of feedstock type and pyrolysis temperature on potential applications of biochar. J. Anal. Appl. Pyrolysis 120, 200–206. https://doi.org/10.1016/j.jaap.2016.05.006

Templeton, G.F., 2011. A Two-Step Approach for Transforming Continuous Variables to Normal: Implications and Recommendations for IS Research. Commun. Assoc. Inf. Syst. 28, 41–58.

Trompowsky, P.M., De Melo Benites, V., Madari, B.E., Pimenta, A.S., Hockaday, W.C., Hatcher, P.G., 2005. Characterization of humic like substances obtained by chemical oxidation of eucalyptus charcoal. Org. Geochem. 36, 1480–1489. https://doi.org/10.1016/j.orggeochem.2005.08.001

Wang, C., Chen, D., Shen, J., Yuan, Q., Fan, F., Wei, W., Li, Y., Wu, J., 2021. Biochar alters soil microbial communities and potential functions 3–4 years after amendment in a double rice cropping system. Agric. Ecosyst. Environ. 311, 107291. https://doi.org/10.1016/j.agee.2020.107291

Wang, L., Chu, J., Wu, J., 2007. Selection of optimum maintenance strategies based on a fuzzy analytic hierarchy process. Int. J. Prod. Econ. 107, 151–163. https://doi.org/10.1016/j.ijpe.2006.08.005

Williams, R.J.P., Fraústo da Silva, J.J.R., 2002. The Involvement of Molybdenum in Life. Biochem. Biophys. Res. Commun. 292, 293–299. https://doi.org/10.1006/bbrc.2002.6518

Zhang, C., Zeng, G., Huang, D., Lai, C., Chen, M., Cheng, M., Tang, W., Tang, L., Dong, H., Huang, B., Tan, X., Wang, R., 2019. Biochar for environmental management : Mitigating greenhouse gas emissions , contaminant treatment , and potential negative impacts. Chem. Eng. J. 373, 902–922. https://doi.org/10.1016/j.cej.2019.05.139

Zhang, H., Chen, C., Gray, E.M., Boyd, S.E., 2017. Effect of feedstock and pyrolysis temperature on properties of biochar governing end use efficacy. Biomass and Bioenergy 105, 136–146. https://doi.org/10.1016/j.biombioe.2017.06.024

Zorzeto, T.Q., Dechen, S.C.F., Abreu, M.F. de, Fernandes Júnior, F., 2014. Caracterização física de substratos para plantas. Bragantia 73, 300–311. https://doi.org/10.1590/1678-4499.0086

Supplementary material

Table S1. Average values of the physical and chemical characteristics of the agricultural wastes poultry litter and swine manure and the industrial wastes construction wood, tire and PVC selected for biochar production

Characteristics	Agricultural wastes		Industrial wastes		
	Poultry litter	Swine manure	Construction wood	Tire	PVC
Bulk density, g cm^{-3}	0.37 ± 0.03	0.32 ± 0.03	0.20 ± 0.01	0.34 ± 0.02	0.87 ± 0.02
WHC, %	145 ± 9.00	99.3 ± 7.00	64.0 ± 2.00	5.00 ± 1.00	4.33 ± 1.00
Volatile matter, %	66.7 ± 0.26	57.6 ± 0.42	43.7 ± 1.78	60.0 ± 0.39	57.2 ± 0.80
Ash content, %	18.1 ± 0.25	34.0 ± 0.21	1.63 ± 0.03	12.8 ± 0.18	20.2 ± 0.27
Fixed carbon, %	0.81 ± 0.23	BDL	46.8 ± 1.71	26.1 ± 0.27	22.2 ± 1.08
EC, dS m^{-1}	2.70 ± 0.05	1.08 ± 0.08	0.14 ± 0.10	0.09 ± 0.01	0.04 ± 0.0
pH in water	9.16 ± 0.02	7.20 ± 0.03	6.94 ± 0.19	7.29 ± 0.01	8.09 ± 0.27
CEC, $cmol_c$ kg^{-1}	35.7 ± 4.43	49.6 ± 8.65	5.49 ± 2.51	3.93 ± 1.55	28.5 ± 5.80
C_{total}, % (w:w)	37.8	30.0	48.7	75.6	41.0
H_{total}, % (w:w)	5.63	5.00	6.51	6.62	6.62
N_{total}, % (w:w)	3.96	2.99	0.19	0.46	0.13
O_{total}, % (w:w)	34.5	27.9	42.9	4.51	32.0
Ca_{total}, g kg^{-1}	51.1 ± 12.8	31.4 ± 2.09	57.9 ± 23.7	0.49 ± 0.01	0.61 ± 0.27
K_{total}, g kg^{-1}	13.8 ± 0.60	5.78 ± 0.56	0.33 ± 0.03	0.22 ± 0.04	0.11 ± 0.01
P_{total}, g kg^{-1}	30.8 ± 2.41	70.4 ± 10.7	0.68 ± 0.12	1.43 ± 0.46	0.42 ± 0.28
Mg_{total}, g kg^{-1}	5.31 ± 0.10	6.56 ± 0.46	0.00 ± 0.00	1.24 ± 0.25	5.58 ± 0.00
S_{total}, g kg^{-1}	1.88 ± 0.08	1.67 ± 0.17	0.29 ± 0.04	1.64 ± 0.59	0.91 ± 0.03
Na_{total}, g kg^{-1}	2.76 ± 1.98	1.39 ± 1.00	0.30 ± 0.23	0.00 ± 00.0	0.05 ± 0.05
Fe_{total}, g kg^{-1}	0.79 ± 0.10	1.10 ± 0.14	0.12 ± 0.09	4.03 ± 0.02	1.21 ± 1.03
Mn_{total}, g kg^{-1}	0.06 ± 0.01	0.05 ± 0.02	0.04 ± 0.00	0.06 ± 0.00	0.02 ± 0.02
Zn_{total}, g kg^{-1}	0.10 ± 0.10	0.71 ± 0.10	0.05 ± 0.00	4.11 ± 1.03	1.81 ± 0.34
Ba_{total}, g kg^{-1}	0.03 ± 0.01	0.06 ± 0.01	0.02 ± 0.00	0.03 ± 0.00	0.06 ± 0.01
Al_{total}, g kg^{-1}	0.49 ± 0.07	0.46 ± 0.04	0.24 ± 0.05	2.00 ± 0.24	3.56 ± 0.05
Cu_{total}, g kg^{-1}	0.06 ± 0.02	0.08 ± 0.01	0.01 ± 0.00	0.06 ± 0.03	1.14 ± 0.15

Adapted from (Rodriguez et al., 2020; Rodriguez et al., 2021). Mean values ± standard deviation. WHC: water holding capacity, pH in water: 1:2.5; EC: electrical conductivity, CEC: cation exchange capacity, BDL: below detection limits. *

Table S2. Rotated factor loadings and commonalities (Com) of the nine factors calculated from the characteristics of biochars produced from the agricultural wastes poultry litter (PL) and swine manure (SM) and from the industrial wastes construction wood (CW), tire (TR) and PVC plastic (PVC), subjected to pyrolysis temperatures of 300, 400, 500, 600 and 700 °C

Biochar Characteristics	Component									Com
	1	2	3	4	5	6	7	8	9	
Pb_{total}	0.94	0.06	-0.17	-0.06	0.08	0.04	-0.07	-0.05	0.13	0.95
Cu_{total}	0.91	0.08	-0.14	0.06	0.11	0.10	-0.06	-0.06	0.13	0.91
Al_{total}	0.91	0.00	-0.13	0.21	0.16	0.10	-0.05	0.02	0.11	0.93
Cd_{total}	0.79	0.21	-0.13	0.09	0.03	-0.06	-0.01	0.17	-0.23	0.78
Ba_{total}	0.55	-0.18	-0.12	0.44	0.17	0.06	0.14	0.48	-0.24	0.88
$Mg_{soluble}$	0.54	0.37	0.06	0.09	0.29	-0.06	0.24	-0.22	0.31	0.74
Cr_{total}	0.54	0.11	-0.09	0.51	0.07	-0.09	0.01	0.00	-0.12	0.59
Biochar yield	0.08	0.90	-0.12	-0.03	0.07	0.06	-0.05	0.08	0.05	0.85
Volatile matter	-0.05	0.89	0.07	0.07	-0.09	-0.19	0.01	0.13	0.10	0.88
Hydrogen	0.20	0.76	-0.29	-0.12	0.19	-0.20	-0.28	-0.03	0.13	0.89
pH	-0.32	-0.72	0.23	0.17	0.18	0.04	-0.24	0.12	-0.08	0.81
CEC	0.01	-0.45	-0.05	0.25	0.15	0.01	0.24	-0.06	0.29	0.44
$K_{soluble}$	-0.07	-0.11	0.86	-0.24	0.11	-0.05	-0.04	-0.01	-0.08	0.84
K_{total}	-0.13	-0.12	0.82	0.36	0.15	-0.06	0.00	-0.04	-0.13	0.88
Na_{total}	-0.18	-0.10	0.82	0.05	0.16	-0.10	0.05	-0.19	0.08	0.80
$S_{soluble}$	-0.20	-0.20	0.68	0.18	-0.03	0.43	-0.04	-0.02	0.00	0.76
Nitrogen	-0.03	0.48	0.60	0.18	0.14	-0.05	0.15	-0.06	-0.12	0.68
$P_{soluble}$	-0.24	0.42	0.53	0.17	0.19	-0.07	0.31	0.03	0.20	0.72
Mo_{total}	-0.02	0.02	0.20	0.86	0.03	0.19	-0.04	-0.17	0.14	0.86
Fe_{total}	0.08	-0.06	0.09	0.85	0.24	0.11	0.14	0.15	-0.12	0.87
B_{total}	0.03	-0.06	0.15	0.82	-0.01	-0.09	-0.01	0.15	-0.20	0.77
Mn_{total}	0.24	-0.02	0.01	0.80	0.11	0.13	0.11	-0.15	0.10	0.77
WRC	0.51	-0.31	-0.13	0.53	0.04	0.33	0.07	0.26	-0.02	0.85
Ash content	0.17	-0.18	0.12	0.09	0.90	0.08	0.08	0.00	-0.19	0.94
Carbon	-0.20	-0.15	-0.08	-0.02	-0.88	0.04	0.04	0.08	-0.20	0.90
Mg_{total}	0.18	-0.09	0.32	0.23	0.85	0.00	0.01	-0.02	-0.04	0.92
Fixed carbon	-0.22	-0.52	-0.16	-0.14	-0.70	0.11	-0.10	-0.09	0.06	0.89
P_{total}	-0.25	-0.12	0.47	0.12	0.52	0.00	0.49	0.09	-0.17	0.86
Zn_{total}	0.22	-0.10	-0.17	0.14	-0.16	0.82	-0.08	0.15	0.00	0.83
S_{total}	-0.11	-0.41	0.24	0.18	0.01	0.78	-0.05	0.04	-0.12	0.89
Ca_{total}	-0.23	-0.24	0.25	-0.01	-0.20	-0.56	-0.32	0.18	0.13	0.68
WMD	0.28	0.01	-0.49	0.03	-0.05	-0.49	-0.34	-0.16	0.11	0.71
EC	-0.19	-0.02	-0.35	-0.14	0.53	-0.06	-0.60	-0.13	0.08	0.85
NP	-0.26	-0.17	-0.04	0.20	0.48	0.03	0.59	0.09	-0.25	0.80
As_{total}	-0.02	0.30	-0.10	-0.08	-0.09	0.07	0.04	0.75	0.18	0.72
Co_{total}	0.09	-0.20	-0.10	0.42	0.10	0.38	0.15	0.54	-0.39	0.85
Oxygen	0.02	0.36	-0.10	-0.15	-0.10	-0.10	-0.18	0.01	0.61	0.59
$Ca_{soluble}$	0.40	-0.19	-0.13	-0.02	-0.04	-0.16	-0.05	0.29	0.53	0.61
Eigenvalues	7.35	7.12	5.05	2.97	2.23	2.00	1.50	1.19	1.08	
Percentage variance	19.34	18.74	13.30	7.82	5.86	5.26	3.94	3.14	2.85	
Cumulative %	19.34	38.07	51.37	59.19	65.05	70.30	74.24	77.38	80.24	

CEC: Cation exchange capacity, WRC: Water retention capacity, WMD: weighted mean diameter, EC: Electric conductivity, NP: Neutralizing power. Com: commonality.

Table S3. Analysis of variance (ANOVA) of the biochar viability indicators (BVI) according to factor loading using characteristics of the biochars produced from the agricultural wastes poultry litter (PL) and swine manure (SM) and from the industrial wastes construction wood (CW), tire (TR) and PVC plastic (PVC), subjected to pyrolysis temperatures of 300, 400, 500, 600 and 700 °C

	Sum of Squares	Degrees of Freedom	Mean Square	t	Significance
Between Groups	2.062	74	0.028	32.293	0.000
Within Groups	0.129	150	0.001		
Total	2.192	224			

Table S4. Classification matrix of the biochars (BC) produced from the agricultural wastes poultry litter (PL) and swine manure (SM) and from the industrial wastes construction wood (CW), tire (TR) and PVC plastic (PVC), subjected to pyrolysis temperatures of 300, 400, 500, 600 and 700 °C, for the biochar quality criteria proposed by Camps-Arbestain et al. (2015)

Biochar	Nutritional requirements (g kg^{-1})				H/C	WMD	NP	BC Index					Classification
	$P_{soluble}$	$K_{soluble}$	$S_{soluble}$	$Mg_{soluble}$				Carbon stability (sBC)	Nutritional Class	Neutralizing Class	Textural Class		
	4.4	4.6	1.5	2.1									
PL+CW300	2.830	19.147	1.27	1.248	0.08	3.52	50.90	3	1	3	3	10	Moderately Viable
PL400	2.879	36.196	2.03	1.108	0.06	2.83	25.44	2	2	3	2	9	Moderately Viable
PL+PVC400	1.291	29.218	0.46	2.538	0.09	4.13	30.17	2	2	3	4	11	Moderately Viable
PVC500	0.007	0.048	0.10	1.406	0.19	4.55	41.16	1	0	3	4	8	Low Viability
CW500	0.021	0.688	0.34	0.010	0.04	5.92	11.95	3	0	2	4	9	Moderately Viable
PL+CW500	1.453	30.223	2.10	0.297	0.03	4.37	57.52	4	2	3	4	13	Highly Viable
CW+PVC600	0.005	1.414	0.08	1.304	0.01	4.59	28.71	2	0	3	4	9	Moderately Viable
PL+CW600	0.530	17.152	0.56	0.166	0.05	3.93	58.75	3	1	3	3	10	Moderately Viable
PL+PVC600	0.006	28.262	0.30	3.137	0.02	4.48	31.48	2	2	3	4	11	Moderately Viable
TR700	0.009	0.575	0.94	0.170	0.10	3.06	56.94	4	0	3	3	10	Moderately Viable
SM700	0.855	16.775	2.60	0.674	0.00	3.22	77.00	1	2	3	3	9	Moderately Viable
CW700	0.006	1.788	0.43	0.007	0.01	6.47	21.41	4	0	3	4	11	Moderately Viable
PL+CW700	0.241	22.576	0.45	1.602	0.01	2.71	52.97	4	1	3	2	10	Moderately Viable
PL+TR700	0.018	28.452	2.41	0.424	0.01	2.77	28.23	3	2	3	2	10	Moderately Viable

WMD: weighted mean diameter, NP: Neutralizing power.

Table S5. Classification matrix of the of the biochars produced from the agricultural wastes poultry litter (PL) and swine manure (SM) and from the industrial wastes construction wood (CW), tire (TR) and PVC plastic (PVC), subjected to pyrolysis temperatures of 300, 400, 500, 600 and 700 °C, for toxic element content IBI (2015)

Biochar	Total micronutrient content (mg kg^{-1})							Total trace-element content (mg kg^{-1})						Na_{total} (mg kg^{-1})	Toxicity classification		
	B	Cu	Fe	Mn	Mo	Ni	Zn	As	Cd	Co	Cr	Pb	Se		Toxic	Dangerous	Saline
PL+CW300	19	66	709	75	2	12	70	1	0	1	66	0	2	2195	Non-toxic	Non-dangerous	Saline
PL400	10	1119	773	118	2	21	1365	0	2	2	1119	446	3	1564	Non-toxic	Dangerous	Saline
PL+PVC400	10	1513	224	7	0	12	2296	0	3	1	1513	1117	2	28	Non-toxic	Dangerous	Non-saline
PVC500	6	36	588	108	0	7	54	1	0	1	36	0	2	490	Non-toxic	Non-dangerous	Non-saline
CW500	38	95	1436	146	3	25	221	0	1	2	95	0	2	4559	Non-toxic	Non-dangerous	Saline
PL+CW500	14	101	863	80	2	6	4601	0	1	4	101	1	3	1421	Non-toxic	Non-dangerous	Saline
CW+PVC600	3	710	348	52	0	12	1191	0	0	1	710	529	2	238	Non-toxic	Dangerous	Non-saline
PL+CW600	35	65	951	95	3	11	120	0	0	2	65	0	2	4378	Non-toxic	Non-dangerous	Saline
PL+PVC600	8	981	484	124	1	35	1620	0	3	2	981	623	3	1745	Non-toxic	Dangerous	Saline
TR700	3	36	546	8	0	8	6171	1	1	8	36	12	2	86	Non-toxic	Non-dangerous	Non-saline
SM700	12	161	1722	42	1	9	1180	0	1	9	161	0	2	3522	Non-toxic	Non-dangerous	Saline
CW700	4	36	434	124	0	20	17	1	0	1	36	0	2	448	Non-toxic	Non-dangerous	Non-saline
PL+CW700	26	179	1105	102	2	24	73	1	0	2	179	0	2	3632	Non-toxic	Non-dangerous	Saline
PL+TR700	14	101	1140	116	3	10	4669	1	1	4	101	35	2	1951	Non-toxic	Non-dangerous	Saline

CAPÍTULO 4

CRESCIMENTO DA CROTALARIA EM REJEITOS DA MINERAÇÃO DE Fe E Mn CONDICIONADOS COM FERTILIZANTES E BIOCARVÕES

RESUMO

Atividades como a mineração podem levar ao aumento da concentração de metais pesados no solo, pela geração de resíduos com altas concentrações de elementos metálicos provenientes dos processos de lavra e refinamento dos metais, causando alteração física, química e biológica dos ecossistemas associados às áreas mineradas. Nessas situações, a chamada atenuação natural assistida com uso de materiais orgânicos como biocarvões, pode levar a melhoria da qualidade do solo e a destinação adequada de resíduos agrícolas e industriais. Objetivou-se avaliar o crescimento da crotalaria (C*rotalaria juncea*) em rejeitos de mineração de Fe e Mn, condicionados com biocarvões derivados de resíduos agrícolas (cama de frango - PL) e industriais (madeira da construção - CW, pneu - TR e plástico PVC - PVC) produzidos por pirólise e em co-pirólise lenta a 600 ºC (PL+CW; PL+TR e PL+PVC). A crotalaria foi cultivada em vasos em casa de vegetação utilizando a dose de 5 % de biocarvão. Avaliaram-se a germinação; altura das plantas, produção de biomassa seca da parte da folha, caule e total e conteúdo de macro e micronutrientes e alguns elementos traços. Além disso, a composição química da solução do solo foi avaliada (0, 15, 30 e 45 após o plantio da crotalaria). De modo geral, verificou-se maiores taxas de germinação, maior crescimento, produção de fitomassa e acúmulo de macro e micronutrientes no rejeito de Mn quando comparado com o rejeito de Fe. O elevado teor de cinzas, pH alcalino e alta CE dos biocarvões, a exceção do derivado de madeira de construção, aumentou o pH e CE da solução do solo, imediatamente após sua aplicação e inibiu a germinação e crescimento da crotalaria. A planta foi responsiva a aplicação de fertilizantes em ambos os rejeitos, porém, com maior produção de fitomassa no rejeito de Mn. Com exceção dos biocarvões produzidos a partir do resíduo de madeira de construção quando aplicados ao rejeito de Mn, não se verificaram efeitos positivos da aplicação de biocarvões aos rejeitos sobre o crescimento e desenvolvimento das plantas.

Palavras-chave: Pirólise e co-pirólise, resíduos orgânicos e sintéticos, revegetação, áreas mineradas.

1. Introdução

No Brasil existem recursos minerais abundantes como minério de ferro (Fe) e manganês (Mn), com reservas estimadas em 32 bilhões de toneladas e 110 milhões de toneladas, respectivamente (Bernhardt e Reilly, 2019). Isso representa 18,8 e 14,5% das reservas mundiais de Fe e Mn, respectivamente (Bernhardt e Reilly, 2019). Em 2017 a produção brasileira de minério de Fe processado foi de 453,70 milhões de toneladas (18,7% da produção mundial), enquanto a de Mn foi 2.88 milhões de toneladas (16,5% da produção mundial) (DNPM, 2018). Como a mineração e processamento desses minérios é continua, quantidades significativas de resíduos sólidos contendo rejeitos de Fe e Mn são geradas a cada ano. De acordo com estimativa de Silva et al. (2012), a quantidade anual de rejeitos sólidos gerados irá praticamente dobrar, passando de 348 milhões de toneladas em 2010 para 684 milhões de toneladas em 2030. Com isso, impactos ambientais negativos associados à disposição desses rejeitos, assim como as extensas áreas destinadas à sua estocagem, representam riscos significativos a segurança do meio ambiente (Lei et al., 2019).

Na maioria das vezes, os rejeitos sólidos são usados na construção de barragens de contenção ou são depositados na própria área minerada e/ou em outros locais, formando "pilhas estéril" (Teixeira et al., 2017). Apesar da concentração de metais nestes rejeitos ser considerada baixa para a indústria de mineração, é alta o suficiente para ser uma fonte contínua de contaminação do solo e a água (Karaca et al., 2018). Com isso, estes rejeitos podem ser um problema ambiental de longo prazo, com danos inaceitáveis ao meio ambiente e riscos à saúde humana (Karaca et al., 2018). As empresas de mineração estão cientes dos efeitos prejudiciais da mineração e buscam alternativas para minimizar os impactos ambientais. Neste sentido, a reversão desses impactos só é possível mediante a intervenção antrópica por meio da recuperação de áreas degradadas, a qual preconiza a adoção de procedimentos para restabelecer a cobertura vegetal, a estabilização e a redução de potenciais riscos de erosão e contaminação de cursos de água, assim como a recuperação da paisagem e suas funções ecológicas (Beesley et al., 2011).

No entanto, áreas mineradas são naturalmente difíceis de serem revegetadas (Anawar et al., 2015). Nessas condições, a qualidade do substrato é geralmente de baixa fertilidade (Fellet et al., 2011) e as propriedades físicas são limitantes ao armazenamento e movimento de água, bem como o desenvolvimento de raízes, entre outras desvantagens (Anawar et al., 2015). A aplicação de fertilizantes orgânicos e/ou inorgânicos para diminuir a biodisponibilidade de

elementos tóxicos (ou seja, estabilização química) em combinação com plantas tolerantes a metais é usada frequentemente em iniciativas de fitoestabilização (Zago et al., 2019). Adicionalmente, Zago et al. (2019) relataram que, entre outras razões, a fertilização visa facilitar e aprimorar a revegetação em solos contaminados, melhorando suas propriedades físico-químicas e biológicas. Carvalho et al. (2018), ao avaliarem a influência do manejo de nutrientes no crescimento de duas espécies vegetais para revegetação de áreas de mineração de Fe, verificaram que a fertilização aumentou o crescimento de ambas as espécies de plantas em Latossolos, solos de canga e rejeitos de mineração de Fe. Além disso, a omissão de macronutrientes reduziu o crescimento de plantas com maior intensidade do que a de micronutrientes, indicando que a falta de N, P e K pode impactar negativamente a reabilitação de áreas minadas.

Biocarvão podem ser definidos como produtos sólidos obtidos a partir da conversão térmica da biomassa em compostos químicos carbonizados, usando altas temperaturas na ausência ou presença limitada de oxigênio (Lehmann e Joseph, 2015). Muitos estudos propuseram que os biocarvões possam ser usados como aditivo ao solo e melhorar as propriedades físicas (Glaser et al., 2002; Are et al., 2018), químicas (Glaser et al., 2002; Chan et al., 2007; Pandit et al., 2018) e biológicas (Lehmann et al., 2011; Zhang et al., 2018) de solos. Além disso, pode atuar como fonte de micro e macronutrientes para as plantas (Prakongkep et al., 2015; Guo et al., 2020). Os biocarvões também possuem elevada CTC, um grande número de grupos funcionais e alta superfície específica, podendo adsorver e complexar metais por meio de múltiplos mecanismos de interação, tais como: atração eletrostática, troca-iônica, adsorção física, complexação de superfície e/ou precipitação (Ahmad et al., 2014). Nesse contexto, biocarvões podem ser uma opção interessante para serem usados em áreas mineradas a serem revegetadas quando combinados com fertilizantes químicos. No entanto, não há informações disponíveis sobre a relação entre biocarvões e fertilizantes químicos e os seus efeitos sinérgicos ou não na germinação e crescimento e desenvolvimento de espécies, tolerantes a condições de excesso de metais pesados, como a crotalaria (*Crotalaria juncea*), visando a fitorremediação de rejeitos de mineração Fe e Mn.

Os biocarvões podem ser utilizados na recuperação de áreas mineradas, proporcionando melhoria das condições para o crescimento e desenvolvimento e de plantas. Partindo desse pressuposto, objetivou-se avaliar o crescimento da crotalaria (C*rotalaria juncea*) em rejeitos de mineração de Fe e Mn, condicionados com biocarvões derivados de resíduos agrícolas (cama

de frango -PL) e industriais (madeira da construção -CW e pneu - TR, plástico PVC - PVC) produzidos por pirólise e co-pirólise lenta a 600 ºC (PL+CW; PL+TR e PL+PVC).

2. Material e Métodos

O ensaio foi instalado em vasos contendo 3,0 dm^3, em casa de vegetação, do Departamento de Solos da Universidade federal de Viçosa (UFV), utilizando rejeitos de mineração de Fe e Mn da Província Mineral de Carajás, município de Parauapebas-PA (S06°02′21.5″ W050°16′34.8″). Os rejeitos utilizados no estudo foram previamente secos, peneirados para obtenção de diâmetro < 2 mm e caracterizados química e fisicamente antes do estabelecimento dos tratamentos (Tabela 1).

A espécie utilizada foi a crotalaria (*Crotalaria juncea)*, escolhida por ser uma leguminosa utilizada frequentemente para a cobertura de solos marginais (Maiti e Maiti, 2015) e pela tolerância a fitotoxidez por metais como Cu (Carramaschi et al., 2011). Além disso, apresenta também rápido crescimento (Galdino et al., 2019).

Tabela 1. Caracterização física e química dos rejeitos da mineração de Fe e Mn provenientes da Província Mineral de Carajás, Parauapebas, Brasil.

Rejeito	pH	K^+	Ca^{2+}	Mg^{2+}	Al^{3+}	H+Al	CTC	S	P	P-Rem	V	MO
	H_2O	----------$cmol_c\ dm^{-3}$----------						---$mg\ dm^{-3}$----		$mg\ L^{-}$	%	$g\ kg^{-1}$
Fe	6,1	0,01	0,21	0,08	ND	0,6	0,9	16,3	3,0	38,5	35,2	0,0
Mn	5,3	0,02	ND	ND	ND	2,5	2,6	44,7	0,3	15.6	2,30	6,6
	Zn	Cr	Cu	Pb	Fe[a]	Mn[a]	Fe[b]	Mn[b]	CRA	Areia	Silte	Argila
	----------$mg\ dm^{-3}$----------						------$g\ dm^{-3}$------		%	----------$g\ kg^{-1}$----------		
Fe	24,89	6,77	65,46	17,97	39,2	60,0	148,74	36,32	18	670	280	50
Mn	15,25	88,95	357,87	119,29	21,4	463,7	33,8	90,8	32	870	110	20

[a] Fe e Mn disponíveis (extrator Mehlich-1); [b] Fe e Mn totais (extraídos com HNO_3 e H_2O_2); CRA: capacidade de retenção de água determinada a 33 kPa; ND: não determinado pelo limite de detecção. pH em água relação 1:2,5; o P, K, Fe e Mn disponíveis: extrator Mehlich-1 (Donagema et al., 2011). Ca, Mg e Al trocáveis: extrator KCl 1 mol L^{-1} e determinados por espectofotometria de absorção atômica (Donagema et al., 2011). A Capacidade de Troca Catiônica a pH 7,0 (CTC): determinada por colorimetria pelo método de Fenato. Fósforo remanescente (P-Rem): determinado após agitação por 1 h, com solução de 0,01 mol L^{-1} de $CaCl_2$, com 60 mg L^{-1} de P (Alvarez e Fonseca, 1990). A textura foi determinada usando o método de pipeta (Gee e Bauder, 1986). Os teores totais de Zn, Cr, Cu, Pb, Fe e Mn: extraídos com HNO_3 e H_2O_2 e determinados por ICP-OES.

Os biocarvões utilizados foram selecionados entre 75 derivados de resíduos agrícola (esterco suíno e cama de frango) e industriais (madeira da construção, pneu e plástico PVC) produzidos por pirólise e co-pirólise lenta em diferentes temperaturas (300, 400, 500, 600, 700ºC). Detalhes sobre o processo de preparação dos resíduos e produção dos biocarvões podem ser encontrados em Rodriguez et al. (2020 e 2021) e Lustosa Filho et al. (2017), respectivamente. Na seleção dos biocarvões considerou-se a análise de componentes principais

(ACP) e índice de viabilidade de biocarvão (IVB) (Camps-Arbestain et al., 2015; IBI, 2015) mais adequados, considerando as propriedades restritivas dos rejeitos de mineração de Fe e Mn ao crescimento e desenvolvimento de plantas (Tabela 1). Sendo assim, os biocarvões utilizados foram aqueles oriundos de pirólise de resíduos de cama de frango (PL), madeira da construção (CW), pneu (TR) e plástico PVC (PVC) e da co-pirólise (relação 1:1, m/m) do primeiro com os demais, no caso: PL+CW, PL+TR e PL+PVC, todos produzidos a 600ºC. Tratamentos-controle dos rejeitos de Fe e Mn com (T_{Fe+} e T_{Mn+}) e sem (T_{Mn} e T_{Fe}) fertilização química também foram acrescentados. A fertilização química foi realizada com soluções de 75 mg dm^{-3} de NH_4NO_3, 100 mg dm^{-3} de $Ca_3(PO_4)_2$, 100 mg dm^{-3} (KCl), 10 mg dm^{-3} de K_2SO_4, 5 mg dm^{-3} de $ZnSO_4$, 2 mg dm^{-3} de H_3BO_3, 2 mg $CuSO_4$-$5H_2O$ e 1 mg dm^{-3} $(NH_4)_6Mo_7O_{24}$-$4H_2O$).

O experimento foi conduzido em blocos casualizados, em esquema fatorial, com tratamentos adicionais (7 × 2 + 4), e quatro repetições. Foram sete biocarvões (PL, CW, TR, PVC, PL+CW, PL+TR e PL+PVC), dois rejeitos de mineração (Fe e Mn) e quatro controles (rejeito de minério de Fe + fertilizante químico – Fe^+; rejeito de minério de Fe sem fertilizante químico, Fe^-; rejeito de minério de Mn + fertilizante químico, Mn^+ e rejeito de minério de Mn sem fertilizante químico, Mn^-). A proporção de biocarvão usada para o condicionamento dos resíduos foi de 5 % (m:m) (Beesley et al., 2011).

Tabela 2. Características físicas e químicas dos biocarvões produzidos pela pirólise de resíduos de cama de frango (PL), madeira de construção (CW), pneu (TR) e plástico PVC (PVC) e por co-pirólise de misturas (1:1, m:m) de resíduos (PL+CW, PL+TR e PL+PVC), em temperatura de 600ºC.

Biocarvões[1]	CRA	pH	CE	CTC	PN	Cinzas	K	Ca	Mg	Na	P	S	Fe	Mn
	g kg^{-1}		dS m^{-1}	$cmol_c$ kg^{-1}	-------%-------		----------g kg^{-1}----------						- -mg kg^{-1}-	
PL	0,45	10,61	10,91	15,52	24,79	27,81	47,24	1,55	0,33	3,54	0,73	1,95	0,5	ND
CW	0,47	9,51	0,09	30,34	6,08	4,22	1,47	2,55	0,02	0,39	0,01	0,55	1,02	ND
TR	0,84	8,55	0,44	21,03	49,73	12,04	0,81	3,96	0,32	0,75	0,01	1,85	0	1,51
PVC	0,79	11,76	146,13	31,87	38,68	49,49	0,09	4,09	0,01	0,1	0,01	0,06	ND	ND
PL+CW	0,48	10,57	1,68	31,46	58,75	21,99	17,15	1,48	0,17	1,38	0,53	0,56	2	ND
PL+TR	0,66	10,74	1,95	27,43	29,54	25,55	25,71	1,57	0,25	2,85	0,45	2,26	1,5	ND
PL+PVC	0,79	8,39	2,95	11,62	31,48	43,09	28,26	2,88	3,14	2,53	0,01	0,3	ND	4

[1] : parte dos dados foram adaptados de (Rodriguez et al., 2020)ND: não determinado pelo limite de detecção. Os elementos B, Co, Cr, Cu, Mo e Pb apresentaram em todos os biocarvões valores abaixo do límite de detecção. Capacidade de retenção de água (CRA) em câmara de pressão a 33 kPa durante 72 h (Zorzeto et al., 2014); condutividade elétrica (CE) e pH em água por potenciometria em solução 1:20 (Al-Wabel et al., 2013); teores de cinzas (ASTM Standard D1762 -84, 2007); poder de neutralização (PN) pelo método titulométrico ácido/base (Rayment e Lyon, 2010); capacidade de troca catiônica (CTC) pelo método de saturação com NH4OAC (1,0 mol L-1) e pelo método de Fenato utilizando colorimetria (Song e Guo, 2012); e os teores totais (Ca, K, P, Mg, S, Na, Fe, Mn, Zn, Mo, B, Ba, Al, Cu, As, Pb, Se, Cd, Co, Cr) de acordo com Enders and Lehmann (2012).

A caracterização química dos biocarvões foi feita em amostras moídas e passadas em peneira de 60 mesh (0,25 mm), secos em estufa a 65 °C ± 2 °C por 48 h. As sementes de crotalaria foram colocadas a uma profundidade de três cm, obtendo-se a germinação aos cinco dias, para um total de cinco plântulas por vaso após 20 dias de plantio, tendo sido feito replantio e desbaste neste intervalo.

As plantas foram avaliadas quanto à porcentagem de germinação, aos cinco dias, e quanto ao crescimento aos 45 dias após a semeadura, seguido do corte das plantas de crotalária, próximo do florescimento (Santana e Ascencio, 2011). Folhas e galhos foram separados, pesadas (peso úmido) e secas em estufa por 72 h a 65 °C, até peso constante para determinação do peso seco. Após moagem (folhas e galhos), em moinho tipo Willey, foi realizada a digestão ácida com HNO_3 e HF concentrados (3:1, v:v), segundo US EPA 3052 (USEPA, 1996), determinando-se as concentrações de P, K, Ca, Mg, Zn, Cu, Mn e Fe por espectroscopia de emissão atômica com plasma indutivamente acoplado (ICP-OES) (He et al., 2008) e N total por destilação e titulação com HCl 0,02 mol L^{-1} (método de Kjeldahl) (Nigussie et al., 2012).

A coleta da solução do solo foi realizada com amostrador de cápsula micro porosa (modelo 1908D2,5L10K05 Rhizon SMS), inserido em cada vaso num ângulo de 45°, com auxílio de uma seringa de 60 mL de plástico para formação de vácuo (Beesley et al., 2013). Após a instalação dos extratores, foi adicionada água deionizada, visando atingir teor de água próximo da capacidade de campo, mantendo-se por um período de 12 horas, visando equilíbrio entre o solo e a fase líquida. Após esse período, foram realizadas as extrações, sendo a primeira coleta 20 dias após a instalação do ensaio e a cada 15 dias, durante 45 dias, o que proporcionou quatro coletas. As amostras de solução do solo foram analisadas quimicamente quanto pH e condutividade elétrica (CE) por potenciometria em solução de água (1:2,5) (v:v); Ca^{2+} e Mg^{2+} extraídos com KCl (1,0 mol L^{-1}) e determinados por espectrometria de emissão atômica (Ca^{2+}, Mg^{2+}); teores de K, Na e P foram extraídos com Mehlich-1 (Fellet et al., 2011; Schulz et al., 2013); teores de elementos totais, S, Fe, Cu, Mn, Zn, Ni, Cr e Pb extraídos após digestão ácida, conforme (Enders e Lehmann, 2012), e determinados por espectroscopia emissão atômica com plasma indutivamente acoplado (ICP-OES).

Os resultados da solução do solo foram sometidos a ANOVA num esquema de parcela subdividida com o tempo de coleta como parcela principal, quando o efeito do tempo for significativo, aplicou-se análise de regressão. Os resultados das variáveis de germinação,

crescimento e conteúdo de nutrientes e metais das plantas foram submetidos a ANOVA e as médias comparadas por contrastes ortogonais (Co) e de interesse (Ci). Utilizou-se o teste F para avaliar a significância da ANOVA e dos contrastes considerando até 5% de probabilidade. Os contrastes ortogonais comparam as medias gerais entre as variáveis obtidas para os rejeitos de Fe e Mn, sendo Co1 = Rejeito Mn *vs* Rejeito Fe; Co2 = controles (Mn^- + Mn^+ + Fe^- + Fe^+) *vs* biocarvões (PL + CW + TR + PVC + PL+CW + PL+TR + PL+PVC); Co3 = controles sem fertilização (Mn^- + Fe^-) *vs* controles fertilizados (Mn^+ + Fe^+); Co4 = biocarvões de pirólise (PL + CW + TR + PVC) *vs* biocarvões de co-pirólise (PL+CW + PL+TR + PL+PVC); Co5 = biocarvões de resíduos de origem sintética (TR + PVC) *vs* biocarvões de resíduos de origem natural (PL + CW); Co6 = biocarvões de resíduos de origem sintética (TR *vs* PVC); Co7 = biocarvões de resíduos de origem natural (PL *vs* CW); C8 = co-pirólise de resíduos de origem sintética com a cama de frango (PL+TR + PL+PVC) *vs* co-pirólise de resíduos de origem natural (PL+CW); C9 = co-pirólise da cama de frango e os resíduos de origem sintética (PL+TR *vs* PL+PVC); C10 = pirólise *vs* co-pirólise dos resíduos de origem natural (PL *vs* PL+CW). Além disso foram feitas comparações a partir de contrastes de interesse, sendo Ci1 = controles fertilizados (Mn^+ + Fe^+) *vs* biocarvões de pirólise (PL + CW + TR + PVC); Ci2 = controles fertilizados (Mn^+ + Fe^+) *vs* biocarvões de co-pirólise (PL+ PL+CW + PL+TR + PL+PVC). A análise de correlação simples de Pearson também foi aplicada para avaliar as relações entre o crescimento e desenvolvimento da crotalaria e o conteúdo de nutrientes e metais na parte aérea, assim como também com os atributos químicos dos rejeitos. Todas as análises foram realizadas utilizando o software SPSS 22 (IMB, 2013).

3. **Resultados**

3.1. Crescimento de planta

A análise de variância mostrou a influência dos diferentes biocarvões e rejeitos sobre a germinação, a produção de biomassa e o acúmulo de nutrientes e metais pesados na parte aérea da crotalaria ($P < 0,05$) (Tabela S1). As médias e comparações por contrastes ortogonais (Co) e de interesse (Ci) encontram-se na Tabela 3 e 4.

As diferenças de comportamento das variáveis avaliadas por meio dos contrastes de médias entre rejeitos de Mn e Fe (Co1 = Rejeito Mn *vs* Rejeito Fe) mostraram os maiores ($p<0,05$) valores das variáveis obtidas no rejeito de Mn, independente do tratamento (Tabela 3), contudo não se observou diferenças significativas ($p<0,05$) para os conteúdos de S, Fe e Mn

(Tabela 4). Ressalta-se que, entre os tratamentos-controle {Co3 = ($Mn^+ + Fe^+$) *vs* ($Mn^- + Fe^-$)}, os maiores ($p<0,05$) valores observados ocorreram quando a fertilização foi feita (+) para todas as variáveis, tendo como exceção a porcentagem de germinação da crotalária (Tabela 3) e conteúdo de Mg (Tabela 4).

Tabela 3. Médias e significância de contrastes ortogonais e de interesse para as variáveis: germinação (Ger), altura da planta (H) e biomassa da crotalária (*Crotalaria juncea*) cultivada em rejeitos de mineração de Fe e Mn condicionados com fertilização química e biocarvões produzidos por pirólise de resíduos de cama de frango (PL), madeira de construção (CW), pneu (TR), plástico PVC (PVC) e co-pirólise (PL+CW; PL+TR e PL+PVC) a 600ºC, e respectivos controles com e sem fertilização química (Fe^+, Fe^-, Mn^+ e Mn^-)

Tratamentos	Ger	H	Biomassa seca		
			Folha	Caule	Total
	%	cm	----------g----------		
	Rejeitos da mineração de Mn				
Mn^-	90,0	15,0	0,13	0,26	0,39
Mn^+	90,0	51,9	3,54	2,84	6,38
PL	82,5	1,75	0,07	0,08	0,15
CW	87,5	55,8	4,22	3,01	7,23
TR	77,5	0,00	0,00	0,00	0,00
PVC	10,0	0,00	0,00	0,00	0,00
PL+CW	87,5	49,0	4,23	2,46	6,69
PL+TR	92,5	33,2	2,03	0,89	2,92
PL+PVC	12,5	0,00	0,00	0,00	0,00
	Rejeitos da mineração de Fe				
Fe^-	55,0	22,6	0,30	0,65	0,95
Fe^+	55,0	50,1	3,05	2,03	5,08
PL	2,50	0,00	0,00	0,00	0,00
CW	67,5	45,4	2,30	1,56	3,86
TR	70,0	44,9	2,12	1,50	3,62
PVC	0,00	0,00	0,00	0,00	0,00
PL+CW	5,00	0,00	0,00	0,00	0,00
PL+TR	15,0	0,00	0,00	0,00	0,00
PL+PVC	0,00	0,00	0,00	0,00	0,00
Contrastes					
Co1 (Rej Mn vs Rej Fe)	-4.25^{**}	-4.86^{**}	-0.71^{**}	-0.43^{**}	-1.14^{**}
Co2 ($Mn^- + Mn^+ + Fe^- + Fe^+$) *vs* (TR + PVC + PL + CW + PL+TR + PL+PVC + PL+CW)	-3.05^{**}	-18.4^{**}	-0.69^{**}	-0.77^{**}	-1.45^{**}
Co3 ($Mn^+ + Fe^+$) *vs* ($Mn^- + Fe^-$)	0.00^{ns}	32.2^{**}	3.08^{**}	1.98^{**}	5.06^{**}
Co4 (TR + PVC + PL + CW) *vs* (PL+TR + PL+PVC + PL+CW)	-1.73^{**}	-4.78^{*}	-0.05^{ns}	-0.21^{ns}	-0.26^{ns}
Co5 (TR + PVC) *vs* (PL + CW)	2.00^{**}	14.5^{**}	1.12^{**}	0.79^{**}	1.90^{**}
Co6 (TR *vs* PVC)	-6.88^{**}	-22.4^{**}	-1.06^{**}	-0.75^{**}	-1.81^{**}
Co7 (PL *vs* CW)	3.63^{**}	49.7^{**}	3.23^{**}	2.24^{**}	5.47^{**}
Co8 (PL+TR + PL+PVC) *vs* (PL+CW)	1.75^{**}	16.2^{**}	1.60^{**}	1.01^{**}	2.61^{**}
Co9 (PL+TR *vs* PL+PVC)	-4.00^{**}	-16.6^{**}	-1.02^{**}	-0.44^{ns}	-1.46^{**}
Co10 (PL *vs* PL+CW)	0.25^{ns}	23.6^{**}	2.08^{**}	1.19^{**}	3.27^{**}
Ci1 ($Mn^+ + Fe^+$) *vs* (TR + PVC + PL + CW)	-2.31^{**}	-32.5^{**}	-2.20^{**}	-1.67^{**}	-3.87^{**}
Ci2 ($Mn^+ + Fe^+$) *vs* (PL+TR + PL+PVC + PL + PL+CW)	-4.04^{**}	-37.3^{**}	-2.25^{**}	-1.88^{**}	-4.13^{**}

$^{*}P<0,05$; $^{**}P< 0,01$; ^{ns}: não significativo.

Quanto à aplicação de biocarvões, quaisquer que sejam eles, as comparações para ambos os rejeitos (Fe e Mn) não apontaram médias ($p<0,05$) superiores em relação a sua não aplicação, seja no caso da presença (+) ou não (-) de fertilização química {Co2 = ($Mn^- + Mn^+ + Fe^- + Fe^+$) *vs* (PL + CW + TR + PVC + PL+CW + PL+TR + PL+PVC). Porém, quando comparam-se a correção química dos rejeitos em relação a sua aplicação conjunta com os biocarvões, sejam

eles pirolisados {(Ci1= (Mn^+ + Fe^+) *vs* (PL + CW + TR + PVC)} ou co-pirolisados {Ci2 = (Mn^+ + Fe^+) *vs* (PL + PL+CW + PL+TR + PL+PVC)}, observaram-se diferenças significativas para todas as variáveis estudadas (P>0,05) (Tabelas 3 e 4), com uma única exceção, em ambos os casos, o conteúdo de Mg (Tabela 4). Nos casos significativos, as maiores médias também ocorreram para os tratamentos-controle (Mn^+ + Fe^+).

Entre os biocarvões avaliados em ambos os rejeitos, aqueles oriundos da pirólise, quando comparados aos obtidos em có-pirólise {Co4 = (PL + CW + TR + PVC) *vs* (PL+TR + PL+PVC + PL+CW)} proporcionaram maiores (p<0,05) valores para a maioria das variáveis, com exceção do acúmulo de Mg na planta (Tabela 4).

Os biocarvões oriundos de resíduos de origem sintética (TR + PVC) não proporcionaram melhores condições para as plantas de crotalária, comparativamente aos de origem natural (PL + CW) (Co5) (Tabelas 3 e 4). Os mesmos resultados ocorreram quando os biocarvões de origens sintética e natural foram produzidos em có-pirólise {Co8 = (PL+TR + PL+PVC) *vs* (PL+CW)}. Nos casos significativos, as maiores médias foram observadas para o tratamento PL+CW, destacando que no rejeito de mineração de Fe, as plantas cultivadas com PL+TR e PL+PVC não conseguiram crescer e produzir biomassa.

As maiores (p<0,05) médias das variáveis foram observadas para os biocarvões TR nas comparações entre aqueles de origem sintética (Co6 = TR *vs* PVC), destacando-se que, quando utilizou-se PVC, as sementes germinaram apenas no rejeito de Mn, mesmo assim com um índice muito baixo (10%). Já, quando compraram-se os biocarvões de origem natural (Co7 = PL *vs* CW), verificou-se diferenças significativas (p<0,05) para todas variáveis estudadas (Tabelas 3 e 4), com exceção ao conteúdo de Fe, com maiores médias para a CW. Destaca-se que no rejeito de Fe, as plantas cultivadas com PL não sobreviveram.

O contraste de médias que compara os efeitos dos biocarvões produzidos em co-pirólise, envolvendo a cama de frango e os resíduos de origem sintética (Co9 = PL+TR *vs* PL+PVC), apresentou as maiores (p<0,05) médias para a maioria das variáveis (p<0,05) quando utilizou PL+TR, tendo como exceção a biomassa do caule da planta (Tabela 3) e o conteúdo de N, Fe e Mn (Tabela 4). Quando a pirólise e co-pirólise dos resíduos de origem natural foi comparada (Co10 = PL *vs* PL+CW), verificou-se que, com exceção da germinação (Tabela 3) e conteúdo de Ca, S, Fe e Mn (Tabela 4), todas as demais variáveis foram significativas (P>0,05), sendo as maiores médias observadas para PL+CW.

Tabela 4. Contrastes ortogonais médios, significância e médias dos conteúdos de N, K, P, Ca, Mg, S, Fe e Mn na crotalaria (*Crotalaria juncea*) cultivada em rejeitos de mineração de Fe e Mn condicionados com fertilização química e biocarvões produzidos por pirólise de resíduos de cama de frango (PL), madeira de construção (CW), pneu (TR), plástico PVC (PVC) e co-pirólise (PL+CW; PL+TR e PL+PVC) a 600ºC, e respectivos controles com e sem fertilização química (Fe^+, Fe^-, Mn^+ e Mn^-)

Tratamentos	N	K	P	Ca	Mg	S	Fe	Mn
	----------mg vaso^{-1}----------							
	Rejeito da mineração de Mn							
Mn^-	0.19	3.98	0.95	2.62	1.86	1.49	0.17	1.14
Mn^+	44.7	49.5	6.95	28.0	3.95	11.1	1.64	14.8
PL	0.07	2.71	0.20	0.25	0.33	0.36	0.13	0.52
CW	56.9	68.1	7.63	62.5	6.00	12.2	1.07	8.38
TR	0.00	0.00	0.00	0.00	0.00	0.00	0.00	0.00
PVC	0.00	0.00	0.00	0.00	0.00	0.00	0.00	0.00
PL+CW	59.7	37.6	9.33	11.52	10.7	8.98	0.76	1.39
PL+TR	11.6	26.3	6.63	16.3	11.7	18.4	0.12	0.75
PL+PVC	0.00	0.00	0.00	0.00	0.00	0.00	0.00	0.00
	Rejeito da mineração de Fe							
Fe^-	1.13	12.2	3.12	9.10	5.88	4.66	0.44	2.77
Fe^+	28.7	40.5	5.32	18.4	3.02	7.85	1.38	10.4
PL	0.00	0.00	0.00	0.00	0.00	0.00	0.00	0.00
CW	17.1	31.2	3.64	23.9	2.48	5.72	0.65	2.99
TR	18.8	28.3	4.66	24.6	6.81	17.4	2.95	16.3
PVC	0.00	0.00	0.00	0.00	0.00	0.00	0.00	0.00
PL+CW	0.00	0.00	0.00	0.00	0.00	0.00	0.00	0.00
PL+TR	0.00	0.00	0.00	0.00	0.00	0.00	0.00	0.00
PL+PVC	0.00	0.00	0.00	0.00	0.00	0.00	0.00	0.00
Contrastes								
Co1	-11.9**	-8.46**	-1.66**	-5.02**	-1.82**	-1.89^{ns}	0.17^{ns}	0.61^{ns}
Co2	-6.96*	-12.6**	-1.79**	-4.61*	-0.96^{ns}	-1.78^{ns}	-0.50*	-5.11**
Co3	36.1**	36.9**	4.10**	17.4**	-0.38^{ns}	6.42**	1.20**	10.6**
Co4	0.29^{ns}	-5.62*	0.64^{ns}	-9.28**	1.78*	0.10^{ns}	-0.45*	-3.16*
Co5	13.8**	18.4**	1.71*	15.5**	0.50^{ns}	0.24^{ns}	-0.27^{ns}	-1.10^{ns}
Co6	-9.39^{ns}	-14.2**	-2.33*	-12.3**	-3.41*	-8.68**	-1.47**	-8.13**
Co7	37.0**	48.3**	5.54**	43.1**	4.07**	8.80**	0.80^{ns}	5.43*
Co8	26.9**	12.2**	3.01**	1.69^{ns}	2.42*	-0.11^{ns}	0.35^{ns}	0.51^{ns}
Co9	-5.82^{ns}	-13.2**	-3.31**	-8.13*	-5.86**	-9.20**	-0.06^{ns}	-0.37^{ns}
Co10	29.8**	17.5**	4.57**	5.63^{ns}	5.18**	4.31^{ns}	0.32^{ns}	0.44^{ns}
Ci1	-25.1**	-28.7**	-4.12**	-9.31**	-1.54^{ns}	-5.03**	-0.91**	-9.08**
Ci2	-24.8**	-34.3**	-3.48**	-18.6**	0.25^{ns}	-4.92*	-1.36**	-12.2**

*P<0,05; **P< 0,01; ^{ns}: não significativo. **Co1** (Rej Mn vs Rej Fe); **Co2** (Mn- + Mn+ + Fe- + Fe+) vs (TR + PVC + PL + CW + PL+TR + PL+PVC + PL+CW); **Co3** (Mn+ + Fe+) vs (Mn- + Fe-); **Co4** (TR + PVC + PL + CW) vs (PL+TR + PL+PVC + PL+CW); **Co5** (TR + PVC) vs (PL + CW); **Co6** (TR vs PVC); **Co7** (PL vs CW); **Co8** (PL+TR + PL+PVC) vs (PL+CW); **Co9** (PL+TR vs PL+PVC); **Co10** (PL vs PL+CW); **Ci1** (Mn+ + Fe+) vs (TR + PVC + PL + CW); **Ci2** (Mn+ + Fe+) vs (PL+TR + PL+PVC + PL + PL+CW).

3.2. Extração da solução do solo

Os resultados relativos ao pH e condutividade elétrica (CE) na solução do solo são apresentados na figura 1 e tabela S3. Na comparação entre as coletas ao longo do tempo, foi observada interação significativa entre a fertilização química e o tempo de coleta para o pH na maioria dos tratamentos, com exceção dos tratamentos fertilizados com biocarvões provenientes de PL+PVC e PL+CW no rejeito de Mn e TR e PL+TR no rejeito de Fe. De forma geral, observa-se que a adição de biocarvão aumentou o pH da solução do solo ao longo do tempo, sendo que os tratamentos adubados com biocarvões de PVC, PL no rejeito de Mn e PVC, PL, PL+CW no rejeito de Fe foram significativamente superiores aos demais tratamentos (Figura 1a-b e Tabela S3). Verificou-se uma resposta quadrática do pH do solo em relação ao tempo de coleta para todos os tratamentos, exceto para o tratamento com PL+CW no rejeito de Fe, onde um modelo linear foi o mais adequado. A CE que indica as concentrações de íons na solução foi significativamente alterada pela interação entre fertilização química e tempo de coleta da solução do solo para grande parte dos tratamentos (Figura 1c-d e Tabela S3). Altos valores de CE foram observados para tratamentos adubados com biocarvões de PVC, PL e PL-PVC no rejeito de Mn, no entanto este último não foi significativo. No rejeito de Fe, maiores valores de CE foram observados para tratamentos fertilizados com biocarvões de PVC e PL ou com biocarvões provenientes da co-pirólise envolvendo PL, no entanto, só houve interação significativa para o tratamento fertilizado com biocarvão de PVC. Entres os casos significativos citado anteriormente em ambos os rejeitos, verificou-se que os dados se ajustaram ao modelo quadrático, exceto para o tratamento com PVC no rejeito de Mn, onde um modelo linear foi o mais adequado.

A interação entre aplicação de fertilizantes químicos/biocarvão e tempo de coleta de solução do solo também afetou significativamente as concentrações de P, K, Ca e Mg (Figura 2 e Tabela S3 e S4) e S, B, Mn e Cr (Figura S1 e Tabela S4). Alguns comportamentos comuns foram observados em ambos os rejeitos, como maiores concentrações de P nos tratamentos cultivados com PVC, PL+TR e PL+CW, enquanto para o K observou-se que nos tratamentos fertilizados com PL+PVC e PL+TR houve maiores concentrações. Para o P, os dados se ajustaram melhor ao modelo quadrático, enquanto para o K o modelo linear descreveu melhor as concentrações na solução do solo ao longo do tempo de coleta. As concentrações de Ca na solução do solo foram superiores nos tratamentos adubados com TR, PL+CW e PL+TR no rejeito de Mn e no tratamento com PL+TR no rejeito de Fe. Em todos os casos citados, os dados

se ajustaram ao modelo quadrático. Ao se analisar as concentrações de Mg na solução do solo ao longo do tempo constatou-se que nos tratamentos fertilizados com NPK e PVC em ambos os rejeitos e PL+TR no rejeito de Fe obtive-se maiores concentrações deste nutriente. Destaca-se que com exceção dos tratamentos com NPK e PL+TR que obtiveram resposta linear a aplicação destas fontes, os demais casos se ajustaram ao modelo quadrático.

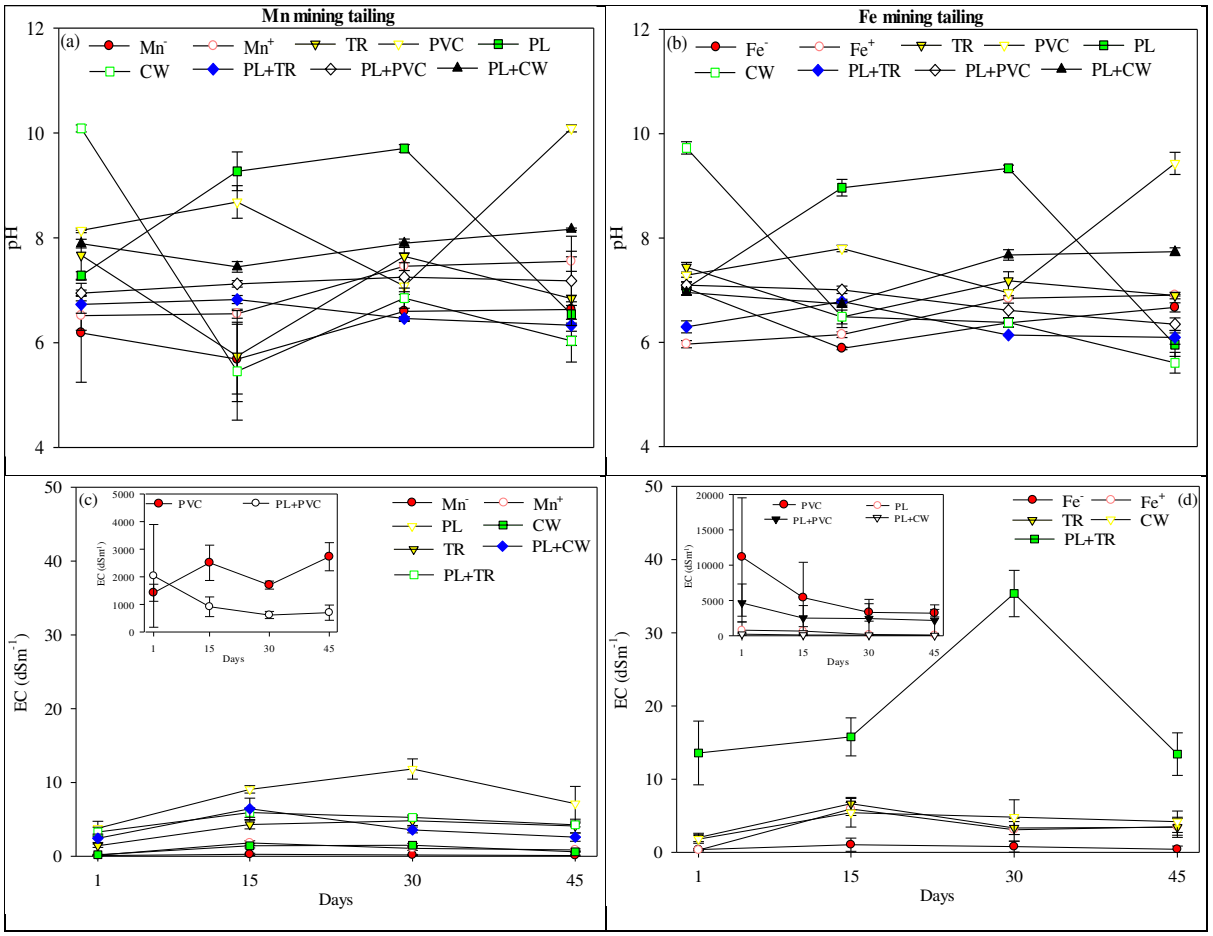

Figura 1. Regressões entre pH e condutividade elétrica (CE) e tempo de coleta da solução do solo no rejeito de mineração de Fe e Mn condicionado com fertilização química e biocarvões produzidos por pirólise de resíduos de cama de frango (PL), madeira de construção (CW), pneu (TR), plástico PVC (PVC) e co-pirólise (PL+CW; PL+TR e PL+PVC) a 600ºC, e respectivos controles com e sem fertilização química (Fe^-, Fe^+, Mn^- e Mn^+). As linhas são as curvas de melhor ajuste.

Em relação a concentração de S na solução do solo, verificou-se que os rejeitos adubados com NPK e com PL+TR, neste último caso apenas no de Fe, apresentaram valor mais elevado para este nutriente. Para os rejeitos adubados com NPK os dados se ajustaram ao modelo quadrático, enquanto para PL+TR houve ajuste linear. Os biocarvões provenientes da pirolise ou co-pirólise envolvendo PL promoveram maiores concentrações de B na solução em ambos

os rejeitos, em todos os casos obteve-se uma resposta quadrática com o aumento do tempo de análise da solução do solo. Para a concentração de Mn na solução verificou-se que os rejeitos fertilizados com biocarvão de PL+PVC obtiveram médias superiores, sendo os dados ajustados ao modelo quadrático. Os tratamentos fertilizados com biocarvões de TR e CW no rejeito de Mn e PL e PL+PVC no rejeito de Fe reduziram significativamente as concentrações de Cr na solução do solo quando comparado ao controle fertilizado. O comportamento Cr na solução em função do tempo de coleta foi representado pelo modelo quadrático para todas as situações citadas acima.

Na tabela 5 estão os contrastes ortogonais entre os tratamentos para pH, CE e elementos na solução do solo. O contraste Co1 usado para comparar o rejeito de Mn *vs* rejeito de Fe mostrou diferenças significativas para o pH, CE, Mn e Cr. Para o pH e concentração de Cr na solução maiores valores foram obtidos no rejeito de Mn, enquanto para CE e concentração de Mn maiores médias foram observadas no rejeito de Fe. Na comparação entre os tratamentos-controle {Co3 = ($Mn^+ + Fe^+$) *vs* ($Mn^- + Fe^-$)}, os maiores valores observados ocorreram quando a fertilização foi feita (+), no entanto com influência significativa ($p<0,05$) apenas para a concentração de K e S (Tabela 5).

A aplicação de biocarvões quando comparada aos controles, presença (+) ou não (-) de fertilização química {Co2 = ($Mn^- + Mn^+ + Fe^- + Fe^+$) *vs* (TR + PVC + PL + CW + PL+TR + PL+PVC + PL+CW) aumentou significativamente ($p<0,05$) o pH, CE e concentração de B na solução, enquanto o inverso só foi observado para a concentração de S na solução. Além disso, quando comparou-se a correção química dos rejeitos em relação a sua aplicação conjunta com os biocarvões, sejam eles pirolisados {(Ci1= ($Mn^+ + TFe^+$) *vs* (TR + PVC + PL + CW)} ou co-pirolisados {Ci2 = ($Mn^+ + TFe^+$) *vs* (PL+TR + PL+PVC + PL + PL+CW)}, observou-se diferenças significativas ($P>0,05$) para o pH, CE e concentração de K e S na solução. Com exceção da concentração de K, em ambos os contrastes, maiores médias foram observados quando os biocarvões foram aplicados em conjunto com a fertilização química (Tabela 5).

Quando se comparou os biocarvões em ambos os rejeitos {Co4 = (TR + PVC + PL + CW) *vs* (PL+TR + PL+PVC + PL+CW)}, aqueles oriundos da co-pirólise apresentaram maiores médias $p<0,05$) para as concentrações de K, Ca e Mn na solução, enquanto os biocarvões provenientes da pirólise obtiveram maior pH. Os biocarvões oriundos de resíduos de origem sintética (TR + PVC) proporcionaram aumento no pH, CE e concentração de S comparativamente aos de origem natural (PL + CW) (Co5).

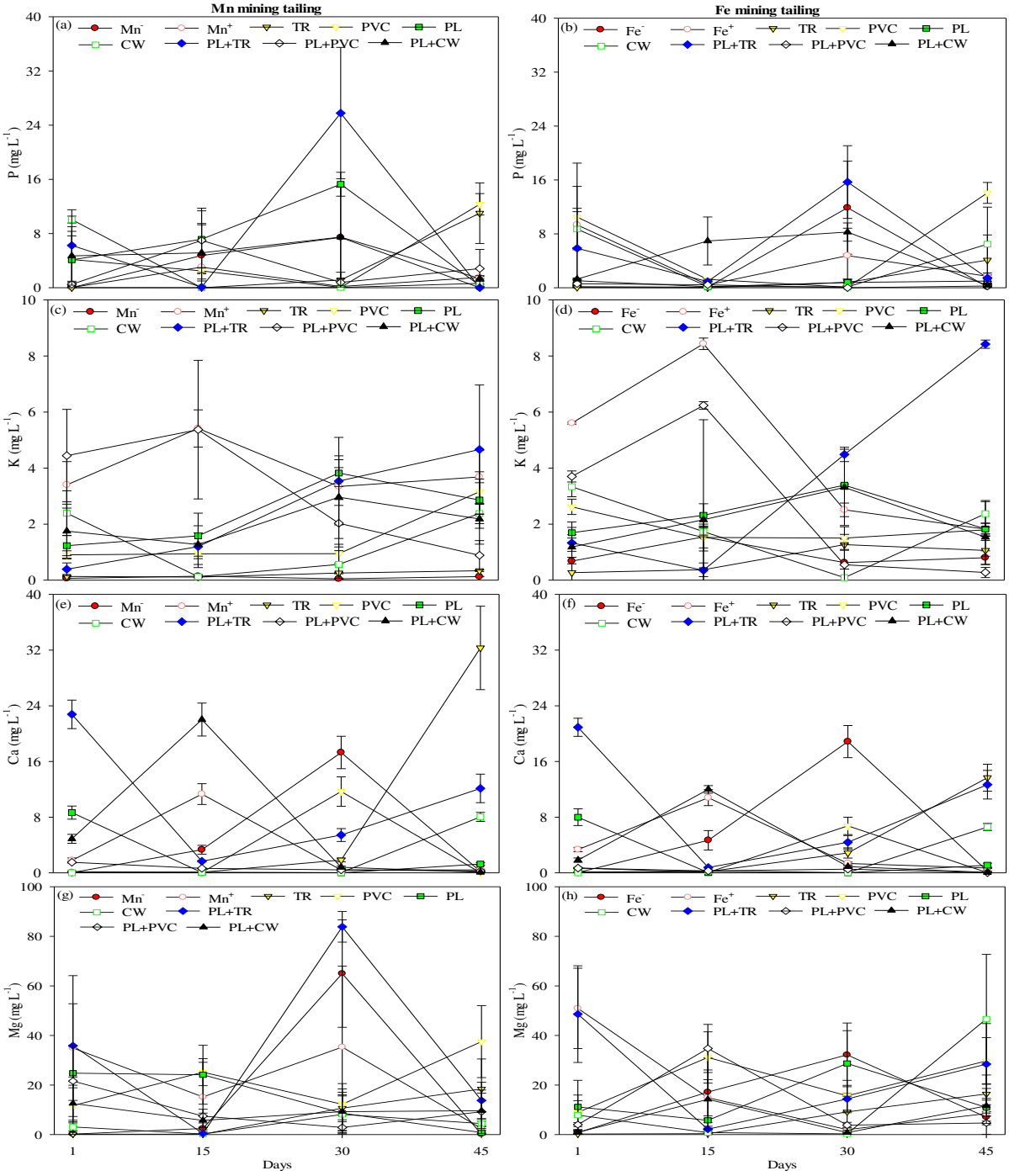

Figura 2. Regressões entre concentrações de P, K, Ca e Mg e tempo de coleta da solução do solo no rejeito de mineração de Fe e Mn condicionado com fertilização química e biocarvões produzidos por pirólise de resíduos de cama de frango (PL), madeira de construção (CW), pneu (TR), plástico PVC (PVC) e co-pirólise (PL+CW; PL+TR e PL+PVC) a 600ºC, e respectivos controles com e sem fertilização química (Fe^-, Fe^+, Mn^- e Mn^+). As linhas são as curvas de melhor ajuste.

Já os biocarvões de origem natural aumentaram as concentrações de K e B na solução do solo (Tabelas 5). Quando os biocarvões de origens sintética e natural foram produzidos em co-pirólise {Co8 = (PL+TR + PL+PVC) *vs* (PL+CW)} constatou-se maior CE na solução dos rejeitos alterados com biocarvões da co-pirólise entre resíduos sintéticos, enquanto os provenientes da co-pirólise de resíduos naturais aumentaram significativamente o pH da solução do solo.

Na comparação entre os biocarvões de origem sintética (Co6 = TR *vs* PVC), maiores ($p<0,05$) médias para a maioria das variáveis foram observadas quando utilizou PVC, tendo como exceção a concentração de Ca na solução. Já, quando compraram-se os biocarvões de origem natural (Co7 = PL *vs* CW), verificou-se diferenças significativas ($p<0,05$) para todas variáveis estudadas, com exceção da CE e concentrações de Mn e Cr (Tabelas 5), com maiores médias para a PL, exceto para a concentração de S.

O contraste ortogonal que compara os efeitos dos biocarvões produzidos em co-pirólise, envolvendo a cama de frango e os resíduos de origem sintética (Co9 = PL+TR *vs* PL+PVC), apresentou as maiores ($p<0,05$) médias para as variáveis pH, CE e concentração de Mn quando utilizou PL+PVC, enquanto para a concentração de Ca maior média foi observada para o PL+TR (Tabela 5). Quando a pirólise e co-pirólise dos resíduos de origem natural foi comparada (Co10 = PL *vs* PL+CW), verificou-se diferença significativa apenas para a pH da solução, neste caso maior média foi observada para PL.

Tratamentos	pH	CE dS cm^{-1}	P	K mg L^{-1}	Ca	Mg	S	B	Mn	Cr
Rejeitos da mineração de Mn										
Mn^-	6.28	0.15	3.04	0.09	5.21	16.9	16.3	21.8	5.53	42.7
Mn^+	7.02	0.96	1.19	3.96	3.48	21.9	22.1	29.7	0.71	25.9
TR	6.98	3.65	3.04	0.21	8.58	7.35	10.7	6.11	2.18	4.46
PVC	8.50	2093	4.75	1.49	2.97	21.6	14.9	50.2	50.2	102
PL	8.20	7.95	6.71	2.37	2.49	14.6	13.2	116	122	13.3
CW	7.11	0.93	2.68	1.36	2.03	3.96	10.5	99.0	282	16.1
PL+TR	6.59	4.68	8.02	2.45	10.5	33.5	32.2	233	140	58.0
PL+PVC	7.12	1069	2.77	3.18	0.70	10.3	18.8	187	171	11.9
PL+CW	7.85	3.75	4.67	2.04	6.95	9.28	18.8	118	49.9	43.4
Rejeitos da mineração de Fe										
Fe^-	6.49	0.65	3.06	0.91	5.95	14.3	15.0	68.1	356	3.70
Fe^+	6.47	3.20	4.06	4.59	4.04	19.1	28.1	138	444	41.7
TR	7.00	3.85	1.23	0.74	4.21	6.51	9.54	77.7	179	9.60
PVC	7.87	5768	6.47	1.86	1.88	21.4	14.5	80.8	241	23.1
PL	7.82	438	0.74	2.31	2.28	14.1	8.94	106	313	2.31
CW	7.05	4.05	3.87	1.88	1.72	13.9	16.9	112	218	26.0
PL+TR	6.33	19.5	5.97	3.65	9.68	23.3	25.6	250	446	43.7
PL+PVC	6.77	2941	0.32	2.69	0.37	11.8	12.0	80.4	690	0.80
PL+CW	7.28	115	4.20	2.05	3.69	6.86	16.1	114	39.4	15.3
Contrastes										
Co1 (Rej Mn vs Rej Fe)	$-2{,}57^{*}$	6110^{**}	$-6{,}96^{ns}$	$3{,}52^{ns}$	$-9{,}1^{ns}$	$-8{,}19^{ns}$	$-11{,}0^{ns}$	165^{ns}	2104^{**}	-151^{*}
Co2 ($Mn^- + Mn^+ + Fe^- + Fe^+$) *vs* (TR + PVC + PL + CW + PL+TR + PL+PVC + PL+CW)	$21{,}1^{**}$	24910^{**}	$31{,}4^{ns}$	$-10{,}4^{ns}$	$-14{,}6^{ns}$	-109^{ns}	-124^{*}	1458^{**}	245^{ns}	$-58{,}5^{ns}$
Co3 ($Mn^+ + Fe^+$) *vs* ($Mn^- + Fe^-$)	$0{,}72^{ns}$	$3{,}36^{ns}$	$-0{,}86^{ns}$	$7{,}55^{**}$	$-3{,}64^{ns}$	$9{,}81^{ns}$	$18{,}9^{**}$	$77{,}8^{ns}$	$83{,}9^{ns}$	$21{,}2^{ns}$
Co4 (TR + PVC + PL + CW) *vs* (PL+TR + PL+PVC + PL+CW)	$7{,}91^{*}$	-5389^{ns}	$-30{,}5^{ns}$	$17{,}7^{**}$	$-58{,}7^{**}$	-127^{ns}	$-52{,}5^{ns}$	157^{ns}	868^{ns}	-501^{*}
Co5 (TR + PVC) *vs* (PL + CW)	$-3{,}27^{**}$	-7838^{**}	$5{,}06^{ns}$	$5{,}05^{**}$	$6{,}3^{ns}$	$17{,}8^{ns}$	$35{,}4^{**}$	479^{**}	614^{ns}	$4{,}84^{ns}$
Co6 (TR *vs* PVC)	$2{,}39^{**}$	7853^{**}	$6{,}95^{ns}$	$2{,}4^{*}$	$-7{,}94^{*}$	$29{,}1^{*}$	$9{,}18^{ns}$	$47{,}1^{ns}$	110^{ns}	111^{**}
Co7 (PL *vs* CW)	$-1{,}24^{*}$	$19{,}2^{ns}$	$7{,}45^{*}$	$2{,}85^{**}$	$16{,}4^{**}$	$39{,}0^{**}$	$30{,}3^{**}$	272^{**}	$85{,}4^{ns}$	$59{,}5^{ns}$
Co8 (PL+TR + PL+PVC) *vs* (PL+CW)	$3{,}03^{**}$	-3237^{*}	$2{,}94^{ns}$	$-0{,}6^{ns}$	$-2{,}17^{ns}$	$19{,}2^{ns}$	$-21{,}6^{ns}$	$-57{,}1^{ns}$	$-78{,}6^{ns}$	$-40{,}3^{ns}$
Co9 (PL+TR *vs* PL+PVC)	$1{,}24^{*}$	-3891^{**}	$5{,}79^{ns}$	$-1{,}79^{ns}$	$9{,}56^{**}$	$-5{,}94^{ns}$	$4{,}14^{ns}$	$-35{,}0^{ns}$	$-77{,}2^{*}$	$46{,}0^{ns}$
Co10 (PL *vs* PL+CW)	$1{,}87^{**}$	441^{ns}	$0{,}9^{ns}$	$1{,}43^{ns}$	$1{,}02^{ns}$	$10{,}9^{ns}$	$-5{,}26^{ns}$	$10{,}0^{ns}$	$-64{,}6^{ns}$	$-26{,}6^{ns}$
Ci1 ($Mn^+ + Fe^+$) *vs* (TR + PVC + PL + CW)	$3{,}47^{*}$	7880^{**}	$15{,}0^{ns}$	$-20{,}6^{**}$	$11{,}5^{ns}$	$-32{,}6^{ns}$	$-65{,}8^{**}$	238^{ns}	-222^{ns}	$12{,}3^{ns}$
Ci2 ($Mn^+ + Fe^+$) *vs* (PL+TR + PL+PVC + PL + PL+CW)	$4{,}58^{**}$	4563^{*}	$3{,}67^{ns}$	$-11{,}0^{**}$	$-6{,}07^{ns}$	$-56{,}2^{ns}$	$-62{,}5^{**}$	218^{ns}	$50{,}8^{ns}$	-116^{ns}

$^{*}P<0{,}05$; $^{**}P< 0{,}01$; ^{ns}: não significativo.

4. Discussão

4.1. Crescimento de planta

De acordo com a interpretação de Alvarez et al. (1999), utilizada para solos agrícolas, os rejeitos de Fe e Mn possuem baixa fertilidade, notadamente pelos baixos teores de P e bases trocáveis (Ca^{2+}, Mg^{2+} e K^{+}) (Tabela 1). A fração argila, característica física que classifica a textura do solo junto com areia e silte, constituiu apenas 20 e 50 g kg^{-1} para o rejeito de Mn e Fe, respectivamente, sendo ambos classificados como textura arenosa (Teixeira et al., 2017). A acidez ativa dos rejeitos, medida pelo pH em água, foi classificada como acidez fraca e média, respectivamente para os rejeitos de Fe e Mn. A CTC muito baixa do rejeito de Fe indica que a argila desses materiais deve dispor de poucos sítios de troca. Por outro lado, o rejeito de Mn mostrou CTC consideravelmente mais alta, no entanto, ainda classificada como baixa. O alto valor de P-rem no rejeito de Fe reflete a baixa capacidade de adsorção de P do mesmo. Os teores de matéria orgânica (MO) foram muito baixos (0,0 e 6,6 g kg^{-1}, respectivamente para os rejeitos de Fe e Mn). Isso se deve as características de textura arenosa dos rejeitos, assim como o próprio processo de extração dos minérios que envolve a supressão da vegetação original. Por outro lado, os teores de S, Zn, Fe e Mn disponíveis foram classificados como altos. As concentrações de Cr, Cu e Pb em ambos os rejeitos ficaram abaixo dos valores de prevenção para metais pesados no solo, segundo (CETESB, 2014).

Os atributos químicos dos rejeitos evidenciam a alta limitação ao crescimento de plantas a serem usadas para revegetação, apresentando como restrições os baixos teores de P, bases trocáveis, MO e CTC. Além de apresentar granulometria que dificulta o crescimento do sistema radicular de plantas, o que indica sérias restrições ao estabelecimento de espécies vegetais. Essas limitações são mais evidentes no rejeito de Fe, devido ao predomínio da fração areia, a ausência de MO e a baixa capacidade de troca catiônica que resulta em reduzida capacidade total de adsorção de cátions neste rejeito.

Na comparação entre os rejeitos (Co1 = Rej Mn *vs* Rej Fe), média de todos os tratamentos em cada rejeito, constatou-se maior produção de biomassa total no rejeito de Mn (2.64 comparado a 1.50 g vaso $^{-1}$ no rejeito de Fe) (Tabela 3). O rejeito de Mn possui maior CTC quando comparado ao rejeito de Fe, portanto, resulta em maior capacidade total de adsorção de cátions e menor capacidade de alterar o pH com adição de biocarvão alcalino. Além disso, as plantas podem ter se desenvolvido melhor no rejeito de Mn devido a maior quantidade de matéria orgânica (MO) neste rejeito (Tabela 1), contrastando com o rejeito de Fe que não

apresentou teor de MO. A matéria orgânica no solo atua tanto como agente condicionador quanto como fornecedor de nutrientes para as plantas. Correlações fortes e significativas (P<0,05) foram observadas entre a produção de biomassa e CTC do rejeito de Mn (r = 0,99), teores de MO (r = 0,99) e pH em água do rejeito (r = -0,99), evidenciando que estes atributos do solo influenciaram o crescimento de plantas, no caso do pH do rejeito, negativamente. Adicionalmente, atributos físicos também podem ter contribuído para efeitos deletérios no desenvolvimento das plantas. O rejeito de Mn possui praticamente o dobro da capacidade de retenção de água (32%, comparado com 18% para do rejeito de Fe), que logicamente possibilitou melhores condições para a germinação e crescimento das plantas. Durante o período experimental, observou-se a formação de uma crosta endurecida nos vasos com rejeito de Fe, que provavelmente contribuiu para uma degradação estrutural. Isso pode ter agido como um impedimento físico ao desenvolvimento radicular.

Tabela 6. Coeficientes de correlação de Pearson em resposta ao cultivo de crotalaria (Crotalaria juncea) cultivada em rejeitos de mineração de Fe e Mn condicionados com aplicação de fertilização química e biocarvões produzidos por pirólise de resíduos de cama de frango (PL), madeira de construção (CW), pneu (TR), plástico PVC (PVC) e co-pirólise (PL+CW; PL+TR e PL+PVC) a 600 ºC, e respectivos controles com e sem fertilização química (Fe^-, Fe^+, Mn^- e Mn^+)

	Ger	H	Bio	Ca	Cd	Cr	Cu	Fe	K	Mg	Mn	Na	P	Pb	S	N	pH_{solo}	CTC_{solo}	MO_{solo}	pH_{BC}	Cinzas	CE_{BC}
Ger	1,00																					
H	0,62**	1,00																				
Bio	0,54**	0,90**	1,00																			
Ca	0,46**	0,76**	0,83**	1,00																		
Cd	0,40**	0,65**	0,64**	0,69**	1,00																	
Cr	0,31**	0,54**	0,61**	0,71**	0,54**	1,00																
Cu	0,36**	0,63**	0,63**	0,70**	0,87*	0,47**	1,00															
Fe	0,31**	0,57**	0,56**	0,57**	0,75**	0,33**	0,92**	1.00														
K	0,54**	0,88**	0,96**	0,91**	0,66**	0,64**	0,64**	0,54**	1,00													
Mg	0,49**	0,62**	0,64**	0,55**	0,34**	0,25*	0,42**	0,39**	0,66**	1,00												
Mn	0,33**	0,58**	0,55**	0,59**	0,83**	0,31**	0,94**	0,94**	0,56**	0,31**	1,00											
Na	0,48**	0,60**	0,56**	0,51**	0,41**	0,26*	0,47**	0,40**	0,56**	0,74**	0,38**	1,00										
P	0,47**	0,78**	0,88**	0,75**	0,58**	0,52**	0,60**	0,53**	0,87**	0,87**	0,47**	0,62**	1,00									
Pb	0,25*	0,44**	0,40**	0,43**	0,64**	0,160	0,84**	0,83**	0,38**	0,29*	0,83**	0,29*	0,37**	1,00								
S	0,49**	0,68**	0,69**	0,71**	0,65**	0,32**	0,80**	0,75**	0,73**	0,81**	0,72**	0,76**	0,79**	0,66**	1,00							
N	0,42**	0,76**	0,94**	0,76**	0,55**	0,61**	0,57**	0,49**	0,87**	0,59**	0,45**	0,43**	0,87**	0,35**	0,58**	1,00						
pH_{solo}	0,00	-0,64	-0,99*	-0,55	-0,76	-0,36	-0,49	-0,09	-0,66	-0,55	0,42	-0,58	-0,58	0,58	-0,59	-0,99**	1,00					
CTC_{solo}	0,00	0,64	0,99*	0,55	0,76	0,36	0,49	0,09	0,66	0,55	-0,42	0,58	0,58	-0,58	0,59	0,99**	-1,00**	1,00				
MO_{solo}	0,00	0,64	0,99*	0,55	0,76	0,36	0,49	-0,09	0,66	0,55	-0,42	0,58	0,58	-0,58	0,59	0,99**	-1,00**	1,00**	1,00			
pH_{BC}	-0,31	0,09	0,14	0,05	0,34	0,07	0,32	0,38	0,19	0,18	0,33	0,38	0,25	0,38	0,27	0,20	-0,90	0,90	0,90	1,00		
Cinzas	0,06	0,23	0,20	0,36	0,40	0,43	0,40	0,39	0,22	0,25	0,39	0,35	0,23	0,37	0,26	0,22	-0,58	0,58	0,58	0,35	1,00	
CE_{BC}	0,25	0,51*	0,45*	0,44*	0,67**	0,360	0,64**	0,68**	0,49*	0,61**	0,65**	0,67**	0,57**	0,60**	0,60**	0,47*	-0,58	0,58	0,58	0,60**	0,65**	1,00

Ger: Germinação; H: Altura da planta; Bio: Biomassa total; Ca, Cd, Cr, Cu, Fe, K, Mg, Mn, Na, P, Pb, S e N: Conteúdo dos respectivos elementos na parte aérea das plantas; pH_{BC}: pH dos biocarvões; Cinzas: Teor de cinzas dos biocarvões; CE_{BC}: Condutividade elétrica dos biocarvões. *P<0,05 e **P<0,01: significativo a 5 e 1% de probabilidade, respectivamente.

Reduções gerais de absorção de nutrientes observadas quando a crotalaria foi cultivada no rejeito de Fe, em comparação com o de Mn, pode estar relacionado com as características do mesmo (baixa CTC e ausência de MO), o que ocasionou o aumento da CE e do pH da solução do solo (Figura 1a-d), sobretudo quando os biocarvões alcalinos foram aplicados. O pH do solo afeta o sistema radicular e sua capacidade de absorver nutrientes. Quando o pH do solo for superior a 8, a planta poderá não conseguir absorver suficientemente alguns micronutrientes como, Fe, Zn e Mn, embora a disponibilidade de P seja elevada (Dhaliwal et al., 2019).

Os tratamento-controle dos rejeitos de Fe e Mn, ambos com adição de fertilizante químico, obtiveram os melhores resultados, independente da comparação, seja em relação a não presença de fertilização (Co3) ou de biocarvões, qualquer que seja ele (Co2, Ci1 e Ci2). O uso de fertilizantes promoveu o aumento no crescimento das plantas de crotalaria em ambos os rejeitos estudados, embora existam diferenças entre os rejeitos na absorção de nutrientes. Neste sentido, a aplicação de fertilizantes aumenta a cobertura vegetal e, portanto, é altamente recomendada para atividades revegetação e reabilitação ambiental que pretendam estabelecer uma cobertura vegetal o mais rápido possível (Carvalho et al., 2018; Silva et al., 2018).

O conteúdo de nutrientes e metais pesados na biomassa aérea das plantas (Tabela 4 e S2) foi influenciado principalmente pela adição de fertilizantes aos rejeitos (Co3, Ci1 e Ci2). A correlação positiva e significativa entre o acúmulo de nutrientes e a produção de biomassa da parte aérea (Tabela 6) sugere que a fertilização é capaz de aumentar concomitantemente o crescimento e a absorção de nutrientes pela crotalaria cultivada em ambos os rejeitos.

Os biocarvões oriundos da co-pirólise, quando comparado com aqueles somente pirolisados (Co4) não favoreceram o desenvolvimento das plantas. Deve-se destacar que os biocarvões refletem a composição dos resíduos utilizados. Portando, a co-pirólise da cama de frango (rica em nutrientes) com os demais resíduos promoveu a confecção de biocarvões com elevado teor de cinzas e nutrientes, especialmente K e Ca. Neste sentido, a aplicação dos biocarvões co-pirolisados em rejeitos com baixa capacidade de tampão, especialmente o rejeito de Fe, aumentou o pH e CE da solução do solo (Figura 1a-d) e reduziu a disponibilidade de nutrientes, principalmente os micronutrientes, como mencionado anteriormente.

Na comparação entre os biocarvões resultantes de resíduos de origem sintética ou natural, verificou-se que resíduos de origem sintética sejam eles via pirólise (Co5) ou co-pirólise com cama de frango (Co8), sobretudo os biocarvões com PVC, influenciaram negativamente a germinação e crescimento das plantas. Adicionalmente, o biocarvão de PVC também teve

desempenho inferior quando comparado ao derivado de pneu, tanto via pirólise (Co6 = PVC *vs* TR) quanto na co-pirólise (Co9 = PL+TR *vs* PL+PVC). A aplicação destes biocarvões (PVC e PL+PVC) reduziram drasticamente a germinação no rejeito de Mn, enquanto no rejeito de Fe não houve germinação da crotalaria. Portando, os resultados deste estudo suscitam uma preocupação com o risco de usar biocarvões derivados de PVC como condicionador orgânico e/ou inorgânico para remediar áreas de mineração. O biocarvão derivado de PVC contém alguns compostos tóxicos, como o hidrocarbonetos policíclicos aromáticos e altos teores de cloro (López et al., 2011; Jouhara et al., 2018), que podem representar algum impacto ambiental negativo, sobretudo quando aplicado em altas doses. A lavagem do biocarvão antes da sua aplicação ao solo poderia minimizar esse impacto.

O efeito inibitório na germinação e no crescimento da crotalaria, especialmente no rejeito de Fe, quando alterado com biocarvões oriundos da pirolise ou co-pirólise de PVC, deve-se provavelmente aos altos valores de CE e teor de cinzas destes biocarvões (Tabela 2). Dependendo do tipo de matéria-prima partir do qual o biocarvão é produzido, este pode conter altas concentrações de nutrientes que podem afetar a germinação das sementes (Gaskin et al., 2008). Durante a pirólise, cátions básicos como Ca, Mg e K contidos na matéria-prima podem ter sido convertidos a óxidos, hidróxidos, sulfatos e carbonatos, os quais, podem atuar como agente calante e elevar a alcalinidade do solo após aplicação do biocarvão (Yuan et al., 2011; Zhang et al., 2017). Portanto, além do pH alcalino do solo, a composição e concentração de sal, especialmente CO_3^{2-} e HCO_3^-, são os principais fatores que inibem a germinação das sementes (Ma et al., 2015). Liu et al. (2014) também relataram que a salinidade excessiva pode influenciar negativamente a germinação e o crescimento das plantas. Esses autores observaram que o solo alterado com composto derivado de lodo de esgoto, rico em sais solúveis de Na, K, Cl, Mg e Ca, inibiu a germinação e o crescimento das sementes de alface (*Lactuca sativa*) e tomate (*Solanum lycopersicum*).

No presente estudo, os biocarvões de PVC e PL+PVC apresentaram teores de cinzas de 49 e 43%, enquanto os biocarvões CW e TR foram menores, no caso, 4.2 e 12%, respectivamente (Tabela 2). Em contrapartida a aplicação de CW e TR no rejeito de Fe aumentou a germinação de 55% do tratamento-controle fertilizado para 67,5 e 70%, respectivamente. A dose aplicada de biocarvão (5%), aumentou imediatamente a CE e pH da solução do solo, sobretudo devido ao alto "poder de neutralização da acidez do solo" e teores de compostos solúveis nas cinzas da maioria dos biocarvões, aliado à baixa capacidade de

tamponamento dos rejeitos, especialmente o de Fe. Solaiman et al. (2012), ao avaliaram a influência de biocarvões e observaram que a germinação das sementes de trigo foi estimulada quando aplicou-se 10 t/ha, porém foi inibida quando 100 t/ha foi utilizada para a maioria dos biocarvões avaliados, o que ressalta que o crescimento das plantas depende tanto da dose aplicada, como das características químicas do biocarvão utilizado e do pH inicial do solo (Heiskanen et al., 2020).

Os tratamentos com biocarvões de resíduos de madeira de construção apresentaram melhores resultados, seja entre biocarvões de origem natural, obtidos pela pirolise (Co7) ou co-pirólise (Co10) e, até mesmo, quando comparados a fertilização química. Por exemplo, no rejeito de Mn, quando o CW e PL+CW foram aplicados ao solo houve aumento de 13,3 e 4.86%, respectivamente, na produção de biomassa total, em comparação ao tratamento-controle com fertilização. O aumento na produção de biomassa no rejeito onde esses biocarvões foram aplicados pode estar associada com as propriedades dos mesmos, como por exemplo, baixa condutividade elétrica (CE) e poder de neutralização (PN), bem como e alta CTC do CW, (0,09 dS m^{-1}; 6,08% e 30,34 $cmol_c$ kg^{-1}, respectivamente). Certamente essas propriedades influenciaram positivamente no crescimento das plantas. Além disso, quando o CW foi aplicado, as plantas absorveram maiores quantidades de N, P, K, Ca, Mg, S, Fe, Mn, B, confirmando a menor alteração na CE do solo (0.93 e 4.05 dS m^{-1} para os rejeitos de Mn e Fe, respectivamente) com a aplicação desse biocarvão, já discutido. Adicionalmente, verificou-se maiores conteúdos de Al, Cr e Pb nas plantas cultivadas com o rejeito de Mn alterado com CW (Tabela S2). Portanto, a adição de CW promoveu maior acúmulo de nutrientes, que se traduziu em maior produção de biomassa, quando comparado ao rejeito apenas fertilizado quimicamente. A maior absorção de metais (Cr e Pb) não comprometeu a produção de biomassa. Esses elementos não são essenciais para o crescimento das plantas, mas são absorvidos pelas plantas em seus tecidos, resultando em efeitos adversos na função fisiológica das plantas quando absorvidos em altas concentrações (Teodoro et al., 2020).

4.2. Solução do solo

Ao incorporar biocarvões derivados de PVC no rejeito de Mn e PVC, PL e PL+CW no rejeito de Fe foi observado um aumento significativo ($P<0.05$) no pH da solução do solo. Este aumento do pH da solução pode ser explicado por diferentes mecanismos: (i) o pH alcalino dos biocarvões (11.8, 10.6 e 10.6, respectivamente para o PVC, PL e PL+CW) (Rodriguez et al.,

2020, 2021) que induz um efeito calagem (capacidade de neutralizar a acidez), aumentando o pH do solo (Masud et al., 2020); (ii) a dissolução de óxidos , hidróxidos e carbonatos metálicos presentes no biocarvão (Houben e Sonnet, 2015); (iii) a presença de grupos funcionais COO^- e O^- na superfície do biocarvão que pode se ligar a H^+ (Yuan et al., 2011; Dai et al., 2017) e (iv) adição de cátions solúveis como Ca, Mg e K (Enders et al., 2012; Dai et al., 2017). Embora o efeito calagem da aplicação de biocarvão possa favorecer a imobilização de "possíveis poluentes" nos rejeitos, um aumento significativo do pH do solo interferiu seriamente e comprometeu o crescimento e o desenvolvimento das plantas (Tabela 3). Os biocarvões provenientes da co-pirólise envolvendo PL no rejeito Fe e PVC e PL em ambos os rejeitos aumentaram significativamente o CE da solução do solo. O aumento da CE da solução após a aplicação destes biocarvões pode ser atribuída a própria CE dos mesmos (e.g., 10.9 e 146 dS m^{-1} para biocarvões derivados de PL e PVC, respectivamente) (Rodriguez et al., 2020) e também ao acréscimo de cinzas presentes no biocarvão e a adição de cátions para a solução do solo que aumenta a força iônica da solução (Chintala et al., 2013; Moreno-Barriga et al., 2017).

A aplicação de fertilizantes e/ou biocarvões aumentou a concentração na solução do solo da maioria dos nutrientes e reduziu a concentração de alguns metais. Destaca-se que os rejeitos são muito pobres em nutrientes. Mais notavelmente, a combinação NPK + biocarvão de PL+TR aumentou significativamente as concentrações na solução do solo de P, K, Ca, B, Mg e S, os dois últimos apenas no rejeito de Fe, em comparação com os rejeitos não adubados ou aqueles adubados apenas com NPK. Uma explicação plausível para o aumento da concentração desses nutrientes na solução do solo nos tratamentos adubados com biocarvão derivado da co-pirólise entre PL+TR, pode estar relacionada a quantidade total adicionada de nutrientes ao solo por essa fonte (28.7, 20.8, 33.5 4.86, 10.7 e 0.016 g kg^{-1} de P, K, Ca, Mg, S e B respectivamente) (Rodriguez et al., 2021), além disso, devido ao alto pH e CEC dessa fonte (10.7 e 27.4 $cmol_c$ kg^{-1}, respectivamente) (Rodriguez et al., 2021), esses nutrientes foram retidos no solo, aumentando assim sua disponibilidade na solução do solo.

O pH da solução do solo foi maior no rejeito de Mn quando comparado ao de Fe (Co1). Um aumento do pH da solução do solo observado para o rejeito de Mn quando comparado ao rejeito de Fe, não era esperado e, neste momento, não pode ser explicado, porque as características do rejeito de Mn (pH, CTC e teor de MO) favorecia uma menor alteração do pH da solução. A condutividade elétrica (CE) na solução do solo do rejeito de Fe foi aproximadamente 3 vezes maior (1033 dS m^{-1}) quando comparado ao rejeito de Mn. Esse

aumento da CE na solução do dolo no rejeito de Fe deve-se ao baixo poder tampão desse rejeito e alta CE de alguns biocarvões (e.g., 2.95, 10.9 e 146 dS m^{-1} para biocarvões derivados de PL+PVC, PL e PVC, respectivamente) (Rodriguez et al., 2020, 2021). As características da maioria dos biocarvões, como alto pH, CE elevada e alto teor de cinzas, influenciou significativamente o pH e CE da solução. Isso fica evidente na comparação dos biocarvões com os controles fertilizados e não fertilizados (Co2), fertilizados *vs* biocarvões de pirólise (Ci1) ou de co-pirólise (Ci2) onde houve aumento significativo do pH e CE da solução quando o biocarvões foram aplicados. Provavelmente, a solubilização de espécies químicas alcalinas presentes nos biocarvões, como calcita ($CaCO_3$) e dolomita ($CaMg(CO_3)_2$, contribuiu para aumentar o pH e CE da solução do solo. Assim, a utilização destes biocarvões é uma estratégia potencial para aumentar o pH de solos ácidos, além de aumentar a concentração de nutrientes (e.g., S e B) na solução do solo.

Em comparação com o controle sem fertilização, nos rejeitos adubados (Co3), a concentração de K e S na solução foram significativamente maiores. Embora tenha ocorrido variação nas concentrações de P, Ca, Mg, B, Mn e Cr (Figure 2 e S1) durante a coleta de solução no solo, estes elementos não foram significativamente afetados pela adição da fertilização. Os biocarvões provenientes do processo de co-pirólise aumentaram a concentração de K, Ca e Mn na solução do solo em comparação com a pirólise (Co4). No processo de co-pirólise as biomassas pobres em nutrientes (TR e PVC) foram misturadas com PL, rica em Ca, K e P, dando origem a biocarvões com elevado teores desses nutrientes (Rodriguez et al., 2021). Portando, é compreensível o aumento na solução do solo desses nutrientes quando comparada aos biocarvões de pirólise, contudo, isso não se traduziu em aumento na produção de biomassa da crotalaria. Os biocarvões de origem sintética são pobres em nutrientes, porém possuem pH elevado e alta CE, especialmente os derivados de PVC. Assim, verificou-se aumento tanto do pH como CE da solução do solo quando estes foram aplicados em comparado com os de origem natural (Co5). Em média, quando os biocarvões de co-pirólise foram aplicados, o pH da solução aumentou de 6.4-7.6. Nesta faixa de pH há redução considerável da disponibilidade de P, B, Fe, Mn, Zn e Cu (Sparks, 2003). Portanto, os aspectos nutricionais devem ter interferido no desenvolvimento das plantas, uma vez que quando esses biocarvões foram aplicados, apenas para o TR no rejeito de Fe houve produção de biomassa da planta. Quando os biocarvões de origem sintética formam co-pirolisados com PL houve uma redução no pH da solução do solo, ainda assim, a CE da solução se manteve extremamente elevada (1009 dS m^{-1}).

O biocarvão derivado de PVC em comparação com TR (Co6), aumentou o pH, CE, e concentração de Mg, K e Mn na solução do solo. Como já mencionado, esse biocarvão possui alto pH e teores de cinzas, e CE elevada, além de maiores teores de K, Mg e S quando comparado ao TR (Rodriguez et al., 2020). Tais características inerentes ao biocarvão supracitadas acima também foram importantes quando se comparou PL *vs* CW, onde houve maior pH e concentração de alguns nutrientes (Mg, K, Ca, P e B) na solução do solo adubado com PL, reforçando assim que biocarvões ricos em nutrientes aumentam a concentração destes na solução do solo.

Devido à alta heterogeneidade das propriedades do biocarvão, condições do solo, desenhos de experimentos e/ou condições ambientais, as respostas das plantas à aplicação do biocarvão no solo são amplamente variadas (Ali et al., 2017; You et al., 2021). Por exemplo, You et al. (2021) verificaram que a aplicação de biocarvão de cavaco de madeira melhorou significativamente a produtividade de plantas (*Mesembryanthemum crystallinum* L.) tolerantes ao sal em solo costeiro sem aplicação de fertilizantes. No entanto, esses autores observaram que não houve diferença significativa na produtividade quando o biocarvão foi aplicado em combinação com fertilizante. Thomas et al. (2013) produziram biocarvões derivados de madeira e carcaça de porco e aplicaram em solos com baixo e alto teor de matéria orgânica e co-contaminados com Cd e Di-etilhexil ftalato. Esses autores verificaram que ambos os biocarvões, especialmente o derivado de carcaça de porco na dose de 2%, aumentaram a produção de biomassa da *Brassica chinensis* L., de forma mais expressiva, no solo com baixo teor de matéria orgânica. Os resultados do nosso estudo mostraram que a aplicação de NPK+biocarvões derivado da pirolise CW ou da co-pirólise deste com PL aumentou a produção de biomassa e absorção de nutrientes da crotalaria cultivada no rejeito de Mn em comparação com aplicação do NPK sozinho (Tabelas 3 e 4). No entanto, para os demais biocarvões, a aplicação combinada com fertilizantes minerais não promoveu nenhum efeito significativo ou até mesmo diminuiu a germinação e a produção de biomassa das plantas de crotalaria. A inconsistência entre estes resultados obtidos pode estar relacionada às características dos biocarvões, como teor de cinzas, pH e quantidade de elementos alcalinos (Ca, K e Mg). Assim a aplicação combinada de biocarvão e fertilizante parece minimizar os efeitos benéficos do biocarvão, já que um dos principais problemas para o crescimento das plantas em rejeitos de mineração é a deficiência de nutrientes (Silva et al., 2018). Assim, o uso de biocarvões rico em nutrientes, podem ser úteis

para melhorar a revegetação em áreas onde há disponibilidade restrita de nutrientes, como pilhas de rejeitos.

Na Província Mineral de Carajás, a maioria das áreas nativas afetadas pela mineração é transformada em cavas exauridas de minas ou pilhas de rejeitos (Ramos et al., 2019). Segundo estes autores, normalmente, a revegetação destas áreas com espécies arbóreas não é recomendada, pois elas podem desestabilizar encostas mais íngremes. Nesse sentido, uso de espécies de crescimento rápido, como a crotalaria, devem ser preferidas (Gastauer et al., 2019). O crescimento rápido e o aporte de biomassa pela crotalaria pode contribuir para a estabilização das propriedades físicas e químicas do solo, para a redução da erosão do solo e para o aumento da quantidade de matéria orgânica no solo nas áreas mineradas a serem revegetadas (Carvalho et al., 2018). No geral, os resultados do experimento em casa de vegetação demonstram benefícios significativos da fertilização para o crescimento das plantas em ambos os rejeitos, em menor proporção da adição de biocarvão (derivado de madeira da construção) no rejeito de Mn. No entanto, deve se enfatizar que, os biocarvões produzidos a partir de diferentes materiais de origem afetaram diretamente as características químicas dos rejeitos e por consequência a resposta fisiológica das plantas. Outro ponto a ser considerado é que apesar do experimento de casa de vegetação demonstrar que uso de biocarvões rico em cinzas e nutrientes podem aumentar a CE da solução e interferir negativamente no crescimento da planta, nas condições de campo de Carájas, doses de 5% podem ser interessantes, pois afinal os processos de erosão e lixiviação podem ser mais intensos. Assim, a necessidade de garantir a revegetação nessas condições podem sugerir que doses mais elevadas de biocarvão possam ser uteis ao desenvolvimento das plantas.

5. Conclusões

Os resultados mostraram que a crotalaria (*Crotalaria juncea*) foi responsiva a aplicação de fertilizantes em ambos os rejeitos, com maior produção de fitomassa no de Mn. No entanto, em contraste com nossa hipótese, os biocarvões foram responsáveis por efeitos deletérios a germinação das sementes e consequentemente ao crescimento das plantas, com exceção dos biocarvões produzidos a partir do resíduo de madeira de construção aplicados no rejeito de Mn. O alto teor de cinzas dos biocarvões e cátions alcalinos, com exceção do proveniente de resíduo de madeira de construção, aumentou o pH e CE da solução do solo a níveis que influenciou negativamente a germinação das sementes e crescimento da crotalaria. É evidente que a

combinação de fertilizante e biocarvões nas condições desse trabalho pode não ser adequada para ambos os rejeitos. Em outras palavras, é necessário confeccionar um biocarvão de acordo com as limitações de cada rejeito e testar a dose que promova maior índice de germinação e que contribua para o desenvolvimento das plantas. Finalmente, estudos adicionais que incluam espécies de plantas nativas do ambiente minerado são necessários; o conhecimento das necessidades nutricionais destas espécies e fatores limitantes ao seu desenvolvimento são de extrema importância, especialmente em projetos de revegetação de áreas mineradas.

6. Referencias

Ahmad M, Rajapaksha AU, Lim JE, Zhang M, Bolan N, Mohan D, Vithanage M, Lee SS, Ok YS. Biochar as a sorbent for contaminant management in soil and water: A review. Chemosphere. Elsevier Ltd; 2014;99:19–33.

Al-Wabel MI, Al-Omran A, El-Naggar AH, Nadeem M, Usman ARA. Pyrolysis temperature induced changes in characteristics and chemical composition of biochar produced from conocarpus wastes. Bioresour Technol. 2013;131:374–379.

Ali S, Rizwan M, Qayyum MF, Ok YS, Ibrahim M, Riaz M, Arif MS, Hafeez F, Al-Wabel MI, Shahzad AN. Biochar soil amendment on alleviation of drought and salt stress in plants: a critical review. Environ Sci Pollut Res. Environmental Science and Pollution Research; 2017;24:12700–12712.

Alvarez V. VH, Novais RF de, Barros NF de, Cantarutti RB, Lopes AS. Interpretação dos resultados das análises de solos. In: Ribeiro AC, Guimarães PTG, Alvarez V. VH, organizadores. Recom para o uso corretivos e Fertil em Minas Gerais, 5ª Aproximação. eds. Viçosa, MG: Comissão de Fertilidade do Solo do Estado de Minas Gerais; 1999. p. 25–32.

Alvarez VVH, Fonseca DM. Definição de doses de fósforo para determinação da capacidade máxima de adsorção de fosfatos e para ensaios em casa de vegetação. Rev Bras da Ciência do Solo. 1990;14:44–55.

Anawar HM, Akter F, Solaiman ZM, Strezov V. Biochar: An Emerging Panacea for Remediation of Soil Contaminants from Mining, Industry and Sewage Wastes. Pedosphere. Soil Science Society of China; 2015;25:654–665.

Are KS, Adelana AO, Fademi IOO, Aina OA. Improving physical properties of degraded soil: Potential of poultry manure and biochar. Agric Nat Resour. Elsevier Ltd; 2018;51:454–462.

ASTM Standard D1762 -84. Standard Test Method for Chemical Analysis of Wood Charcoal.

West Conshohocken: ASTM International; 2007.
Beesley L, Marmiroli M, Pagano L, Pigoni V, Fellet G, Fresno T, Vamerali T, Bandiera M, Marmiroli N. Biochar addition to an arsenic contaminated soil increases arsenic concentrations in the pore water but reduces uptake to tomato plants (Solanum lycopersicum L.). Sci Total Environ. 2013;454–455:598–603.
Beesley L, Moreno-Jiménez E, Gomez-Eyles JL, Harris E, Robinson B, Sizmur T. A review of biochars' potential role in the remediation, revegetation and restoration of contaminated soils. Environ Pollut. Elsevier Ltd; 2011;159:3269–3282.
Bernhardt D, Reilly JF. Mineral Commodity Summaries. U.S. Geol. Surv. Reston, USA; 2019.
Camps-Arbestain M, Amonette JE, Singh B, Wang T, Schmidt HP. A biochar classification system and associated test methods. In: Lehmann J, Joseph S, organizadores. Biochar Environ Manag Sci Technol Implement. London: aylor and Francis; 2015. p. 165–194.
Carramaschi A, Zancheta F, Abreu CA De, Zambrosi CB, Erismann NDM, Magalhães AM. cultivadas em solução nutritiva. Bragantia. 2011;70:737–744.
Carvalho JM, Ramos SJ, Furtini Neto AE, Gastauer M, Caldeira CF, Siqueira JO, Silva MLS. Influence of nutrient management on growth and nutrient use efficiency of two plant species for mineland revegetation. Restor Ecol. 2018;26:303–310.
CETESB CADEDSP. Relatório de estabelecimento de valores orientadores para solo e água subterrânea no estado de São Paulo. São Paulo: CETESB; 2014.
Chan KY, Van Zwieten L, Meszaros I, Downie A, Joseph S, Journal A. Agronomic values of green waste biochar as a soil amendment. Aust J Soil Res. 2007;45:629–634.
Chintala R, Mollinedo J, Schumacher TE, Papiernik SK, Malo DD, Clay DE, Kumar S, Gulbrandson DW. Nitrate sorption and desorption in biochars from fast pyrolysis. Microporous Mesoporous Mater. Elsevier Inc.; 2013;179:250–257.
Dai Z, Zhang X, Tang C, Muhammad N, Wu J, Brookes PC, Xu J. Potential role of biochars in decreasing soil acidification - A critical review. Sci Total Environ. Elsevier B.V.; 2017;581–582:601–611.
Dhaliwal SS, Naresh RK, Mandal A, Singh R, Dhaliwal MK. Dynamics and transformations of micronutrients in agricultural soils as influenced by organic matter build-up: A review. Environ Sustain Indic. Elsevier Ltd; 2019;1–2:100007.
DNPM - Departamento Nacional de Producão Mineral. Brazilian mineral yearbook: main

metallic commoditie. Brasılia: DNPM; 2018. p. 34.
Donagema GK, Campos DVB de, Calderano SB, Teixeira WG, Viana JHM. Manual de métodos de análise de solo. 2 edição. EMBRAPA. Centro Nacional de Pesquisa de Solos, organizador. Rio de Janeiro; 2011.
Enders A, Hanley K, Whitman T, Joseph S, Lehmann J. Characterization of biochars to evaluate recalcitrance and agronomic performance. Bioresour Technol. Elsevier Ltd; 2012;114:644–653.
Enders A, Lehmann J. Comparison of Wet-Digestion and Dry-Ashing Methods for Total Elemental Analysis of Biochar. Commun Soil Sci Plant Anal. 2012;43:1042–1052.
Fellet G, Marchiol L, Delle Vedove G, Peressotti A. Application of biochar on mine tailings: Effects and perspectives for land reclamation. Chemosphere. Elsevier Ltd; 2011;83:1262–1267.
Galdino AG, Camara FT, Santana LD, Pinto AA, Silva JM. Potencial De Emergência Das Espécies De Clotalária Juncea E Crotalaria Chroleuca Em Função Da Profundidade De Semeadura. Nucleus. 2019;16:15–20.
Gaskin JW, Steiner C, Harris K, Das KC, Bibens B. Effect of Low-Temperature Pyrolysis Conditions on Biochar for Agricultural Use. Trans ASABE. 2008;51:2061–2069.
Gastauer M, Souza Filho PWM, Ramos SJ, Caldeira CF, Silva JR, Siqueira JO, Furtini Neto AE. Mine land rehabilitation in Brazil: Goals and techniques in the context of legal requirements. Ambio. 2019;48:74–88.
Gee GW, Bauder JW. Particle-size Analysis. In: KLUTE A, organizador. Methods soil Anal Phys Mineral methods. 2.ed. Madison: American Society of Agronomy, Soil Science Society of America; 1986. p. 383–411.
Glaser B, Lehmann J, Zech W. Ameliorating physical and chemical properties of highly weathered soils in the tropics with charcoal - A review. Biol Fertil Soils. 2002;35:219–230.
Guo X, Liu H, Zhang J. The role of biochar in organic waste composting and soil improvement: A review. Waste Manag. Elsevier Ltd; 2020;102:884–899.
He R, Ruan A, Jiang C, Shen D. Responses of oxidation rate and microbial communities to methane in simulated landfill cover soil microcosms. Bioresour Technol. 2008;99:7192–7199.
Heiskanen J, Hagner M, Ruhanen H, Mäkitalo K. Addition of recyclable biochar, compost and fibre clay to the growth medium layer for the cover system of mine tailings: a bioassay in a greenhouse. Environ Earth Sci. Springer Berlin Heidelberg; 2020;79:1–16.

Houben D, Sonnet P. Impact of biochar and root-induced changes on metal dynamics in the rhizosphere of Agrostis capillaris and Lupinus albus. Chemosphere. Elsevier Ltd; 2015;139:644–651.
IBI IBI. Standardized Product Definition and Product Testing Guidelines for Biochar That Is Used in Soil [Internet]. International Biochar Initiative; 2015.
Jouhara H, Ahmad D, van den Boogaert I, Katsou E, Simons S, Spencer N. Pyrolysis of domestic based feedstock at temperatures up to 300 °C. Therm Sci Eng Prog. Elsevier; 2018;5:117–143.
Karaca O, Cameselle C, Reddy KR. Mine tailing disposal sites: contamination problems, remedial options and phytocaps for sustainable remediation. Rev Environ Sci Biotechnol. Springer Netherlands; 2018;17:205–228.
Lehmann J, Joseph S. Biochar for Environmental Management: Science, Technology and Implementation. 2 ed. London: Routledge.; 2015.
Lehmann J, Rillig MC, Thies J, Masiello CA, Hockaday WC, Crowley D. Biochar effects on soil biota - A review. Soil Biol Biochem. Elsevier Ltd; 2011;43:1812–1836.
Lei M, Tang L, Du H, Peng L, Tie B, Williams PN, Sun G. Safety assessment and application of iron and manganese ore tailings for the remediation of As-contaminated soil. Process Saf Environ Prot. Institution of Chemical Engineers; 2019;125:334–341.
Liu H tao, Gao D, Chen T bin, Cai H, Zheng G di. Improvement of salinity in sewage sludge compost prior to its utilization as nursery substrate. J Air Waste Manag Assoc. 2014;64:546–551.
López A, de Marco I, Caballero BM, Laresgoiti MF, Adrados A. Influence of time and temperature on pyrolysis of plastic wastes in a semi-batch reactor. Chem Eng J. 2011;173:62–71.
Lustosa Filho JF, Penido ES, Castro PP, Silva CA, Melo LCA. Co-Pyrolysis of Poultry Litter and Phosphate and Magnesium Generates Alternative Slow-Release Fertilizer Suitable for Tropical Soils. ACS Sustain Chem Eng. 2017;5:9043–9052.
Ma H, Yang H, Lü X, Pan Y, Wu H, Liang Z, Ooi MKJ. Does high pH give a reliable assessment of the effect of alkaline soil on seed germination? A case study with Leymus chinensis (Poaceae). Plant Soil. 2015;394:35–43.
Maiti SK, Maiti D. Ecological restoration of waste dumps by topsoil blanketing, coir-matting and seeding with grass–legume mixture. Ecol Eng. Elsevier B.V.; 2015;77:74–84.

Masud MM, Baquy MA Al, Akhter S, Sen R, Barman A, Khatun MR. Liming effects of poultry litter derived biochar on soil acidity amelioration and maize growth. Ecotoxicol Environ Saf. Elsevier Inc.; 2020;202:110865.

Moreno-Barriga F, Faz Á, Acosta JA, Soriano-Disla M, Martínez-Martínez S, Zornoza R. Use of Piptatherum miliaceum for the phytomanagement of biochar amended Technosols derived from pyritic tailings to enhance soil aggregation and reduce metal(loid) mobility. Geoderma. Elsevier; 2017;307:159–171.

Nigussie A, Kissi E, Misganaw M, Ambaw G. Effect of biochar application on soil properties and nutrient uptake of lettuces (Lactuca sativa) grown in chromium polluted soils. Am J Agric Environ Sci. 2012;12:369–376.

Pandit NR, Mulder J, Hale SE, Martinsen V, Schmidt HP, Cornelissen G. Biochar improves maize growth by alleviation of nutrient stress in a moderately acidic low-input Nepalese soil. Sci Total Environ. The Authors; 2018;625:1380–1389.

Prakongkep N, Gilkes RJ, Wiriyakitnateekul W. Forms and solubility of plant nutrient elements in tropical plant waste biochars. J Plant Nutr Soil Sci. 2015;178:732–740.

Ramos SJ, Gastauer M, Mitre SK, Caldeira CF, Silva JR, Furtini Neto AE, Oliveira G, Souza Filho PWM, Siqueira JO. Plant growth and nutrient use efficiency of two native Fabaceae species for mineland revegetation in the eastern Amazon. J For Res. 2019;1–7.

Rayment GE, Lyon DJ. Soil Chemical Methods - Australasia. Australia: CSIRO Publishing: Collingwood; 2010.

Rodriguez JA, Lustosa Filho JF, Melo LCA, de Assis IR, de Oliveira TS. Influence of pyrolysis temperature and feedstock on the properties of biochars produced from agricultural and industrial wastes. J Anal Appl Pyrolysis. 2020;149:104839.

Rodriguez JA, Lustosa Filho JF, Melo LCA, de Assis IR, de Oliveira TS. Co-pyrolysis of agricultural and industrial wastes changes the composition and stability of biochars and can improve their agricultural and environmental benefits. J Anal Appl Pyrolysis. 2021;155:105036.

Santana GF., Ascencio J. Capacidad de crecimiento de Crotararia juncea L . en condiciones de deficiencia de fósforo. Agron Trop. 2011;61:221–230.

Schulz H, Dunst G, Glaser B. Positive effects of composted biochar on plant growth and soil fertility. Agron Sustain Dev. 2013;33:817–827.

Silva APM da, Viana JP, Cavalcante ALB. Diagnóstico dos Resíduos Sólidos da Atividade de

Mineração de Substâncias Não Energéticas - Relatório de Pesquisa [Internet]. IPEA (Instituto Pesqui. Econômica Apl. Brasília: IPEA; 2012. p. 30.
Silva JR, Gastauer M, Ramos SJ, Mitre SK, Furtini Neto AE, Siqueira JO, Caldeira CF. Initial growth of Fabaceae species: Combined effects of topsoil and fertilizer application for mineland revegetation. Flora. Elsevier; 2018;246–247:109–117.
Solaiman ZM, Murphy D V., Abbott LK. Biochars influence seed germination and early growth of seedlings. Plant Soil. 2012;353:273–287.
Song W, Guo M. Quality variations of poultry litter biochar generated at different pyrolysis temperatures. J Anal Appl Pyrolysis. Elsevier B.V.; 2012;94:138–145.
Sparks DL. Environmental soil chemistry. 2nd Editio. Academic Press, London, UK; 2003.
Teixeira AF dos S, Kemmelmeier K, Marascalchi MN, Stürmer SL, Carneiro MAC, Moreira FM de S. Arbuscular mycorrhizal fungal communities in an iron mining area and its surroundings: Inoculum potential, density, and diversity of spores related to soil properties. Ciência e Agrotecnologia. 2017a;41:511–525.
Teixeira PC, Donagemma GK, Fontana A, Teixeira WG. Manual de métodos de análise de solo [Internet]. 3. ed. rev. Brasília, DF: Embrapa; 2017b.
Teodoro M, Trakal L, Gallagher BN, Šimek P, Soudek P, Pohořelý M, Beesley L, Jačka L, Kovář M, Seyedsadr S, Mohan D. Application of co-composted biochar significantly improved plant-growth relevant physical/chemical properties of a metal contaminated soil. Chemosphere. 2020;242:125255.
USEPA PUSE. Microwave assisted Acid digestion of Sediments, Sludges, Soils and Oils – Method 3052 –SW –. https://www.epa.gov/sites/production/files/2015-12/documents/3052.pdf; 1996. p. 20.
You X, Yin S, Suo F, Xu Z, Chu D, Kong Q, Zhang C, Li Y, Liu L. Biochar and fertilizer improved the growth and quality of the ice plant (Mesembryanthemum crystallinum L.) shoots in a coastal soil of Yellow River Delta, China. Sci Total Environ. Elsevier B.V.; 2021;775:144893.
Yuan J-H, Xu R-K, Zhang H. The forms of alkalis in the biochar produced from crop residues at different temperatures. Bioresour Technol. 2011;102:3488–3497.
Zago VCP, das Dores NC, Watts BA. Strategy for phytomanagement in an area affected by iron ore dam rupture: A study case in Minas Gerais State, Brazil. Environ Pollut. 2019;249:1029–1037.

Zhang L, Jing Y, Xiang Y, Zhang R, Lu H. Responses of soil microbial community structure changes and activities to biochar addition : A meta-analysis. Sci Total Environ. Elsevier B.V.; 2018;643:926–935.

Zhang T, Zhu X, Shi L, Li J, Li S, Lü J, Li Y. Efficient removal of lead from solution by celery-derived biochars rich in alkaline minerals. Bioresour Technol. 2017;235:185–192.

Zorzeto TQ, Dechen SCF, Abreu MF de, Fernandes Júnior F. Caracterização física de substratos para plantas. Bragantia. 2014;73:300–311.

Material Suplementar

Tabela S1. Análise de variância (ANOVA) da germinação, crescimento, biomassa seca da folha, caule e total e conteúdo de nutrientes e metais na parte aérea da crotalaria (*Crotalaria juncea*) cultivada em rejeitos de mineração de Fe e Mn condicionados com fertilização química e biocarvões produzidos por pirólise de resíduos de cama de frango (PL), madeira de construção (CW), pneu (TR), plástico PVC (PVC) e co-pirólise (PL+CW, PL+TR e PL+PVC) a 600ºC, e respectivos controles com e sem fertilização química (Fe^-, Fe^+, Mn^- e Mn^+)

		Quadrado médio											
				Biomassa seca			Conteúdo de macronutrientes e Na						
Fontes de variação	GL	Germinação	Crescimento	Total	Caule	Folha	N	Ca	K	Mg	Na	P	S
Bloco	3	6,42**	84,34	3,09*	0,66	0,97*	372,07	173,144	230,05*	15,36	0,02	21,76*	26,27
Tratamento	17	60,86**	2128,37**	29,17**	4,78**	10,51**	1702,87**	1067,39**	1828,55**	58,48**	1,23**	42,62**	160,22**
Rejeito (R)	1	279,01**	701,84**	25,80**	3,28**	10,68**	2441,69**	504,81**	1622,39**	108,11**	0,82	68,59**	81,70
Biocarvão (BC)	6	65,82**	2736,39**	34,63**	5,69**	12,34**	1891,84**	1904,51**	2463,01**	54,47**	1,19**	44,24**	158,46**
Rej x BC	6	32,60**	1760,14**	21,62**	3,18**	8,28**	1472,33**	745,72**	1158,69**	85,50**	2,03**	44,77**	240,94**
Testemunha	3	16,33**	1421,27**	35,48**	5,78**	12,80**	1906,41**	491,76**	1913,39**	11,534	0,26	27,31**	68,78
Fator*Testemunha	1	101,53**	1454,45**	1,47	1,27	0,01	6,42	8,56	245,74	11,91	0,05	9,10	1,75
Erro	51	1,29	64,47	1,03	0,38	0,27	178,73	64,92	75,06	8,28	0,25	6,50	26,83
CV(%)		23,33	39,1	48,98	72,93	42,29	100,71	73,53	51,90	98,16	119,95	94,79	105,72

		Conteúdo de micronutrientes e metais							
Bloco	GL	Fe	Mn	B	Zn	Cu	Cr	Mo	Pb
Tratamento	3	1,14	49,32	0,07	22,02	9,17E-04	2,10E-03	6,57E-05	2,02E-04
Rejeito (R)	17	2,55**	114,45**	0,34**	28,31	1,79E-3**	4,29E-3**	3,79E-4**	9,42E-05
Biocarvão (BC)	1	0,65	19,34	0,07	32,39	2,85E-05	4,48E-03	5,07E-4**	6,87E-07
Rej x BC	6	2,55*	88,52*	0,40**	36,04	1,57E-03	8,67E-3**	4,65E-4**	9,17E-05
Testemunha	6	3,04**	95,59*	0,17**	37,59	1,60E-03	1,56E-03	5,11E-4**	1,42E-04
Fator*Testemunha	3	2,01	165,35**	0,49**	0,06	2,69E-3*	2,20E-03	9,25E-06	6,12E-05
Erro	1	0,66	87,45	0,14*	6,73	5,20E-04	3,50E-05	3,80E-05	7,90E-07
CV(%)	51	0,90	33,14	0,03	22,28	7,20E-04	1,49E-03	4,66E-05	8,98E-05
		183,53	174,42	73,63	676,68	176,49	205,14	150,24	323,08

*P<0,05 e **P<0,01: significativo a 5 e 1% de probabilidade, respectivamente.

Tabela S2. Contrastes ortogonais médios, significância e médias dos conteúdos de Zn, B, Na, Al, Cd, Cr, Cu e Pb na crotalaria (Crotalaria juncea) cultivada em rejeitos de mineração de Fe e Mn condicionados com fertilização química e biocarvões produzidos por pirólise de resíduos de cama de frango (PL), madeira de construção (CW), pneu (TR), plástico PVC (PVC) e co-pirólise (PL+CW, PL+TR e PL+PVC) a 600ºC, e respectivos controles com e sem fertilização química (Fe^-, Fe^+, Mn^- e Mn^+)

Tratamentos	Zn	B	Na	Al	Cd	Cr	Cu	Pb
	----------mg $vaso^{-1}$----------							
	Rejeito da mineração de Mn							
Fe^-	0.013	0.052	0.108	0.071	0.001	0.003	0.004	0.000
Fe^+	0.277	0.773	0.710	0.802	0.006	0.049	0.057	0.008
PL	0.001	0.005	0.116	0.074	0.000	0.002	0.002	0.000
CW	0.052	0.821	0.570	0.136	0.003	0.117	0.048	0.009
TR	0.000	0.000	0.000	0.000	0.000	0.000	0.000	0.000
PVC	0.000	0.000	0.000	0.000	0.000	0.000	0.000	0.000
PL+CW	0.161	0.333	1.195	0.162	0.000	0.059	0.014	0.007
PL+TR	0.504	0.254	1.867	0.039	0.002	0.006	0.022	0.002
PL+PVC	0.000	0.000	0.000	0.000	0.000	0.000	0.000	0.000
Fe^-	0.029	0.171	0.373	0.157	0.002	0.005	0.008	0.001
Fe^+	0.153	0.644	0.534	0.576	0.004	0.039	0.042	0.006
PL	0.000	0.000	0.000	0.000	0.000	0.000	0.000	0.000
CW	0.021	0.435	0.826	0.080	0.001	0.059	0.019	0.001
TR	11.344	0.497	1.232	1.276	0.003	0.000	0.057	0.018
PVC	0.000	0.000	0.000	0.000	0.000	0.000	0.000	0.000
PL+CW	0.000	0.000	0.000	0.000	0.000	0.000	0.000	0.000
PL+TR	0.000	0.000	0.000	0.000	0.000	0.000	0.000	0.000
PL+PVC	0.000	0.000	0.000	0.000	0.000	0.000	0.000	0.000
Contrastes								
C1	1.171^{ns}	-0.055^{ns}	-0.178^{ns}	0.090^{ns}	0.000^{ns}	-0.015^{ns}	-0.002^{ns}	0.000^{ns}
C2	0.745^{ns}	-0.243^{**}	-0.016^{ns}	-0.275^{ns}	-0.002^{**}	-0.007^{ns}	-0.016^{*}	-0.001^{ns}
C3	0.194^{ns}	0.597^{**}	0.382^{ns}	0.575^{*}	0.004^{**}	0.040^{*}	0.043^{**}	0.007^{ns}
C4	-1.317^{ns}	-0.122^{**}	0.167^{ns}	-0.162^{ns}	-0.001^{ns}	-0.01^{ns}	-0.010^{ns}	-0.002^{ns}
C5	-2.817^{ns}	0.191^{**}	0.070^{ns}	-0.247^{ns}	0.001^{ns}	0.044^{**}	0.003^{ns}	-0.002^{ns}
C6	-5.672^{*}	-0.249^{**}	-0.616^{**}	-0.638^{*}	-0.001^{ns}	0.000^{ns}	-0.029^{*}	-0.009^{*}
C7	0.036^{ns}	0.625^{**}	0.640^{**}	0.071^{ns}	0.002^{**}	0.087^{**}	0.033^{**}	0.005^{ns}
C8	-0.046^{ns}	0.103^{ns}	0.131^{ns}	0.071^{ns}	0.000^{ns}	0.028^{ns}	0.002^{ns}	0.003^{ns}
C9	-0.252^{ns}	-0.127^{ns}	-0.934^{**}	-0.020^{ns}	-0.001^{ns}	-0.003^{ns}	-0.011^{ns}	-0.001^{ns}
C10	0.080^{ns}	0.164^{*}	0.540^{*}	0.044^{ns}	0.000^{ns}	0.029^{ns}	0.006^{ns}	0.003^{ns}
C11	1.212^{ns}	-0.489^{**}	-0.279^{ns}	-0.493^{*}	-0.004^{**}	-0.022^{ns}	-0.034^{**}	-0.004^{ns}
C12	-0.104^{ns}	-0.611^{**}	-0.111^{ns}	-0.656^{**}	-0.005^{**}	-0.033^{*}	-0.044^{**}	-0.006^{ns}

$^{*}P<0,05$; $^{**}P< 0,01$; ^{ns}: não significativo. **Co1** (Rej Mn vs Rej Fe); **Co2** (Mn- + Mn+ + Fe- + Fe+) vs (TR + PVC + PL + CW + PL+TR + PL+PVC + PL+CW); **Co3** (Mn+ + Fe+) vs (Mn- + Fe-); **Co4** (TR + PVC + PL + CW) vs (PL+TR + PL+PVC + PL+CW); **Co5** (TR + PVC) vs (PL + CW); **Co6** (TR vs PVC); **Co7** (PL vs CW); **Co8** (PL+TR + PL+PVC) vs (PL+CW); **Co9** (PL+TR vs PL+PVC); **Co10** (PL vs PL+CW); **Ci1** (Mn+ + Fe+) vs (TR + PVC + PL + CW); **Ci2** (Mn+ + Fe+) vs (PL+TR + PL+PVC + PL + PL+CW).

Tabela S3. Análise de regressão das características químicas e macronutrientes da solução do solo dos rejeitos de Fe e Mn condicionados com biocarvões produzidos por pirólise de resíduos de cama de frango (PL), madeira de construção (CW), pneu (TR), plástico PVC (PVC) e co-pirólise (PL+CW; PL+TR e PL+PVC) a 600ºC, e respectivos controles com e sem fertilização química (Fe^-, Fe^+, Mn^- e Mn^+)

	CE	R^2	pH	R^2	$Mg_{solúvel}$	R^2	$K_{solúvel}$	R^2	$Ca_{solúvel}$	R^2
					Rejeito de Mn					
Mn^-	$\hat{Y}$ =1,24+0,25**x-0,0042**x	0,51	$\hat{Y}$ =6,07-0,011*x+0,0006**x^2	0,55	$\hat{Y}$ =-13,74+4,16**x-0,081**x^2	0,45	$\hat{Y}$ =0,08+5E-4**x+3E-6**x^2	0,07	$\hat{Y}$ =-3,35+1,22**x-0,024**x^2	0,59
Mn+	$\hat{Y}$ =0,18+0,108**x-0,0021**x^2	0,5	$\hat{Y}$ =6,39+0,027**x	0,85	$\hat{Y}$ =33,92-0,53**x	0,38	$\hat{Y}$ =$\bar{Y}$ =3,96		$\hat{Y}$ =3,11+0,38*x-0,011**x^2	0,39
PL	$\hat{Y}$ =2,94+0,63**x-0,012**x^2	0,97	$\hat{Y}$ =6,93+0,27**x-0,006**x^2	0,97	$\hat{Y}$ =28,19-0,59**x	0,92	$\hat{Y}$ =$\bar{Y}$=2,37		$\hat{Y}$ =8,91-0,68**x+0,012**x^2	0,94
CW	$\hat{Y}$ =0,11+0,12**x-0,002**x^2	0,99	$\hat{Y}$ =9,90-0,28**x+0.0044**x^2	0,72	$\hat{Y}$ =$\bar{Y}$ =3,96		$\hat{Y}$ =$\bar{y}$=1,36		$\hat{Y}$ =0,68-0,26*x+9,2E-3**x^2	0,94
TR	$\hat{Y}$ =1,24+0,25**x-0,004**x^2		$\hat{Y}$ =7,37-0,06**x+0,001**x^2	0,11	$\hat{Y}$ =-2,82+0,45**x	0,91	$\hat{Y}$ =0,12-1E-4**x+1E-4**x^2	0,92	$\hat{Y}$ =2,39-0,95**x+0,04**x^2	0,95
PVC	$\hat{Y}$ =1615,46+20,97*x	0,85	$\hat{Y}$ =8,60-0,106**x+0,0003**x^2	0,53	$\hat{Y}$ =11,66+0,044**x	0,46	$\hat{Y}$ =$\bar{Y}$=1,48		$\hat{Y}$ =-2,40+0,72**x-0,014**x^2	0,42
PL+TR	$\hat{Y}$ =3,25+0.21**x-0,004**x^2	0,87	$\hat{Y}$ =6,83-0,011**x	0,78	$\hat{Y}$ =$\bar{Y}$ =33,47		$\hat{Y}$ =0,094+0,103**x	0,97	$\hat{Y}$ =23,16-1,68**x+0,03**x^2	0,89
PL+PVC	$\hat{Y}$ =$\bar{Y}$ =664,73		$\hat{Y}$ =$\bar{Y}$ =7,12		$\hat{Y}$ =22,96-1,39*x-0,024*x^2	0,99	$\hat{Y}$ =5,37-0,096**x	0,77	$\hat{Y}$ =$\bar{Y}$ =0,70	
PL+CW	$\hat{Y}$ =2,68+0,04**x-0,006**x^2	0,61	$\hat{Y}$ =$\bar{Y}$ =7,85		$\hat{Y}$ =$\bar{Y}$ =9,28		$\hat{Y}$ =$\bar{Y}$=2,04		$\hat{Y}$ =7,44+0,66**x-0,019**x^2	0,44
					Rejeito de Fe					
Fe^-	$\hat{Y}$ =$\bar{Y}$ =0,65		$\hat{Y}$ =7,01-0,08**x+0.002**x^2	0,74	$\hat{Y}$ =-3,59+2,49**x-0,049**x^2	0,88	$\hat{Y}$ =$\bar{Y}$ =0,91		$\hat{Y}$ =-3,52+1,38**x-0,03**x^2	0,64
Fe^+	$\hat{Y}$ =0,64+0.32**x-0.006**x^2	0,54	$\hat{Y}$ =5,93+0,024**x	0,89	$\hat{Y}$ =53,79-3,28**x+0,051**x^2	0,99	$\hat{Y}$ =7,29-0,12*x	0,55	$\hat{Y}$ =4,45+0,29x9E-3*x^2	0,48
PL	$\hat{Y}$ =$\bar{Y}$=438,17		$\hat{Y}$ =6,67+0,27**x-0,006**x^2	0,97	$\hat{Y}$ =$\bar{Y}$ =14,14		$\hat{Y}$ =$\bar{Y}$=2,31		$\hat{Y}$ =8,21-0,63**x+0,01**x^2	0,94
CW	$\hat{Y}$ =1,77+0,27**x-0.005**x^2	0,97	$\hat{Y}$ =9,73-0,22**x+0,003**x^2	0,92	$\hat{Y}$ =11,88-2,05**x+0,062**x^2	0,95	$\hat{Y}$ =$\bar{Y}$=1,88		$\hat{Y}$ =0,58-0,02**x+7,3E-3**x^2	0,92
TR	$\hat{Y}$ =2,41+0.24**x-0.005**x^2	0,42	$\hat{Y}$ =$\bar{Y}$ =7,00		$\hat{Y}$ =-2,40+0,39**x	0,91	$\hat{Y}$ =$\bar{Y}$=0,74		$\hat{Y}$ =0,66-0,27**x+12E-3**x^2	0,98
PVC	$\hat{Y}$ =11519,81-487,64*x+0,005*x^2	0,99	$\hat{Y}$ =7,60-0,069x-0,0023**x^2	0,7	$\hat{Y}$ =$\bar{Y}$ =21,36		$\hat{Y}$ =$\bar{Y}$=1,86		$\hat{Y}$ =-0,77+0,37**x-7E-3*x^2	0,35
PL+TR	$\hat{Y}$ =$\bar{Y}$=19,54		$\hat{Y}$ =$\bar{Y}$ =6,33		$\hat{Y}$ =48,88-3,56**x0,071**x^2	0,85	$\hat{Y}$ =-0,32+0,17*x	0,82	$\hat{Y}$ =21,43-1,66**x+0,033**x^2	0,91
PL+PVC	$\hat{Y}$ =$\bar{Y}$=2941,43		$\hat{Y}$ =7,18+0,02**	0,96	$\hat{Y}$ =$\bar{Y}$ =11,81		$\hat{Y}$ =5,19-0,11*x	0,54	$\hat{Y}$ =0,59-4,5E-3*x-2E-4x^2	0,6
PL+CW	$\hat{Y}$ =$\bar{Y}$=115,35		$\hat{Y}$ =6,76+0,023**	0,71	$\hat{Y}$ =$\bar{Y}$ =6,86		$\hat{Y}$ =$\bar{Y}$=2,05		$\hat{Y}$ =$\bar{Y}$ =3,69	

(*) indica diferenças significativa (p<0,05); (**) indica diferenças significativa (p<0,01); R^2=coeficiente de regressão.

Tabela S4. Análise de regressão macro e micronutrientes e metal da solução do solo dos rejeitos de Fe e Mn condicionados com e biocarvões produzidos por pirólise de resíduos de cama de frango (PL), madeira de construção (CW), pneu (TR), plástico PVC (PVC) e co-pirólise (PL+CW; PL+TR e PL+PVC) a 600ºC, e respectivos controles com e sem fertilização química (Fe^-, Fe^+, Mn^- e Mn^+)

	$P_{solúvel}$	R^2	$S_{solúvel}$		$B_{solúvel}$	R^2	$Mn_{solúvel}$	R^2	$Cr_{solúvel}$	R^2
					Rejeito de Mn					
Mn^-	$\hat{Y}$ =-1,06+0,68**x-0,014**x^2	0,93	$\hat{Y}$ =-6,03+3,56**x-0,074**x^2	0,89	$\hat{Y}$ =$\bar{Y}$ =21,76		$\hat{Y}$ =3,11+0,93*x-0,024*x^2	0,38	$\hat{Y}$ =-35,310,44**x-0,20x^2	0,42
Mn^+	$\hat{Y}$ =$\bar{Y}$=1,19		$\hat{Y}$ =30,03+0,16x-0,015**x^2	0,65	$\hat{Y}$ =$\bar{Y}$ =29,75		$\hat{Y}$ =-0,34+0,13*x-3,2E-3*x^2	0,38	$\hat{Y}$ =98,67-7,13**x+0,11**x^2	0,91
PL	$\hat{Y}$ =1,69+0,96**x-0,021**x^2	0,69	$\hat{Y}$ =$\bar{Y}$=13,22		$\hat{Y}$ =229,87-13,53**x+0,24**x^2	0,87	$\hat{Y}$ =$\bar{Y}$ =122,53		$\hat{Y}$ =$\bar{Y}$ =13,24	
CW	$\hat{Y}$ =10,27-0,77*x+0,013x^2	0,92	$\hat{Y}$ =18,76-1,49**x+0,033**x^2	0,88	$\hat{Y}$ =32,59-4,61*x+0,22**x^2	0,99	$\hat{Y}$ =$\bar{Y}$ =282,06		$\hat{Y}$ =61,95-4,48**x+0,071**x^2	0,92
TR	$\hat{Y}$ =0,67-0,29x+0,011**x^2	0,96	$\hat{Y}$ =0,96+0,044x+0,014**x^2	0,97	$\hat{Y}$ =-0,20-0,072*x+0,01x^2	0,99	$\hat{Y}$ =-0,82-0,11**x+4,9E-3*x^2	0,99	$\hat{Y}$ =-0,31+0,26x-1,5*E-3x^2	0,76
PVC	$\hat{Y}$ =5,55-0,60**x+0,016**x^2	0,87	$\hat{Y}$ =$\bar{Y}$=14,95		$\hat{Y}$ =$\bar{Y}$ =50,16		$\hat{Y}$ =$\bar{Y}$ =50,23		52,92+9,87**x-0,22**x^2	0,16
PL+TR	$\hat{Y}$ =0,69+1,15**x-0,024**x^2	0,24	$\hat{Y}$ =$\bar{Y}$=32,16		$\hat{Y}$ =36,46+12,55**x-0,11*x^2	0,98	$\hat{Y}$ =$\bar{Y}$ =139.66		$\hat{Y}$ =9,68-3,88**x+0,17**x^2	0,99
PL+PVC	$\hat{Y}$ =$\bar{Y}$ =2,77		$\hat{Y}$ =31,37-0,22x+0,01*x^2	0,87	$\hat{Y}$ =407,02-15,48**x+0,17**x^2	0,77	$\hat{Y}$ =596,53-40,34*x+0,63x^2	0,88	$\hat{Y}$ =$\bar{Y}$ =11,89	
PL+CW	$\hat{Y}$ =3,86+0,30x-0,008**x^2	0,73	$\hat{Y}$ =$\bar{Y}$=18,85		$\hat{Y}$ =185,29-8,73*x+0,17**x^2	0,99	$\hat{Y}$ =$\bar{Y}$ =49,91		$\hat{Y}$ =46,96-4,74**x+0,13**x^2	0,81
					Rejeito de Fe					
Fe^-	$\hat{Y}$ =-2,43+0,73**x-0,014**x^2	0,42	$\hat{Y}$ =-2,68+2,58**x+0,052**x^2	0,89	$\hat{Y}$ =33,87+7,36x-0,16*x^2	0,42	$\hat{Y}$ =174,25+62,23*x-1,57*x^2	0,38	$\hat{Y}$ =$\bar{Y}$ =3,69	
Fe^+	$\hat{Y}$ =8,64-0,44*x+0,007x^2	0,53	$\hat{Y}$ =33,06-0,87*x+0,019x^2	0,63	$\hat{Y}$ =208,04-3,08**x	0,95	$\hat{Y}$ =297,71+61,65**x1,59**x^2	0,54	$\hat{Y}$ =87,57-2,015**x	0,96
PL	$\hat{Y}$ =$\bar{Y}$ =0,74		$\hat{Y}$ =$\bar{Y}$=8,94		$\hat{Y}$ =127,265,99*x-0,20**x^2	0,86	$\hat{Y}$ =842,11-38,32*x+0,44x^2	0,99	2,74+0,019*x-0,0011*x^2	0,13
CW	$\hat{Y}$ =9,38-0,85**x-0,017**x^2	0,99	$\hat{Y}$ =13,82-0,72**x+0,025**x^2	0,86	$\hat{Y}$ =$\bar{Y}$ =112,24		$\hat{Y}$ =714,31-44,92**x+0,67*x^2	0,99	$\hat{Y}$ =53,31-5,19**x+0,11**x^2	0,99
TR	$\hat{Y}$ =$\bar{Y}$ =1,23		$\hat{Y}$ =-0,63+0,14x+0,008*x^2	0,95	$\hat{Y}$ =6,87+7,92x-0,14*x^2	0,24	$\hat{Y}$ =-71,71+34,96*x-0,69x^2	0,39	$\hat{Y}$ =$\bar{Y}$ =9,60	
PVC	$\hat{Y}$ =11,97-1,18**x+0,027**x^2	0,98	$\hat{Y}$ =$\bar{Y}$=14,50		$\hat{Y}$ =$\bar{Y}$ =80,77		$\hat{Y}$ =106,56-30,07x+1,039**x^2	0,95	$\hat{Y}$ =$\bar{Y}$ =23,08	
PL+TR	$\hat{Y}$ =2,73+0,54**x-0,0012**x^2	0,17	$\hat{Y}$ =15,69+0,44**x	0,39	$\hat{Y}$ =272,52-10,28**x+0,27**x^2	0,99	$\hat{Y}$ =162,1158,96**x+2,06**x^2	0,94	$\hat{Y}$ =46,05-2,46x+0,068*x^2	0,84
PL+PVC	$\hat{Y}$ =$\bar{Y}$ =0,32		$\hat{Y}$ =32,98-2,21**x+0,04**x^2	0,99	$\hat{Y}$ =226,23-16,70**x+0,29**x^2	0,98	$\hat{Y}$=223,49179,82**x+3,23**x^2	0,95	$\hat{Y}$ =1,42-0,028*x+3E5**x^2	0,60
PL+CW	$\hat{Y}$ =0,34+0,72**x-0,016**x^2	0,98	$\hat{Y}$ =18,32-0,095		$\hat{Y}$ =158,27-8,15**x+0,18**x^2	0,96	$\hat{Y}$ =$\bar{Y}$ =39,41		$\hat{Y}$ =-10,28+1,12*x	0,60

(*) indica diferenças significativa (p<0,05); (**) indica diferenças significativa (p<0,01); R^2=coeficiente de regressão.

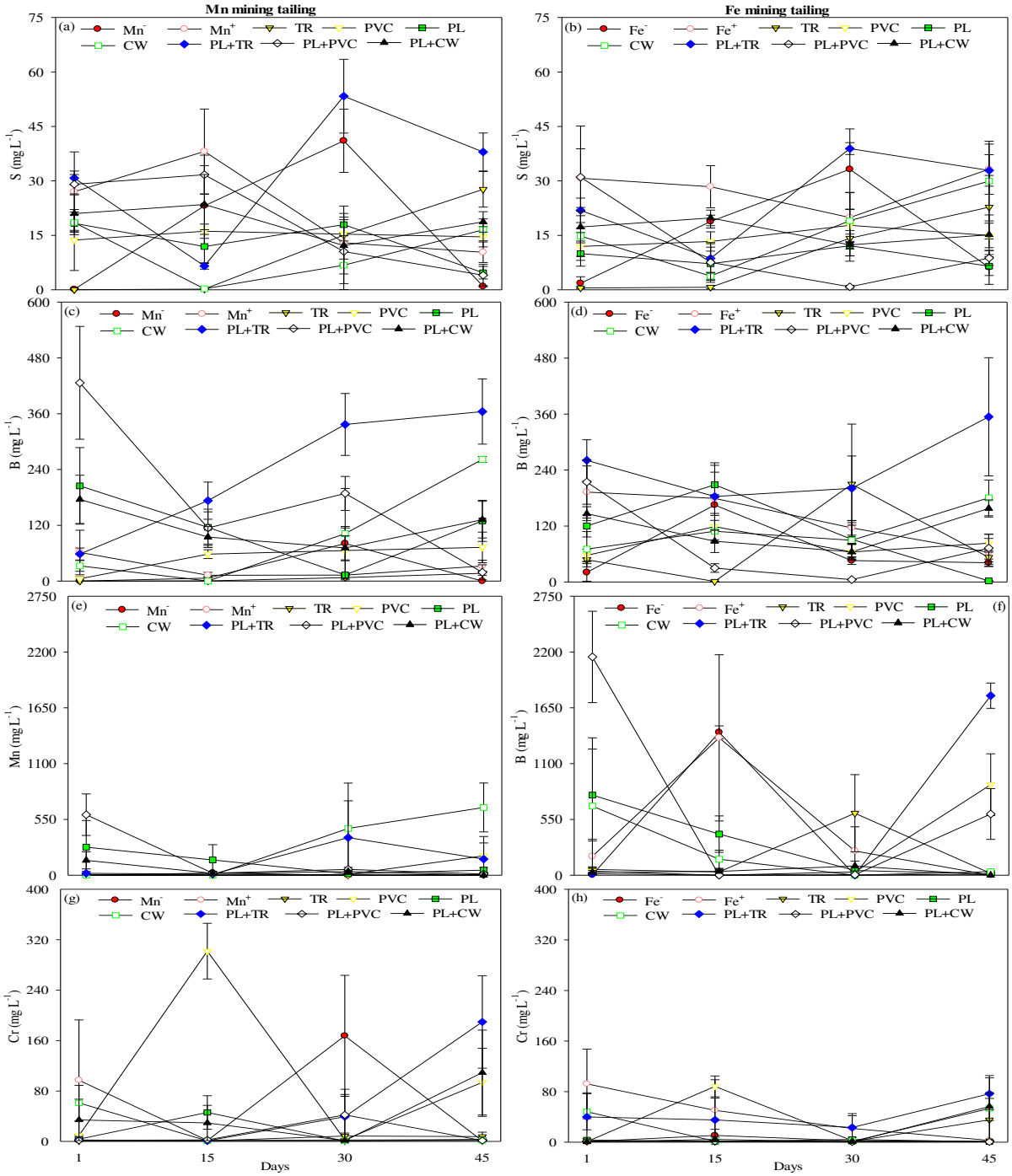

Figura S1. Regressões entre S, B, Mn e Cr e o tempo de coleta da solução do solo no rejeito de mineração de Fe e Mn condicionado com fertilização química e biocarvões produzidos por pirólise de resíduos de cama de frango (PL), madeira de construção (CW), pneu (TR), plástico PVC (PVC) e co-pirólise (PL+CW; PL+TR e PL+PVC) a 600ºC, e respectivos controles com e sem fertilização química (Fe^-, Fe^+, Mn^- e Mn^+). As linhas são as curvas de melhor ajuste.